Question to Fabiola Gianotti: Do you think science can be a force for peace?

"Absolutely, because science is universal and unifying. Universal, because it is based on objective facts, the laws of nature, and not on opinions. An apple falls in the same way, whether it falls in Isaac Newton's garden in 17th-century England, or today in Switzerland, China or the United States. Unifying, because the thirst for knowledge and the desire to understand how things work are intrinsic to humanity. Thus, science has no passport, belief or gender, and can help connect people in our fractured world."

"…Today, CERN is not only a world-class scientific facility and the world leader in high-energy particle physics: it is a value system, embracing and promoting knowledge, innovation, training and education, collaboration across borders, inclusion, diversity and open science."

Наука универсальна и объединяет. Универсальна, потому что она основана на объективных фактах, законах природы, а не на мнениях. Яблоко падает одинаково, будь то в саду Исаака Ньютона в Англии XVII века или сегодня в Швейцарии, Китае или Соединенных Штатах. Объединяет, потому что жажда знаний и желание понять, как всё работает, присущи человечеству. Таким образом, у науки нет паспорта, убеждений или пола, и она может помочь объединить людей в нашем раздробленном мире.

Search for long-range di-hadron correlations in high-multiplicity p+p collisions at $\sqrt{s_{NN}}$ =200 GeV with STAR



Prithwish Tribedy for the STAR collaboration

(Brookhaven National Laboratory)

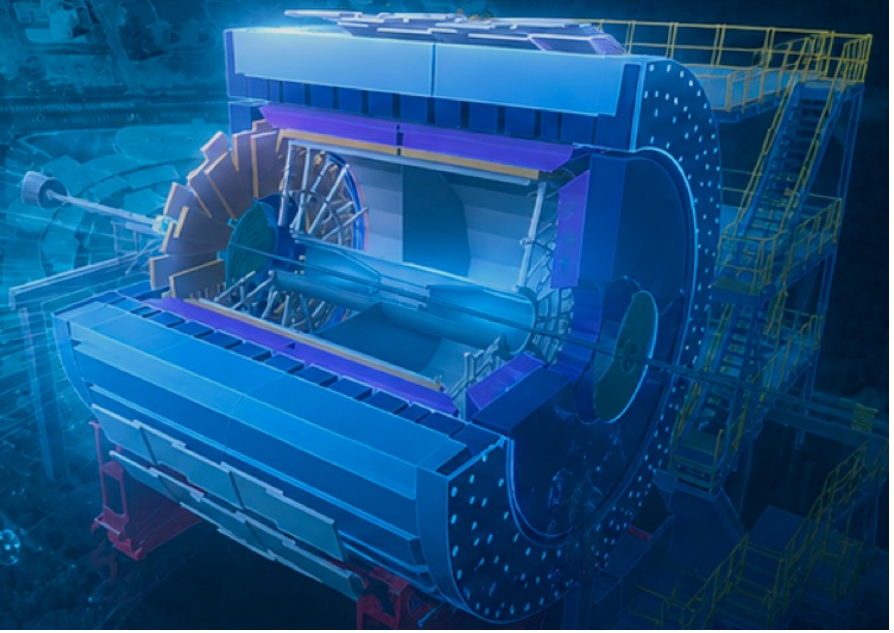

The 54th International Symposium on Multiparticle Dynamics (ISMD 2026), NCU in Chungli, Taiwan, Aug 17-21, 2026

From heavy ions to the ultra-small system frontier

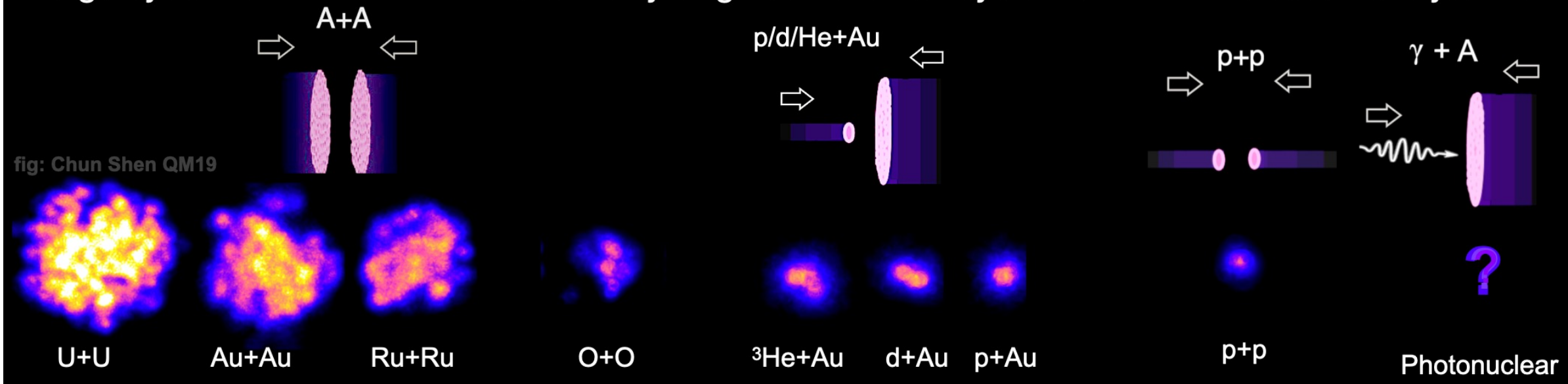

Before:
Can long-range collective correlations seen in A+A emerge in systems as small as p+p?

This work: What are the minimal conditions for collective long-range behavior to dominate the measured correlation?

- System size
- Collision energy
- Event activity

Run-24 experimental reach

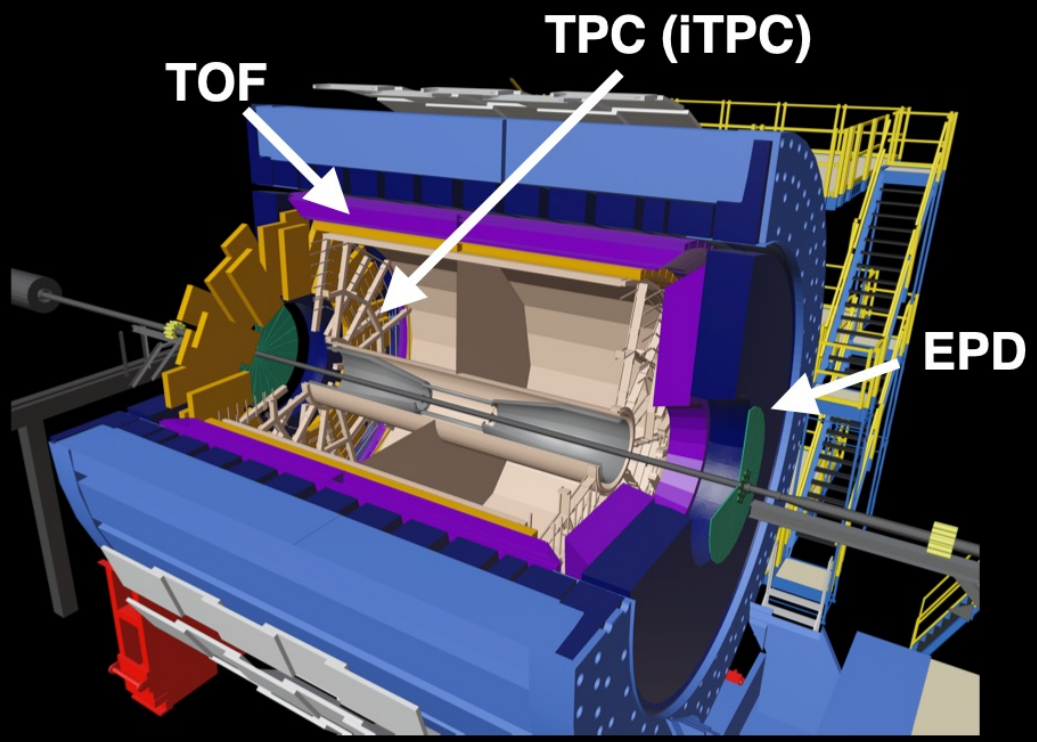

iTPC tracking: $|\eta|<1.5$
Low-luminosity p+p running
MB + dedicated HM trigger

Event activity: reconstructed TPC tracks

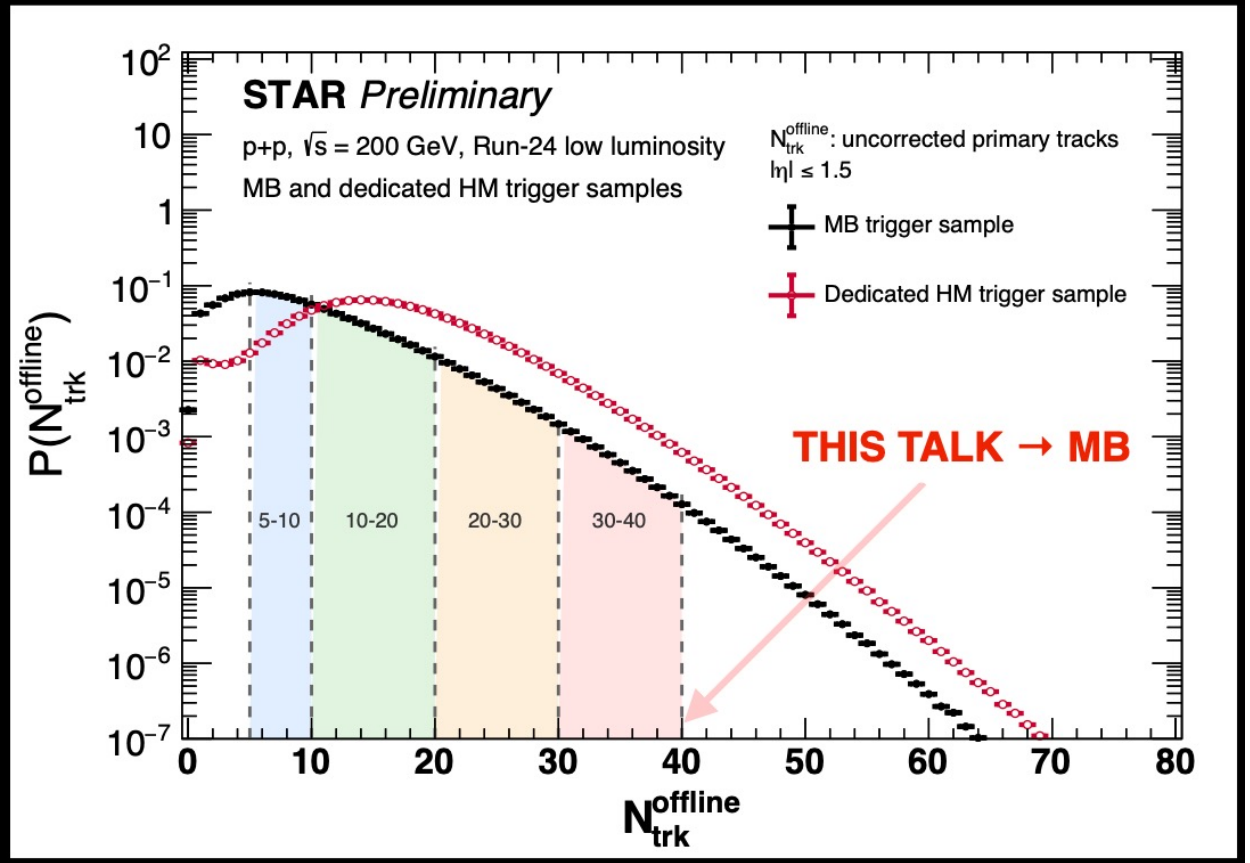

Pileup studied with TOF + event/track-quality variations

This talk: first minimum-bias benchmark; analysis of the high-multiplicity sample is ongoing

Summary

First benchmark of the STAR p+p long-range correlation program

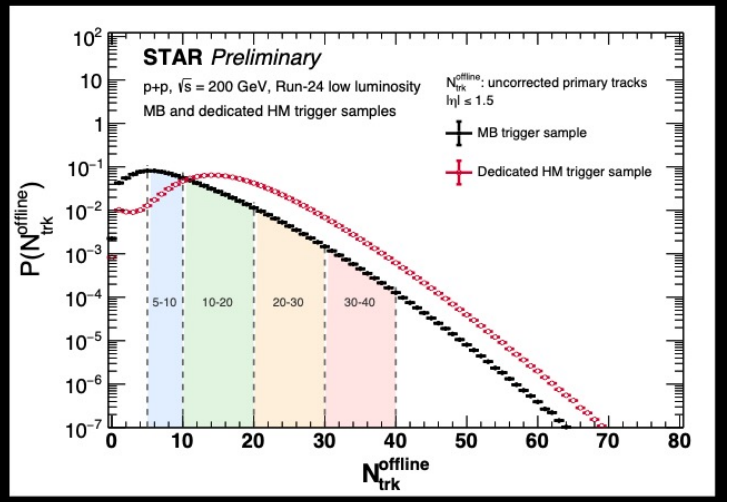

Run-24 enables a new regime at RHIC

- Low-luminosity p+p, extended iTPC acceptance, dedicated HM trigger

Minimum-bias benchmark

- Long-range C_2 is positive and robust across three analysis methods
- C_3 remains non-positive for $N_{trk}^{offline}(|\eta| < 1.5) < 40$

Model comparison (PYTHIA & IP-Glasma+MUSIC)

- Positive C_2 alone is not unique to collective dynamics, sign of C_3 is a good discriminator
- Data C_2-C_3 pattern remains qualitatively consistent with a non-collective-dominated regime

Goal: identify the regime where collective long-range correlations become the dominant structure in the measured p+p correlation at RHIC

Science
AAAS

Supplementary Materials for

Tracking the baryon number with nuclear collisions

STAR Collaboration

Corresponding author: C. Y. Tsang, star-publication@bnl.gov

Science **393**, 727 (2026)
DOI: 10.1126/science.ads5962

The PDF file includes:

Materials and Methods
Figs. S1 to S5
References

https://www.bnl.gov/newsroom/news.php?a=122692

Gluons May Play Central Role in Baryon Number Conservation

Quark-connecting 'gluon junction' could be primary carrier of baryon number, essential to stability of protons, atoms, and all visible matter

August 13, 2026

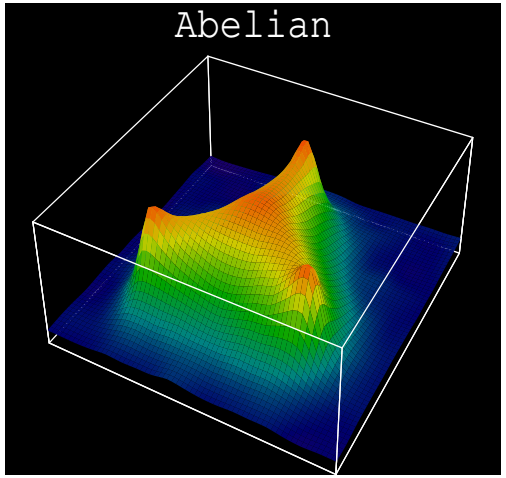

hep-lat/0401026v2
V. Bornyakov et al.

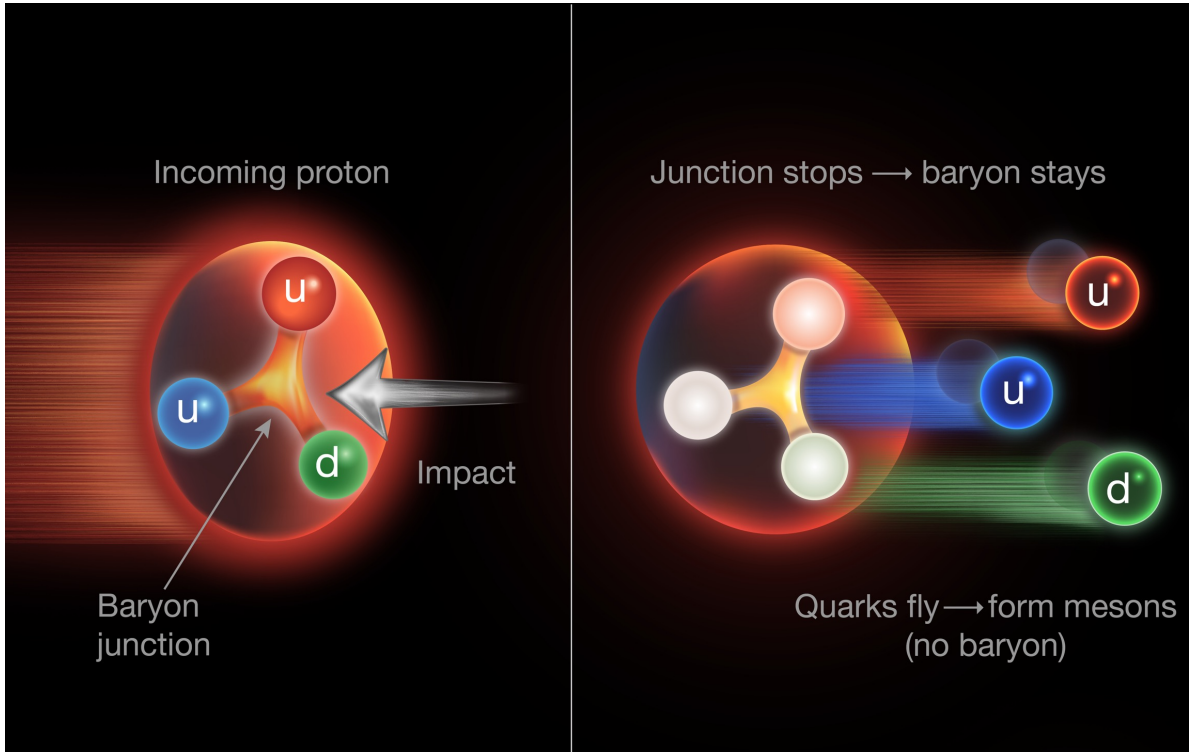

New results from the STAR detector at RHIC suggest that gluons, the gluelike particles that hold quarks together inside protons, play a central role in the conservation of baryon number — an essential part of a particle's quantum identity. These findings suggest that baryon number is carried by a Y-shaped "junction" of gluons connecting the proton's three main quarks. The study, published in the journal *Science*, challenges a long-held view that baryon number is solely carried by those three quarks.

"Traditionally, scientists have assumed that each of the three 'valence' quarks inside a proton or neutron carries 1/3 of the baryon number," said Zhangbu Xu, a professor at Kent State University with a joint appointment at BNL.

"The baryon junction, or g-junction, was predicted by physicists in the 1970s to explain how gluons hold those valence quarks together within protons (Veneciano et al). Then, in 1996, D. Kharzeev [Phys. Lets B 378 (1996) 238], a theoretician at Stony Brook University and BNL, proposed that the baryon junction could be the true carrier of baryon number, instead of the valence quarks. In *Science*, the STAR team describes their innovative strategy to test this idea."

"Data collected from different types of particle collisions at RHIC, suggest that the baryon number is not simply carried by individual quarks, our findings strongly support the idea that baryon number is more favourably carried and transported by gluons, the particles that hold quarks together, when arranged in this special configuration."

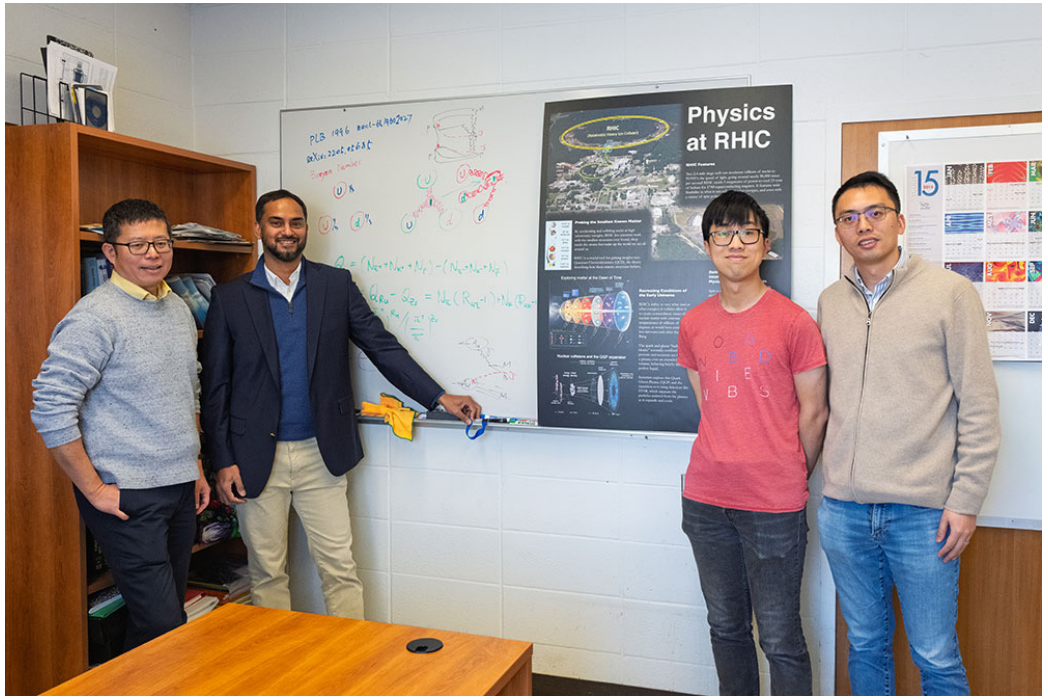

Zhangbu Xu (Kent SU, BNL), Prithwish Tribedy (BNL), Chun Yuen (Tommy) Tsang (ANL), and Rongrong Ma (BNL).

Zhangbu Xu; "Using data collected from different types of particle collisions at RHIC, our results suggest that the baryon number is not simply carried by individual quarks. Our findings strongly support the idea that baryon number is more favourably carried and transported by gluons, the particles that hold quarks together, when arranged in this special configuration."



Nicole Lewis (a STAR Coll. physicist at Rice University, began this study when she was a postdoc at BNL in 2020.

Baryon number conservation (BNC) ensures that the total number of baryons remains the same before and after collisions. The idea of BNC extends to the entire universe. Nicole Lewis: "Since the Big Bang, the number of p's and n's all together never changes as a function of time. The reasons for BNC are not well understood. It's one of the mysteries of the universe, related to why we have more matter than antimatter.

It's believed that the lifetime of a proton is longer than the lifespan of the universe. This allows atomic nuclei to form and be stable — which means matter, as we interact with it in the universe, can exist."

Tommy Tsang; In the STAR detector, we consistently see an excess of baryons coming out of the collisions perpendicular to the direction of the colliding beams, it is not surprising since our collisions start with matter."

"This baryon excess caused the STAR team to question the assumption that valence quarks are solely responsible for carrying the baryon number. To produce the observed excess, it would require all three quarks of a single colliding proton to "stop" and undergo a transformation from matter to energy and then back to matter in the centre of the detector, with all those newly created baryons spraying out away from the beamline."

Prithwish Tribedy: "at high energy, gluons within the proton split and multiply. With more and more gluons, each individual gluon, including those that make up the junction, carries less and less of the proton's overall momentum, while the valence quarks, also still present, continue to carry the bulk of the proton's forward oomph. That means, at the instant of the collision, the slower-moving three-pronged gluon structure should be easier to stop and transform into new particles than the speeding quarks.

Then, these entities immediately partner up with new particles: each quark might partner up with an antiquark to form two-quark particles called mesons, while the 3-pronged g-junction, like a Y shaped magnet, pulls in three new quarks from the vacuum to become a new baryon."

Rongrong Ma: "The higher the number of particles produced in a collision, the greater the observed excess of "midrapidity" baryons is, compared with what would be expected from the naive picture of quarks as the sole carriers of baryon number.

That so many of the baryons produced emerge perpendicular to the beamline provides compelling support for the existence of the baryon junction.

This research challenges the long-held idea that baryon number is simply divided among and carried by the three quarks. This new understanding reshapes how we think about the structure of matter and deepens our knowledge of the most fundamental element that is responsible for the universe in its current form."

https://www.bnl.gov/newsroom/news.php?a=122692

Baryon transport in photonuclear events

Studying baryon transport in γ+Au interactions provides another avenue for identifying the baryon number carrier.

The key to selecting γ+Au events is the asymmetric rapidity dependence of produced particles. Model calculations indicate that in such collisions a large amount of activity is expected in the Au-going direction due to nucleus fragmentation, while little-to-no activity is expected in the γ-going direction. Most importantly, a few neutrons from the fragmenting Au nucleus are expected to be traveling in the Au-going direction, while the γ-going side is expected to see one or two neutrons due to Coulomb excitations. In addition, the rapidity distribution of charged tracks around mid-rapidity is expected to be strongly asymmetric, with more particles in the Au-going direction.

[Science, August, 2026]

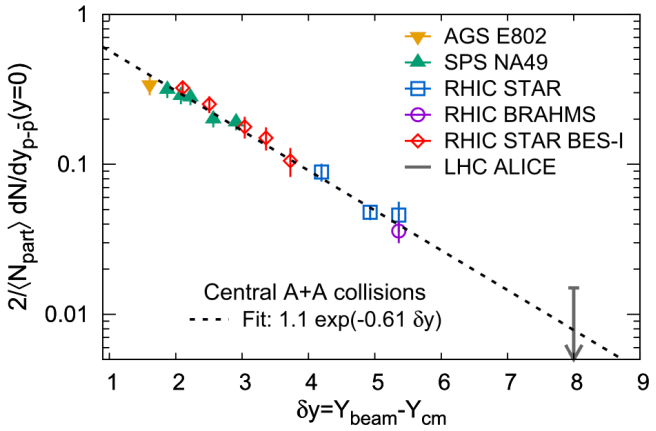

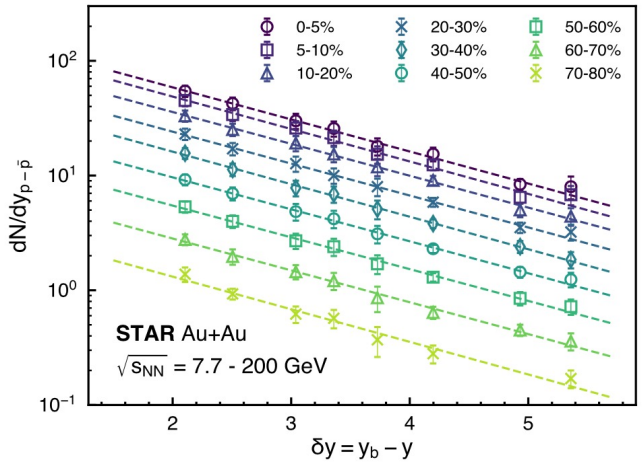

The dotted line is an exponential fit to the data:

$$\frac{dN_{p-\bar{p}}/dy}{N_{part}/2} = N_B \exp(-\alpha_B \delta y)$$

The assumption that baryon number could be carried by a NP Y-shaped topology of g-junctions, rather than by the valence quarks as in the QCD standard model is explained by the apparent substantial baryon excess in the mid-rapidity region that could not be adequately accounted for in most conventional models of quark and diquark transport. The y-density of net-baryons near mid-rapidity in g-junction concept indeed follows an exp drop with a slope of $\alpha_B = -0.61 \pm 0.03$ (AGS, SPS and RHIC) with the rapidity loss variable ($\sim\exp(-\alpha J(y-Y\text{beam}))$) determined by the Regge intercept of the g-junction (α_J). $\alpha_B = 0.61 \pm 0.03$ is qualitatively consistent with the value of $\alpha_J \simeq 0.42 - 1$ predicted by Regge theory.

[Science, August, 2026]

Test of baryon junction hypothesis with isobar collisions

In 2018, RHIC delivered a set of isobar collisions of $^{96}_{44}$Ru+ $^{96}_{44}$Ru and $^{96}_{40}$Zr+ $^{96}_{40}$Zr at the centre-of-mass energy per nucleon-nucleon pair of 200 GeV. If the total charge and baryon number are shifted differently from beam rapidity to mid-rapidity, it would indicate that baryon number is not correlated with the valence quarks and may likely be carried by the g-junction. The net charge here is defined based on the yields of pion, kaon and (anti)proton: $Q=(N\pi+ +NK+ +Np)-(N\pi- +NK- +N\,\bar{p})$.

The net-charge difference at mid-rapidity between the two collision systems $\Delta Q = Q^{Ru} - Q^{Zr}$. Use double ratios $R2_{\pi} = (N^{\mathrm{Ru}}_{\pi^+}/N^{\mathrm{Ru}}_{\pi^-})/(N^{\mathrm{Zr}}_{\pi^+}/N^{\mathrm{Zr}}_{\pi^-})$

$$= 1 + [(N^{\mathrm{Ru}}_{\pi^+}/N^{\mathrm{Ru}}_{\pi^-}) - (N^{\mathrm{Zr}}_{\pi^+}/N^{\mathrm{Zr}}_{\pi^-})]/(N^{\mathrm{Zr}}_{\pi^+}/N^{\mathrm{Zr}}_{\pi^-}),$$

$$\simeq 1 + (N^{\mathrm{Ru}}_{\pi^+}/N^{\mathrm{Ru}}_{\pi^-}) - (N^{\mathrm{Zr}}_{\pi^+}/N^{\mathrm{Zr}}_{\pi^-}),$$ expanding to first order in $(N\pi+ /N\pi- - 1)$.

[Science, August, 2026]

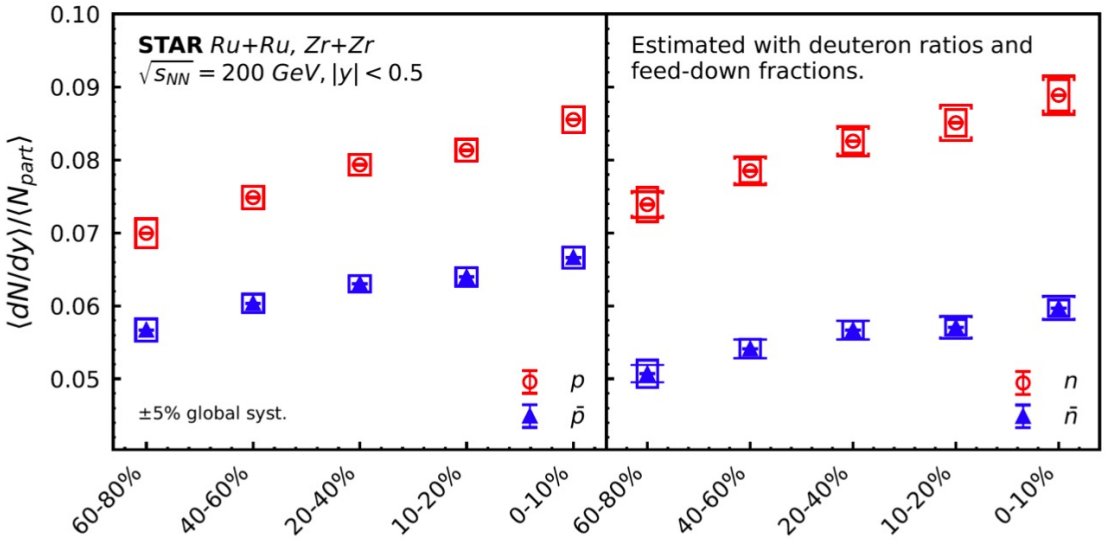

Yields of protons (left) and neutrons (right), as well as their antiparticles, as a function of centrality.

[Science, August, 2026]

Comparison between data and UrQMD:

Distributions of net-charge difference (left) and average net-baryon yield (right), scaled by ⟨*N*part⟩ between Ru+Ru and Zr+Zr at $\sqrt{s} = 200$ GeV.

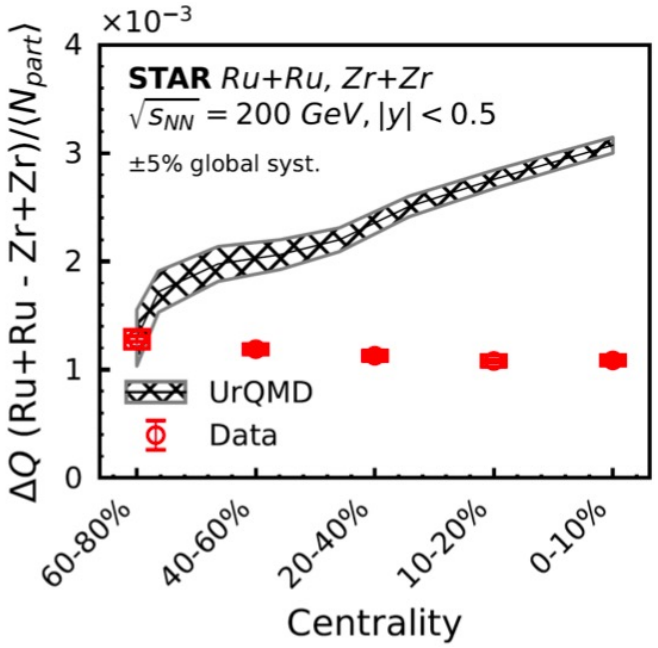

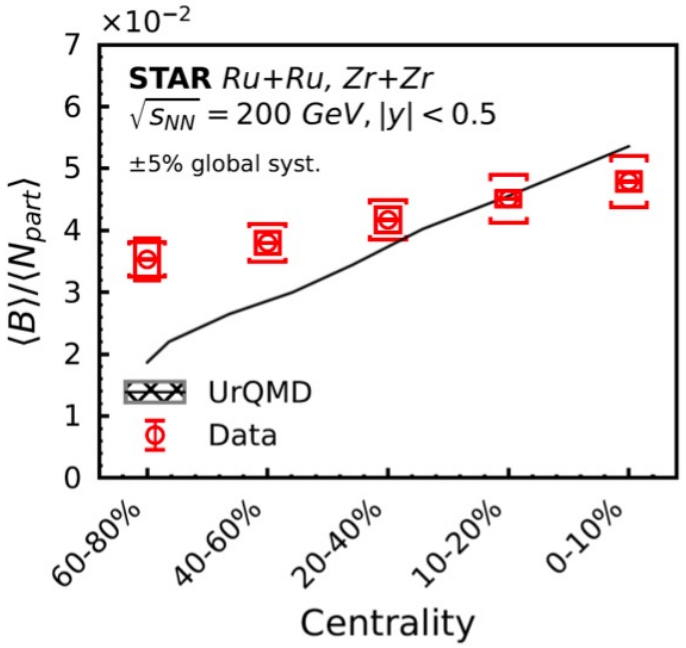

The following event generators and tunes are tested: PYTHIA 6.4 (default tune, Perugia0 (P0) tune, Perugia2012 (P12) tune), PYTHIA 8.1 (default tune), PYTHIA 8.3 (CR Mode 2) and HERWIG 7.2.

Table 1 Comparisons between data [7,9] and various event generators and tunes [12–15,21,22,63] for quantities related to baryon stopping, as well as model predictions for B/Q in 200 GeV $p+p$ collisions. Values in parentheses are for primordial production, while others are for inclusive production. Listed uncertainties are the quadrature sums of statistical and systematic uncertainties for data, and statistical only for simulations

	$\bar{p}/p$ (200 GeV, $\|y\| < 0.1$)	$\bar{p}/p$ (900 GeV, $\|y\| < 0.5$)	$\bar{p}/p$ (7 TeV, $\|y\| < 0.5$)	$dN_{p-\bar{p}}/dy$ slope	B/Q (200 GeV, $\|y\| < 0.5$)
Data	0.819 ± 0.047	(0.957 ± 0.015)	(0.991 ± 0.015)	0.61 ± 0.03	–
PYTHIA 6.4	0.928 ± 0.008	0.966 ± 0.003 (0.961 ± 0.004)	0.986 ± 0.003 (0.984 ± 0.003)	0.86 ± 0.05	0.300 ± 0.016
PYTHIA 6.4 (P0)	0.851 ± 0.008	0.948 ± 0.004 (0.946 ± 0.004)	0.987 ± 0.003 (0.985 ± 0.004)	0.76 ± 0.03	0.879 ± 0.049
PYTHIA 6.4 (P12)	0.815 ± 0.007	0.912 ± 0.003 (0.911 ± 0.004)	0.966 ± 0.003 (0.968 ± 0.003)	0.38 ± 0.02	1.519 ± 0.095
PYTHIA 8.1	0.913 ± 0.008	0.968 ± 0.003 (0.964 ± 0.004)	0.989 ± 0.003 (0.987 ± 0.003)	0.89 ± 0.04	0.567 ± 0.032
PYTHIA 8.3 (CR Mode 2)	0.837 ± 0.006	0.928 ± 0.003 (0.926 ± 0.003)	0.981 ± 0.002 (0.982 ± 0.003)	0.73 ± 0.02	0.986 ± 0.033
HERWIG 7.2	0.858 ± 0.005	0.969 ± 0.002 (0.914 ± 0.003)	1.028 ± 0.002 (1.006 ± 0.002)	1.17 ± 0.04	0.558 ± 0.014

Semi-inclusive γ + *p*/A at RHIC kinematics provide an opportunity to search for the signatures of the g-junction and to shed light onto the mechanisms of observed baryon excess in the mid-rapidity region in HIC. Such measurements can be further validated in A+A collisions at the LHC and *e* + *p*/A collisions at the EIC. [Eur. Phys. J. C (2024) 84:590]

[Science, August, 2026]

Differential Measurements of ϕ-meson Global Spin Alignment and Off-diagonal Spin Density Matrix Elements in Au+Au Collisions at STAR

Zhenyu Ye for STAR collaboration

Lawrence Berkeley National Laboratory

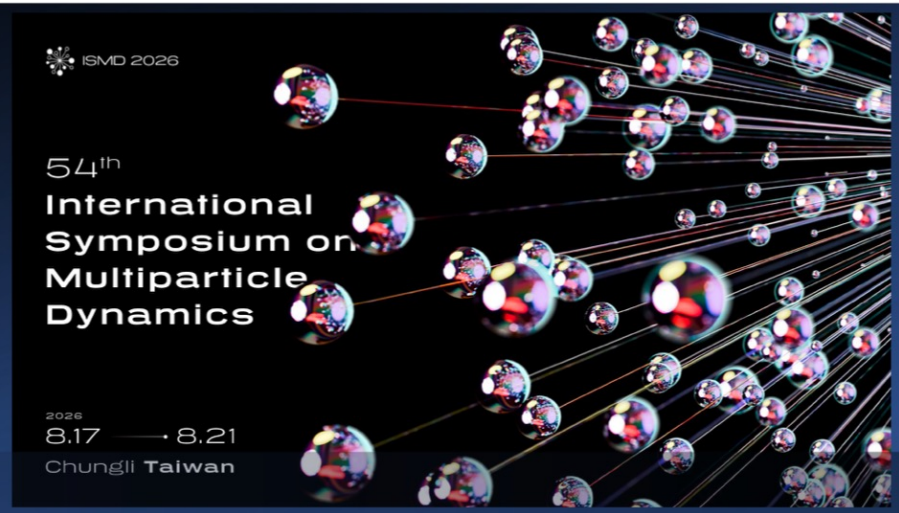

Orbital Angular Momentum in Heavy-Ion Collisions

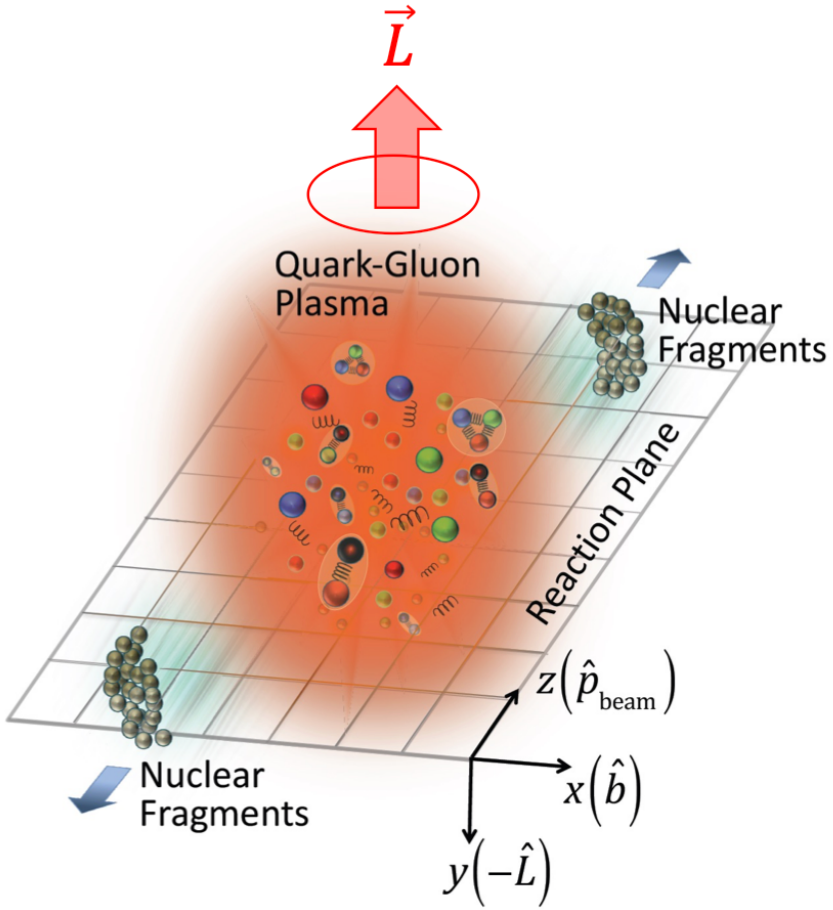

- The collision system in a non-central ultra-relativistic heavy-ion collision carries a large orbital angular momentum (OAM) perpendicular to the reaction plane (RP) formed by the impact parameter and beam direction.
- Part of the OAM is transferred to the QGP in the form of fluid vorticity, which can polarize the quark spin along the OAM direction through spin-orbit coupling.
- The quark spin polarization can be studied through global polarization of hyperons or global spin alignment of vector mesons.

Global spin polarization in heavy ion collisions

$$\frac{dN}{d\cos\theta^*} = \frac{1}{2}\left(1 + \alpha_H |\vec{\mathcal{P}}_H| \cos\theta^*\right)$$

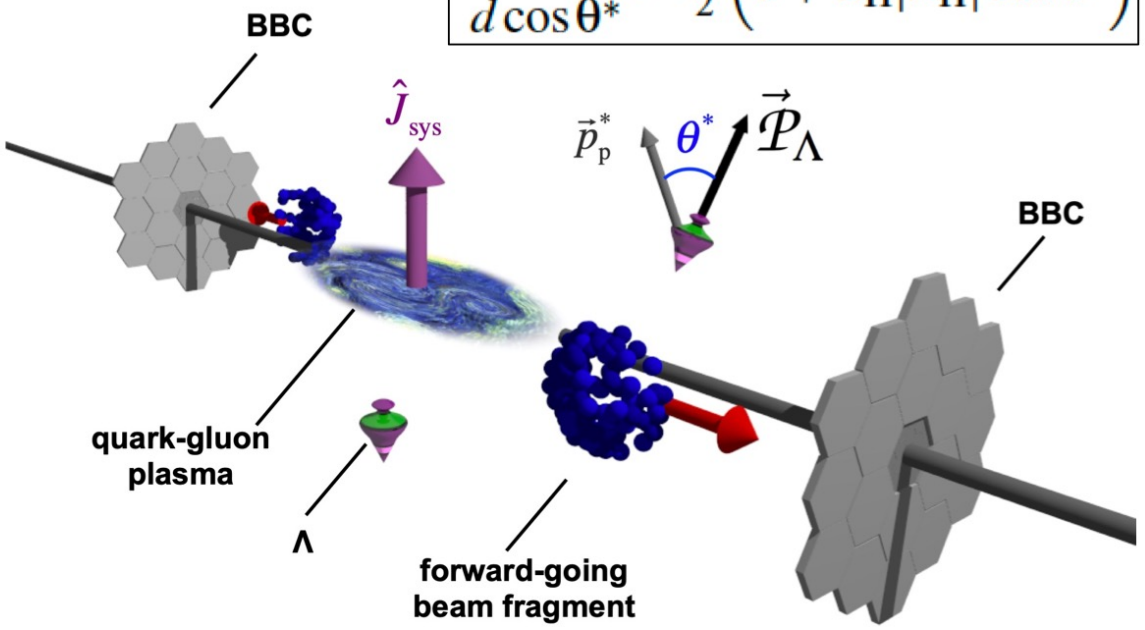

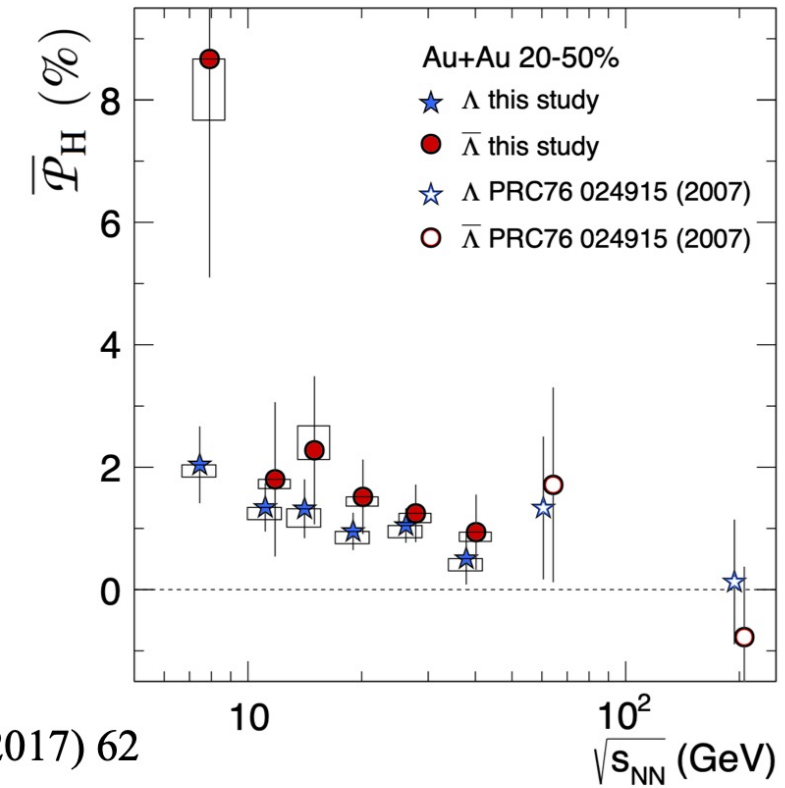

[1] STAR Coll., **Nature** 548 (2017) 62

The first discovery of global spin polarization P_H of Λ-hyperon in Au+Au collisions by STAR in RHIC Beam-Energy Scan Phase-I (BES-I) suggests the creation of most vortical system with $\omega = (9 \pm 1)\times 10^{21} s^{-1}$ [1]

Vector meson spin density matrix

The spin density matrix elements (SDMEs) of a spin-1 vector meson:

- The diagonal elements indicate the probability in the spin-m state (m=-1,0,1)
- The off-diagonal elements indicate quantum coherences among 3 spin states
- $\rho_{00} \neq 1/3$ indicates spin alignment of vector meson

$$\rho = \begin{pmatrix} \rho_{-1-1} & \rho_{-1,0} & \rho_{-11} \\ \rho_{0-1} & \rho_{00} & \rho_{01} \\ \rho_{1-1} & \rho_{10} & \rho_{11} \end{pmatrix}$$

For a 2-body decay of a vector meson into pseudo-scalar mesons (e.g. $\phi \rightarrow K^+K^-$), the angular distribution of a daughter in the vector meson's rest frame is:

$$\begin{aligned} \frac{d^2N}{d\cos\theta^* d\beta} = \frac{3}{8\pi}\big[& (1-\rho_{00}) + (3\rho_{00}-1)\cos^2\theta^* \\ & - \sqrt{2}\mathrm{Re}\,(\rho_{10}-\rho_{0-1})\sin 2\theta^* \cos\beta \\ & + \sqrt{2}\mathrm{Im}\,(\rho_{10}-\rho_{0-1})\sin 2\theta^* \sin\beta \\ & - 2\mathrm{Re}\,(\rho_{1-1})\sin^2\theta^* \cos 2\beta \\ & + 2\mathrm{Im}\,(\rho_{1-1})\sin^2\theta^* \sin 2\beta\big], \end{aligned}$$

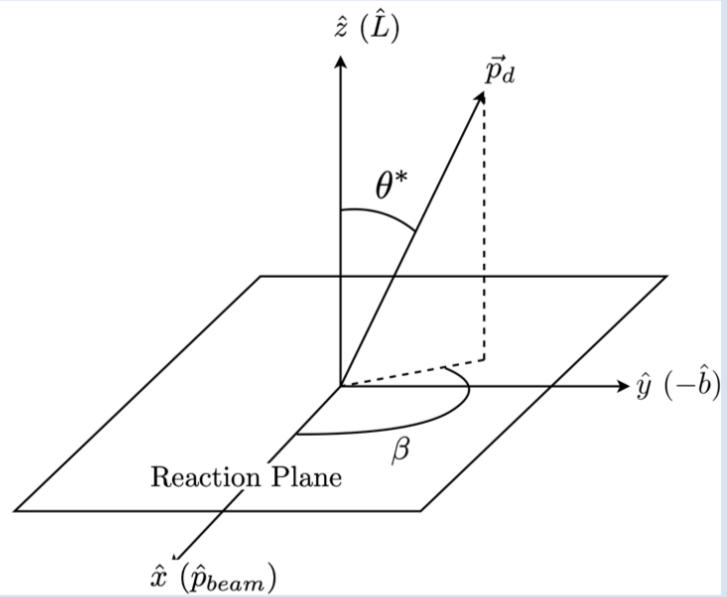

Global spin alignment in heavy ion collisions

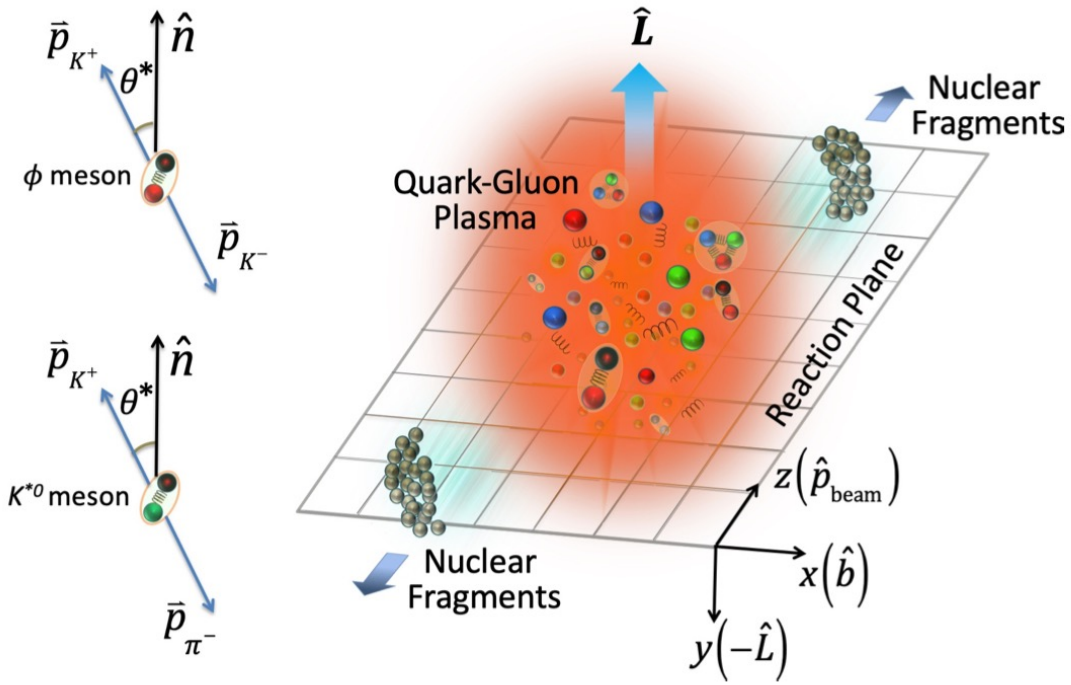

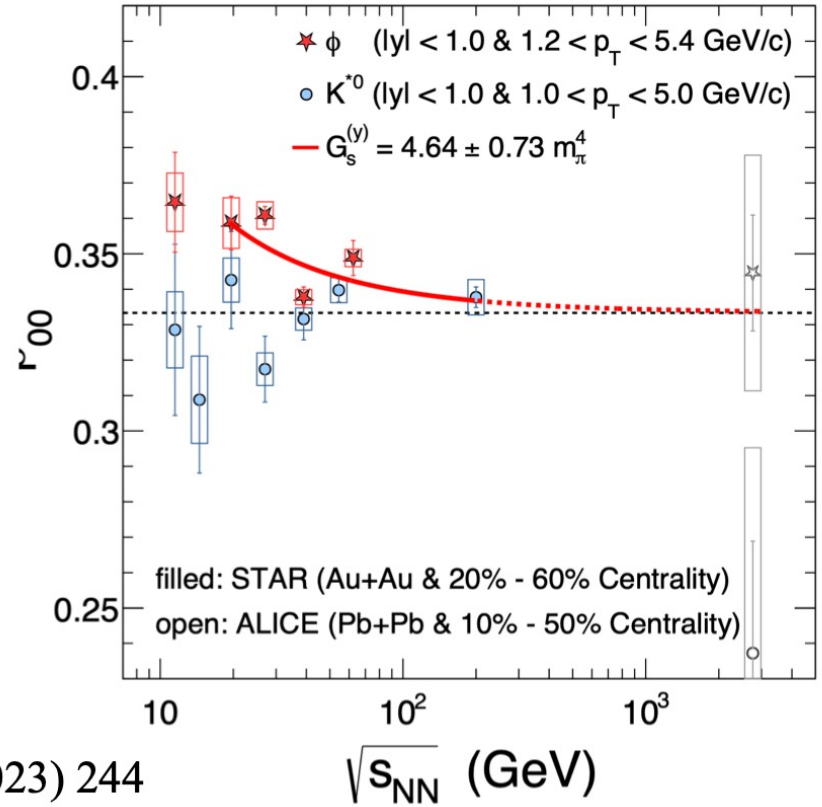

[2] STAR Coll., **Nature** 614 (2023) 244

The observed pattern of $\phi(s\bar{s})$- and $K^{0*}(d\bar{s})$-meson ρ_{00} and the magnitudes of ϕ-meson ρ_{00} and Λ-hyperon P_H in Au+Au collisions by STAR in BES-I can not be explained by conventional mechanisms [2].

The global spin alignment for ϕ is unexpectedly large, while that for K^{*0} is consistent with zero. The observed spin-alignment pattern and magnitude for the ϕ cannot be explained by conventional mechanisms, while a model with a connection to strong force fields, based on Kadanoff- Baym equations [a set of coupled integro-differential equations in time that describe the non-equilibrium evolution of two-time Green's functions in interacting quantum many-body systems] in the closed-time-path formalism. This connection, if fully established, will open a potential new avenue for studying the behaviour of strong force fields. The key observation is that there is correlation inside the ϕ meson wave function between the ϕ field that polarizes the strange quark and that polarizes the strange antiquark. This is reflected by the fact that the contributions to ρ_{00} are all in squares of fields which are nonvanishing even if the fields may strongly fluctuate in space-time.

Global spin polarization and alignment

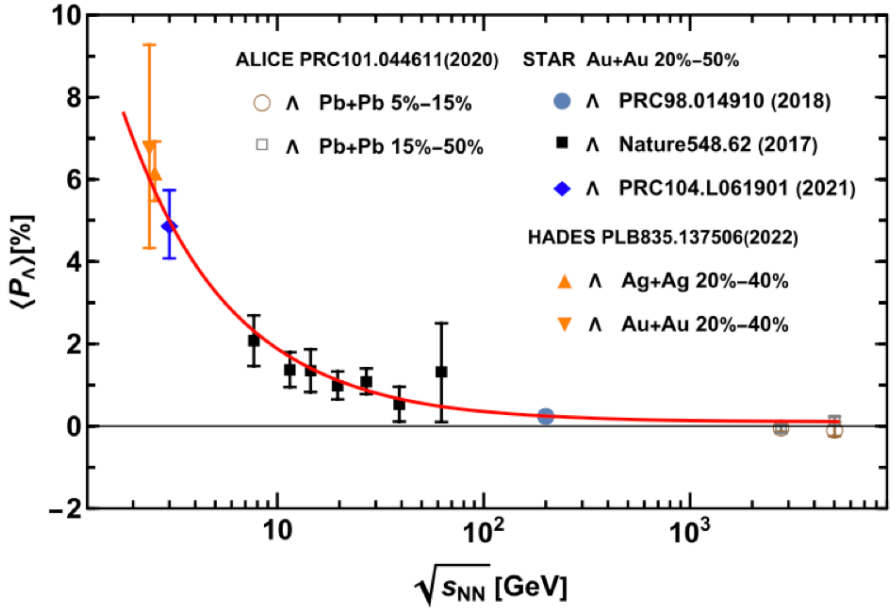

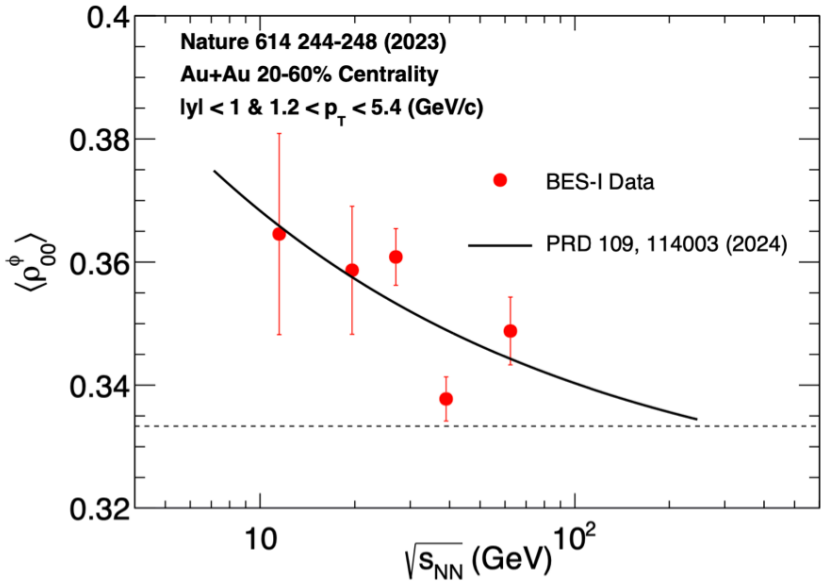

Fits parameterized by:

$$\langle P_\Lambda \rangle \sim \langle P_s \rangle,$$

$$\langle \rho_{00}^{\phi} \rangle \sim \frac{1 - \bar{c}_{zz;\phi}^{(s\bar{s})} - \langle P_s \rangle^2}{3 + \bar{c}_{zz;\phi}^{(s\bar{s})} + \langle P_s \rangle^2},$$

$$\langle P_s \rangle = a s_{NN}^{-b} + c,$$

$$\bar{c}_{zz;\phi}^{(s\bar{s})} = e s_{NN}^{-f} + d.$$

[3] J.-P. Lv, Z.-H. Yu, Z.-T. Liang, Q. Wang, and X.-N. Wang, **Phys. Rev. D** 109 (2024) 114003

A quark recombination model for hadronization in heavy-ion collisions can simultaneously describe the observed Λ-hyperon P_H and ϕ-meson ρ_{00} signals by introducing local strange-quark-antiquark spin correlations [3].

SDMEs, quark spin polarizations and correlations

(Spin density matrix elements)

- **Relations of vector meson SDMEs to quark and anti-quark polarizations, $P_{q_1 i}$ and $P_{\bar{q}_2 j}$, and quark-antiquark spin correlations, $c_{ij}^{(q_1\bar{q}_2)}$ [3] :**

$$C_V = 3 + c_{xx}^{(q_1\bar{q}_2)} + c_{yy}^{(q_1\bar{q}_2)} + c_{zz}^{(q_1\bar{q}_2)} + P_{q_1 x}P_{\bar{q}_2 x} + P_{q_1 y}P_{\bar{q}_2 y} + P_{q_1 z}P_{\bar{q}_2 z}$$

$$\rho_{00} = \frac{1}{C_V}\left[1 + c_{xx}^{(q_1\bar{q}_2)} + c_{yy}^{(q_1\bar{q}_2)} - c_{zz}^{(q_1\bar{q}_2)} + P_{q_1 x}P_{\bar{q}_2 x} + P_{q_1 y}P_{\bar{q}_2 y} - P_{q_1 z}P_{\bar{q}_2 z}\right]$$

$$\mathrm{Re}(\rho_{10} - \rho_{0-1}) = \frac{\sqrt{2}}{C_V}\left[c_{xz}^{(q_1\bar{q}_2)} + c_{zx}^{(q_1\bar{q}_2)} + P_{q_1 x}P_{\bar{q}_2 z} + P_{q_1 z}P_{\bar{q}_2 x}\right]$$

$$\mathrm{Im}(\rho_{10} - \rho_{0-1}) = -\frac{\sqrt{2}}{C_V}\left[c_{yz}^{(q_1\bar{q}_2)} + c_{zy}^{(q_1\bar{q}_2)} + P_{q_1 y}P_{\bar{q}_2 z} + P_{q_1 z}P_{\bar{q}_2 y}\right]$$

$$\mathrm{Re}(\rho_{1-1}) = \frac{1}{C_V}\left[c_{xx}^{(q_1\bar{q}_2)} - c_{yy}^{(q_1\bar{q}_2)} + P_{q_1 x}P_{\bar{q}_2 x} - P_{q_1 y}P_{\bar{q}_2 y}\right]$$

$$\mathrm{Im}(\rho_{1-1}) = -\frac{1}{C_V}\left[c_{xy}^{(q_1\bar{q}_2)} + c_{yx}^{(q_1\bar{q}_2)} + P_{q_1 x}P_{\bar{q}_2 y} + P_{q_1 y}P_{\bar{q}_2 x}\right]$$

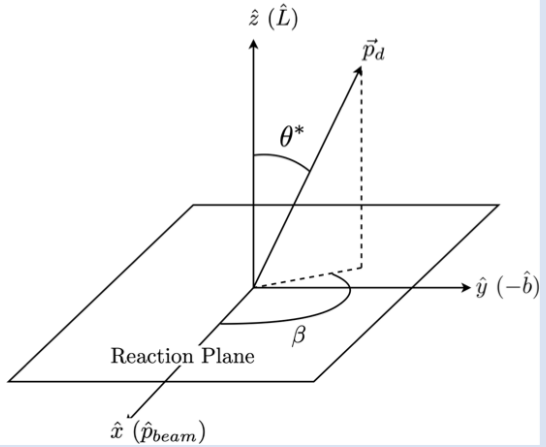

- **It will be interesting to measure off-diagonal SDMEs.**

[3] J.-P. Lv, Z.-H. Yu, Z.-T. Liang, Q. Wang, and X.-N. Wang, **Phys. Rev. D** 109 (2024) 114003

1D vs 2D methods to extract SDMEs

- **Previous 1D method integrates over β [4]:**

$$\frac{dN}{dcos\theta^*} = \frac{3}{4}[(1-\rho_{00}) + (3\rho_{00}-1)cos^2\theta^*]$$

- **2D method considers both θ^* and β distributions [4]:**

$$\begin{aligned}\frac{d^2N}{d\cos\theta^* d\beta} = \frac{3}{8\pi}\big[&(1-\rho_{00}) + (3\rho_{00}-1)\cos^2\theta^* \\ &- \sqrt{2}\mathrm{Re}\,(\rho_{10}-\rho_{0-1})\sin 2\theta^*\cos\beta \\ &+ \sqrt{2}\mathrm{Im}\,(\rho_{10}-\rho_{0-1})\sin 2\theta^*\sin\beta \\ &- 2\mathrm{Re}\,(\rho_{1-1})\sin^2\theta^*\cos 2\beta \\ &+ 2\mathrm{Im}\,(\rho_{1-1})\sin^2\theta^*\sin 2\beta\big],\end{aligned}$$

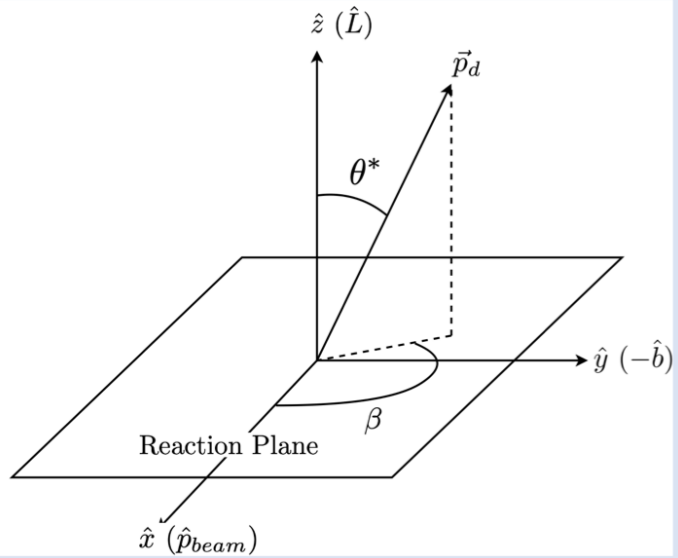

[4] G. Wilks, X, Sun, Z. Ye, **Phys. Rev. C** 113 (2026) 044911

ϕ-meson yields extraction

Raw Yield Extraction

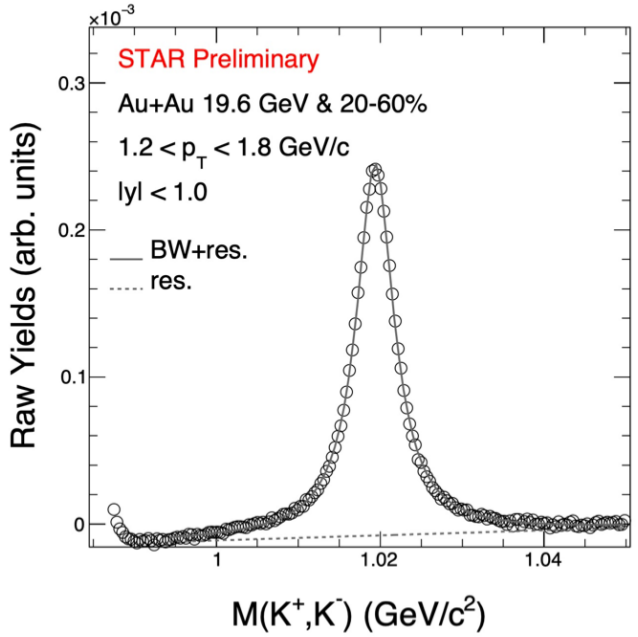

Corrected Yields

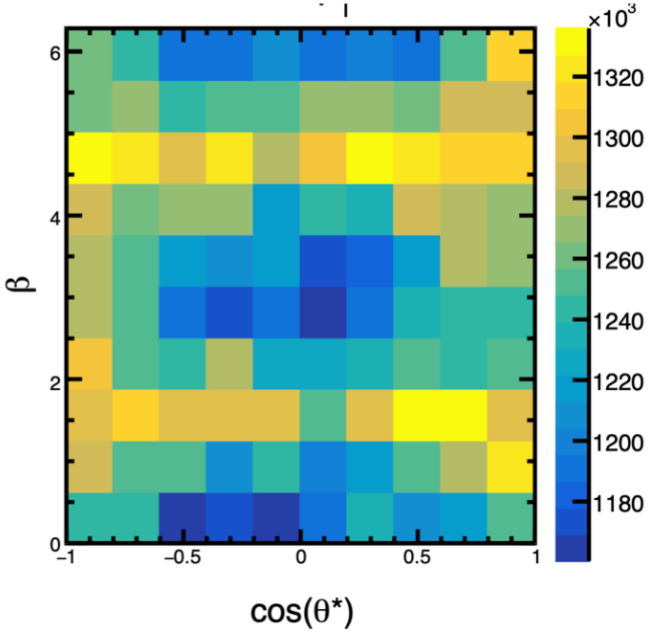

- Using mixed events to estimate background and extract ϕ-meson yields in 10 cosθ* bin x 10 β bins.
- Fit invariant mass distribution with Breit-Wigner + 1st polynomial:

$$\frac{dN}{dM(K^+K^-)} = \frac{1}{2\pi}\frac{AF}{(m-m_\phi)+(\Gamma/2)^2} + poly1(m-m_\phi)$$

- Yields vs. (cosθ*, β) are corrected for the detector acceptance, tracking and PID related efficiencies.

ϕ-meson SDME extraction

Au+Au 19.6 GeV
20-60% Centrality
$1.2 < p_T < 1.8$ GeV/c, $|y| < 1$

Corrected yields from data

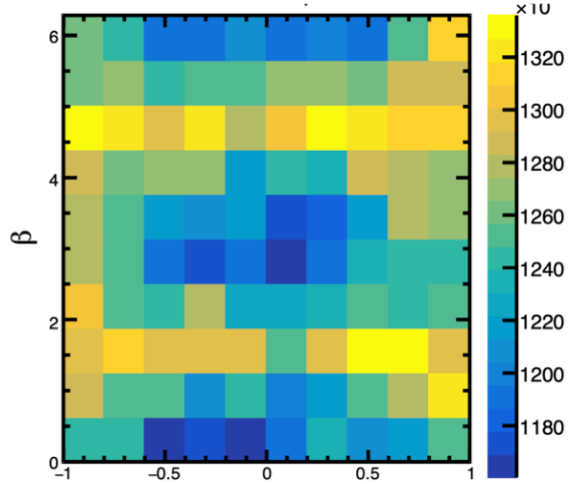

Fit to corrected yields

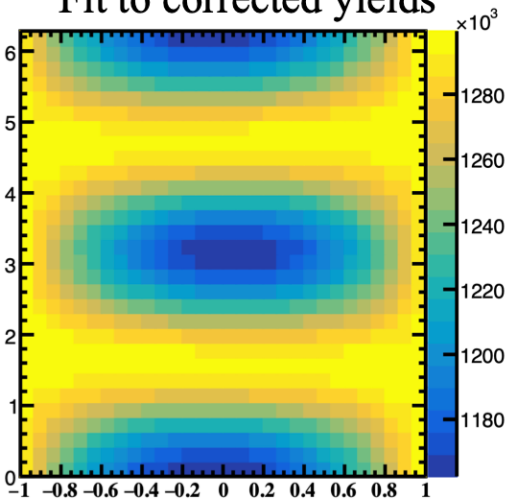

1D projections

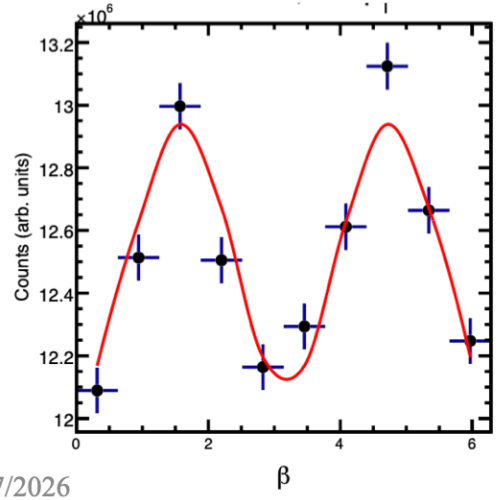

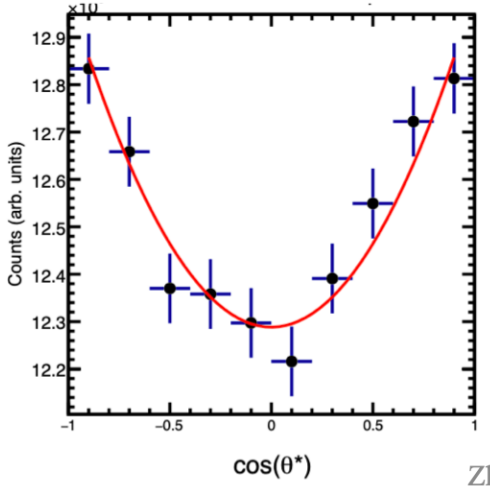

- **Fit data to Eq (1) to extract SDMES relative to the mth order EP.**

$$\frac{d^2N}{d\cos\theta^{*\Psi_m} d\beta^{\Psi_m}} = N_0 \Big[1 - \rho_{00}^{\Psi_m} + \left(3\rho_{00}^{\Psi_m} - 1\right)\cos^2\theta^{*\Psi_m} - \sqrt{2}\mathrm{Re}\left(\rho_{10}^{\Psi_m} - \rho_{0-1}^{\Psi_m}\right)\sin 2\theta^{*\Psi_m}\cos\beta^{\Psi_m} + \sqrt{2}\mathrm{Im}\left(\rho_{10}^{\Psi_m} - \rho_{0-1}^{\Psi_m}\right)\sin 2\theta^{*\Psi_m}\sin\beta^{\Psi_m} - 2\mathrm{Re}\left(\rho_{1-1}^{\Psi_m}\right)\sin^2\theta^{*\Psi_m}\cos 2\beta^{\Psi_m} + 2\mathrm{Im}\left(\rho_{1-1}^{\Psi_m}\right)\sin^2\theta^{*\Psi_m}\sin 2\beta^{\Psi_m} \Big] \quad (1)$$

- **Apply event plane corrections [4].**

[4] G. Wilks, X, Sun, Z. Ye, **Phys. Rev. C** 113 (2026) 044911

ϕ-meson off-diagonal SDMEs

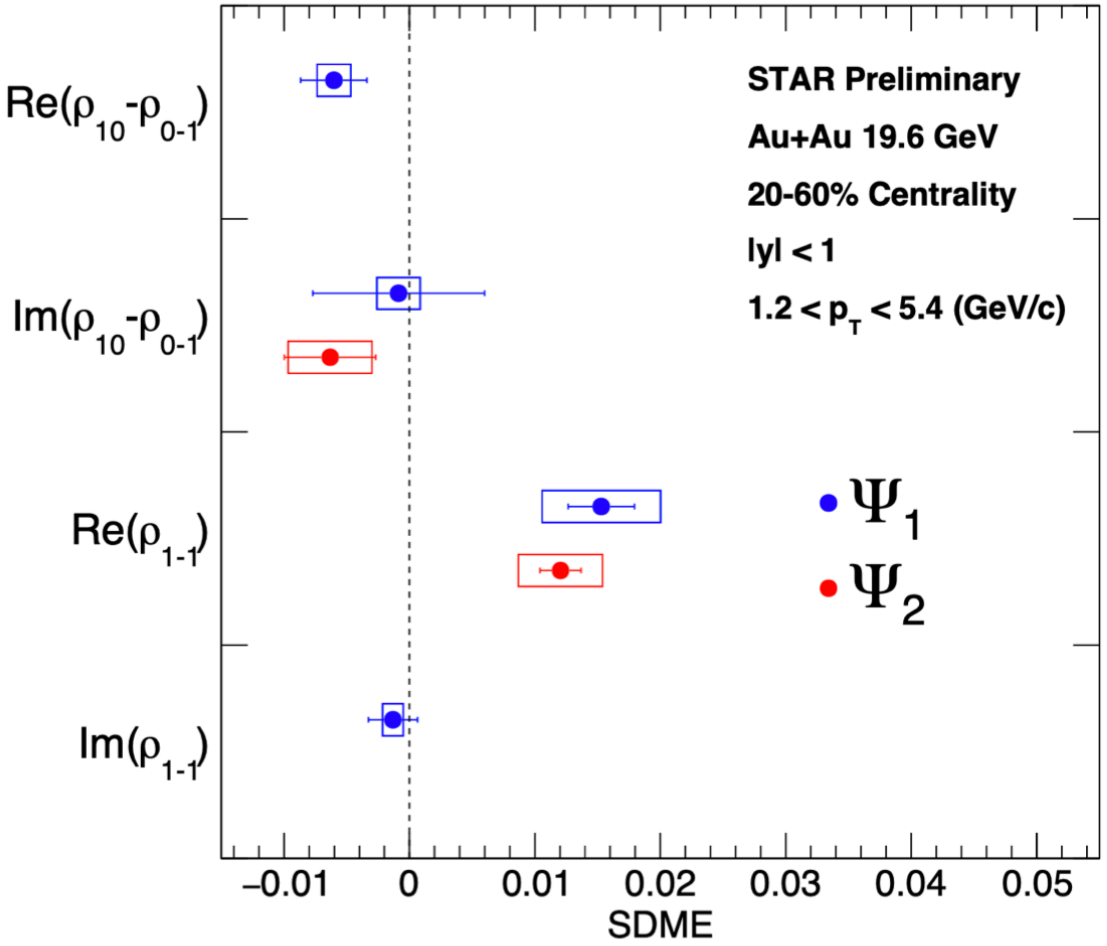

SDME	Ψ_1	Ψ_2
$\mathrm{Re}(\rho_{10} - \rho_{0-1}) < 0$	2σ	N/A
$\mathrm{Im}(\rho_{10} - \rho_{0-1}) \approx 0$	-0.2σ	-1.2σ
$\mathrm{Re}(\rho_{1-1}) > 0$	2.8σ	**3.2σ**
$\mathrm{Im}(\rho_{1-1}) \approx 0$	-0.6σ	N/A

Summary

- **Confirmation of $\rho_{00} > 1/3$ with 5.2σ significance in Au+Au collisions at RHIC.**
- First measurements of ϕ-meson off-diagonal SDMEs.
  - **First evidence of Re(ρ_{1-1}) > 0 with 3.2σ significance.**
  - All other off-diagonal terms are consistent with 0.
- The results suggest non-zero strange-quark-antiquark spin correlations [3].

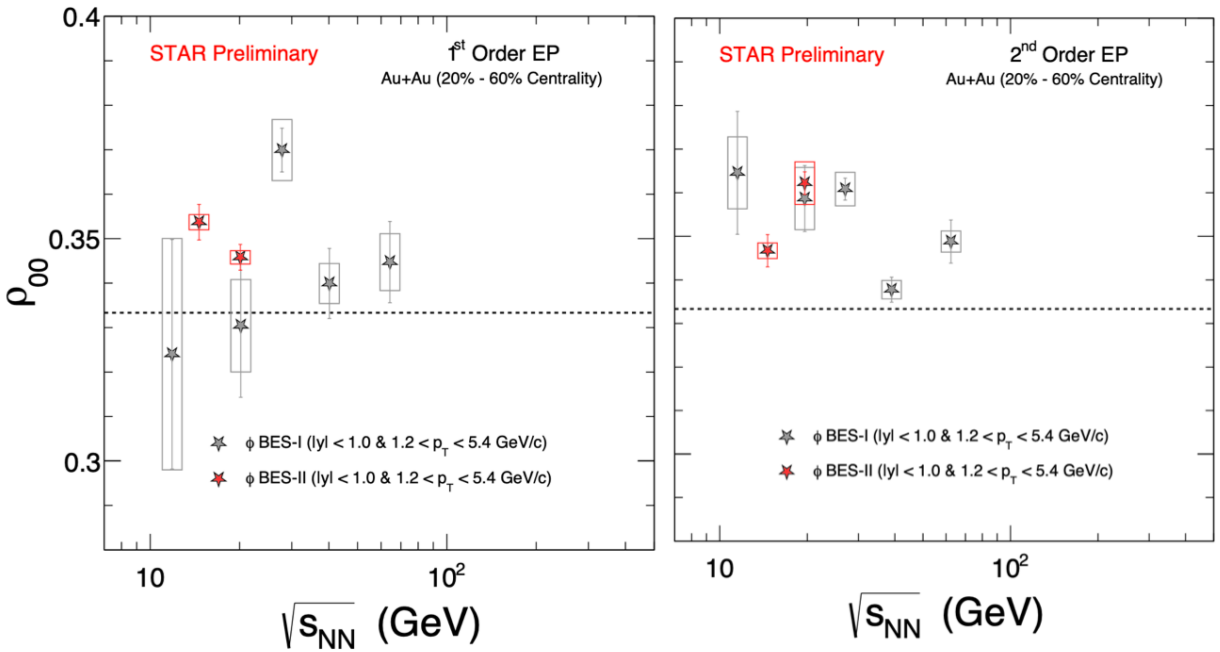

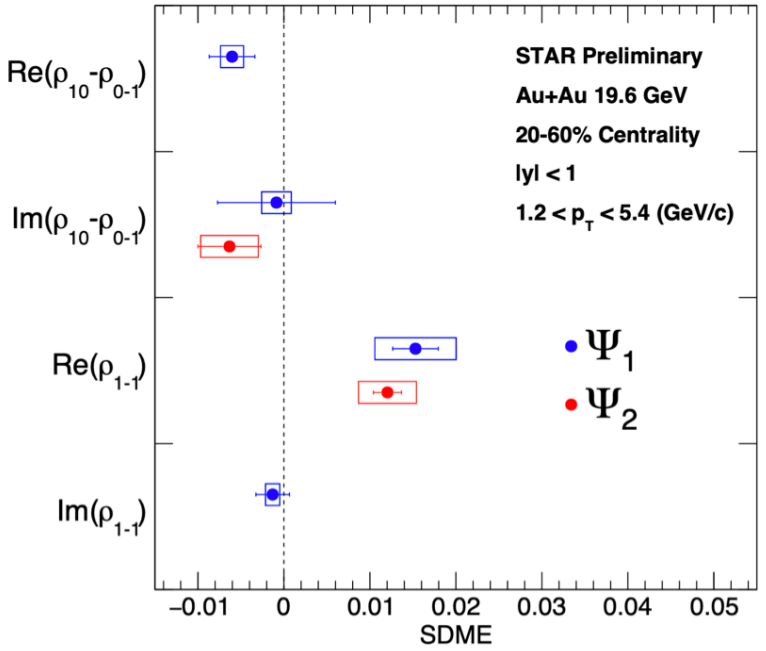

Longitudinal decorrelations in Xe+Xe collisions

Koichi Murase

The University of Osaka

Including ongoing works with

A. Sakai, Y. Nara

Nagasaki Institute of Applied Science, Akita International University

E. Miyoshi, A. Cendikia, C. Nonaka

Hiroshima University

Computational resources

SQUID

Supercomputer for Quest to Unsolved Interdisciplinary Datascience

A part of calculations is performed within **K25A04** on the supercomputer **SQUID** in the D3 Center of the University of Osaka

Outline

- Introduction
- Longitudinal flow decorrelations in Xe+Xe
- Model and results (ongoing study)

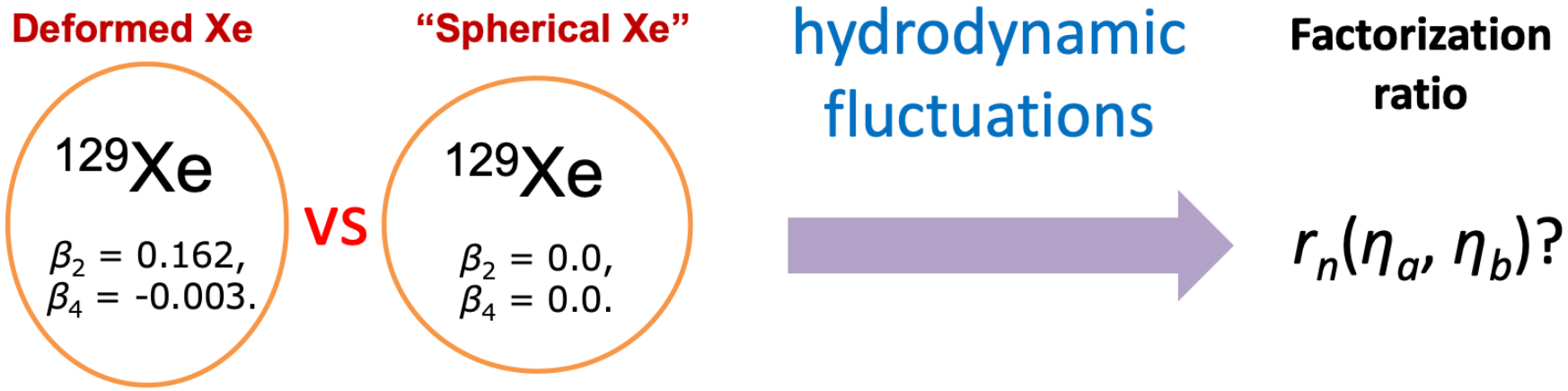

High-energy heavy-ion collisions (HIC)

Colliders



LHC $\sqrt{s_{NN}}$ ~ 2.76—5.44 TeV

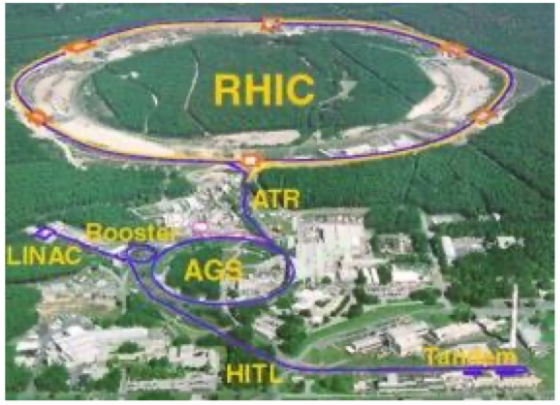

RHIC $\sqrt{s_{NN}}$ ~ 3.0—200 GeV

Colliding nuclei

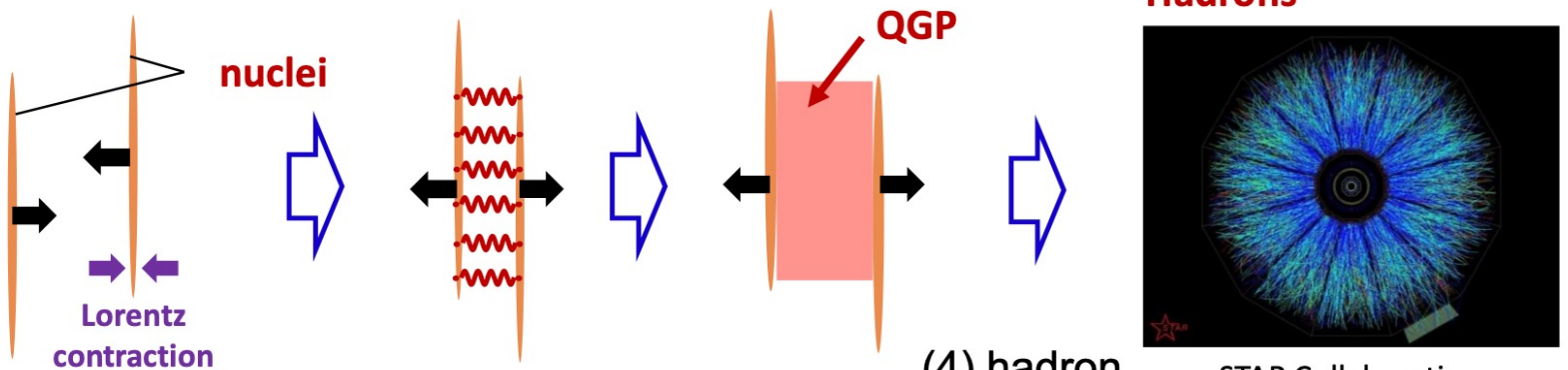

Various collision systems

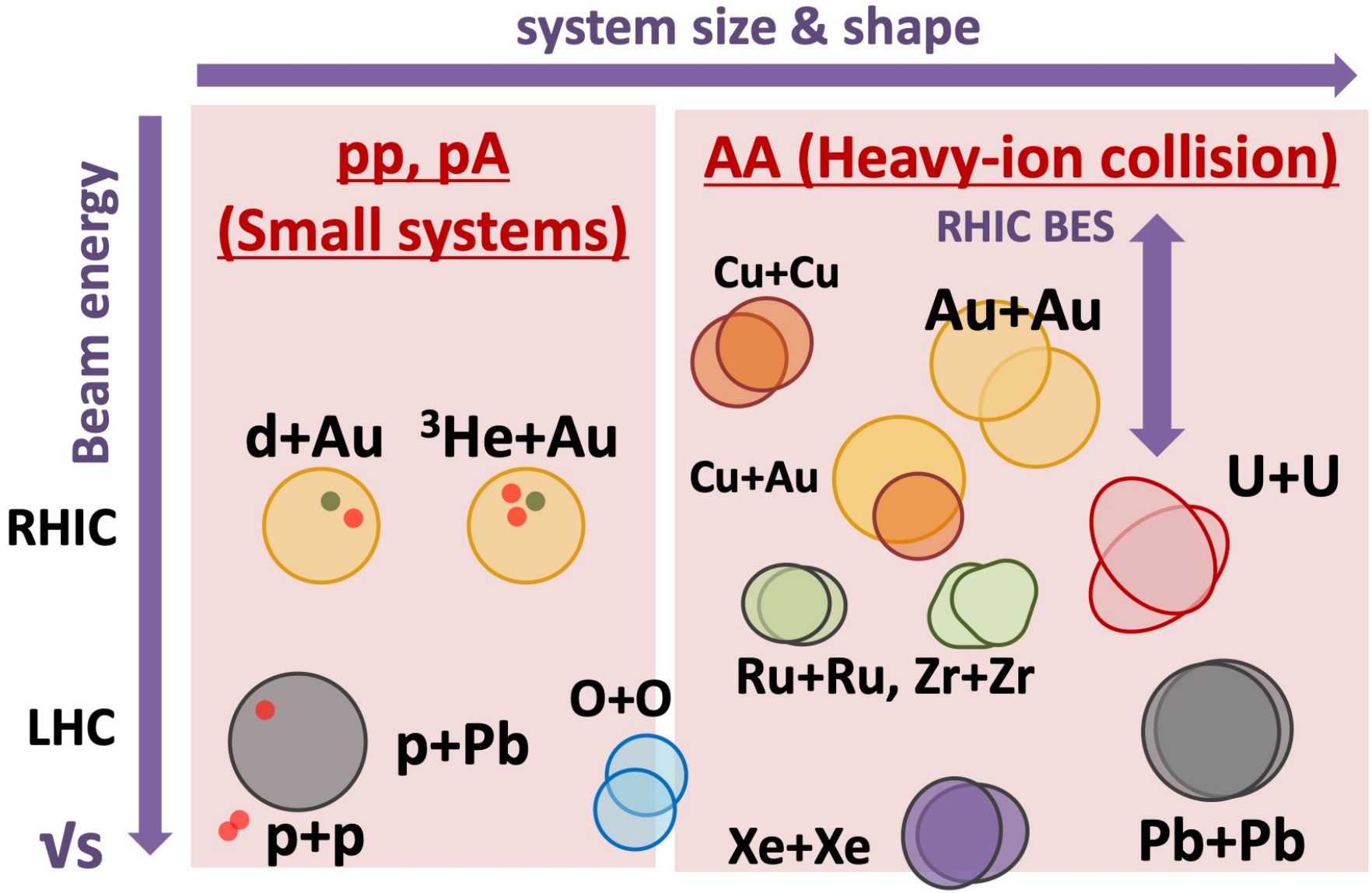

Nuclear shapes/structures in HIC

- $^{238}U+^{238}U$ vs $^{197}Au+^{197}Au$, $^{63}Cu+^{197}Au$
  @ $\sqrt{s}$ = 193-200 GeV
  A. Goldschmidt, Z. Qiu, U. Heinz (2012, 2015), etc.

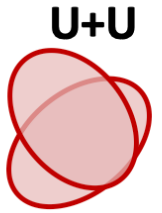

- $^{96}Zr+^{96}Zr$ (Z=40) vs $^{96}Ru+^{96}Ru$ (Z=44) "**Isobar**"
  @ $\sqrt{s}$ = 7.7-200 GeV
  Opposite effect as CME,
  STAR (2021, 2022), etc.



- $^{129}Xe+^{129}Xe$ @ $\sqrt{s}$ = 5.44 TeV
  vs $^{208}Pb+^{208}Pb$ @ $\sqrt{s}$ = 5.02 TeV
  A. Behera, M. Nie, J. Jia (2020), ATLAS (2021),
  H. Mäntysaari et al (2024), etc.

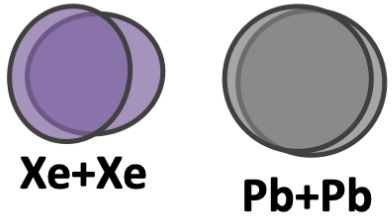

- $^{16}O+^{16}O$, p+O @ $\sqrt{s}$ = 200 GeV, 7 TeV
- $^{20}Ne+^{20}Ne$, …

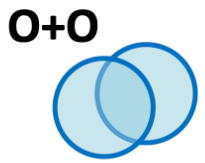

Key observables: v_n, [p_T], … ← Nucleon distribution

v_n "flow": Final momentum anisotropy of hadrons (measured in exp)

Matter response (hydro/hadron)

$$\frac{1}{N'}\frac{\mathrm{d}N'}{\mathrm{d}\phi} = \frac{1}{2\pi}\left[1 + 2\sum_{n=1}^{\infty} v_n \cos n(\phi - \Psi_n)\right].$$

ε_n: Initial spatial anisotropy in hydro initial condition

$$\epsilon_n e^{i\Phi_n} = -\int d^2x_T e^{in\phi_s} w_n(r_T)\rho(\boldsymbol{x}_T) \Big/ \int d^2x_T w_n(r_T)\phi(\boldsymbol{x}_T),$$

Fourier expansion wrt spatial φ of transverse initial entropy density $\rho(x)$.

$\rho(x)$: Initial entropy/energy density, etc.

[$w(r) = r^2$ is weight]

Initial model

Nucleon distribution inside nuclei

Size

1-body nucleon (n/p) distribution (Woods-Saxon, etc.)

Shape (deformation)

***A*-body wavefunc**

More structures…

Nucleon-nucleon correlation

Summary

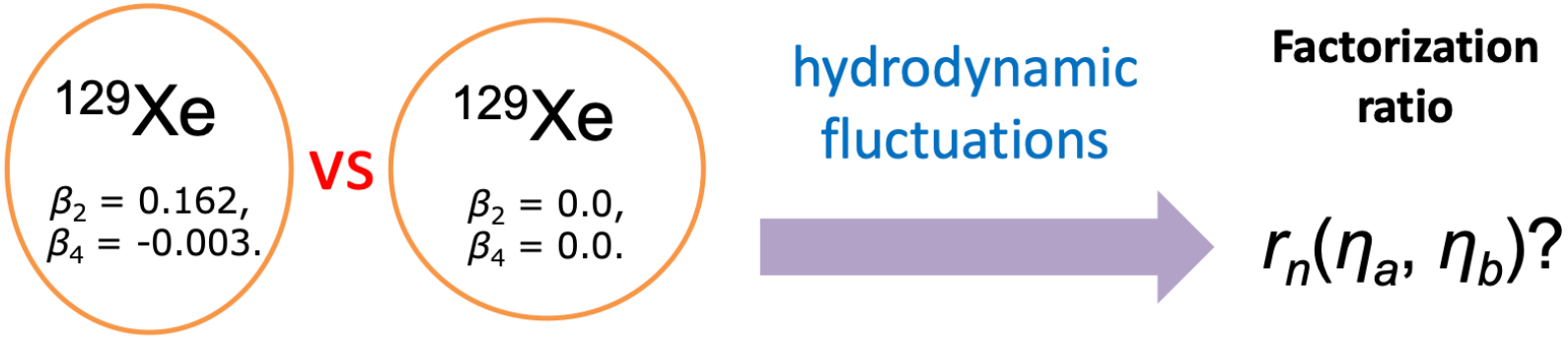

Interplay of hydrodynamic fluctuations and deformation in Xe+Xe

- HF causes smaller longitudinal decorrelation at central collisions w/ larger ε_2 by deformation.
- ESE shows that larger q_2 suppresses decorrelation (smaller slope F_2)

Outlook

- Analysis in ultra central events (tip-tip, body-body) w/ large stat.
- Comparison with Pb+Pb, initial longitudinal fluct, rescattering, no HF
- [p_T]-decorrelations $r_{pT}(\eta_a, \eta_b)$, triaxiality, Bayesian analysis

Collective signatures in thermal photons and initial fluctuations of EM-fields in event-by-event 3+1D relativistic resistive MHD

2026/08/17

Talk by: Nicholas J. Benoit (PostDoc at Academia Sinica)

Collaborators: T. Miyoshi (HU), C. Nonaka (HU, SKCM2), A. Sakai (Nagasaki Inst. of App. Sci.), and H. R. Takahashi (KU)

Paper: Phys. Rev. C 112, 024911 + writing in-progress

Summary of our work

We present the first model with:

1) initial event-by-event fields

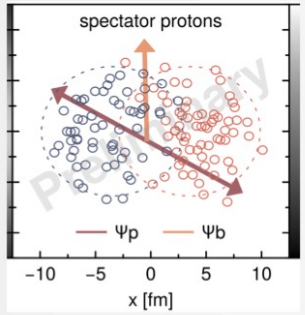

2) Relativistic Resistive MagnetoHydrodynamics

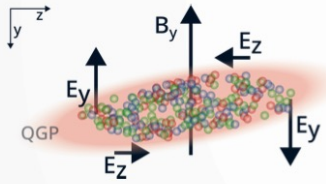

3) thermal photons with EM field corrections



=

EM fields and Prompt + thermal photons

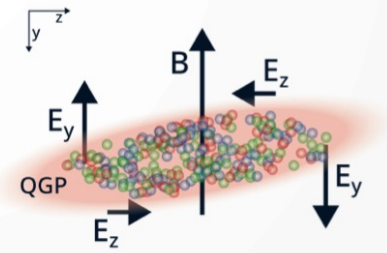

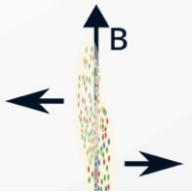

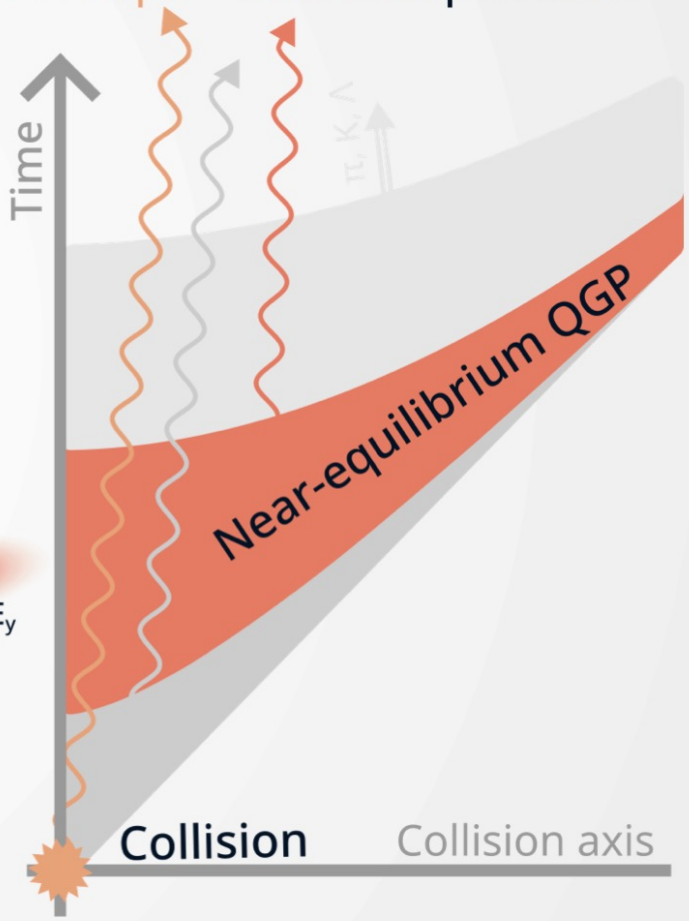

Direct photon puzzle

Motivation for iebe-RRMHD:

~10 years models successfully applied to hadron collectivity can not fully explain photon flow or yield

Proposed solution 1: Model all the photon stages

Multi Messenger Model

J. Churchill, L. Yan, S. Jeon, and C. Gale
Phys. Rev. C 103, 024904 (2021)

Proposed solution 2: Include other exotic sources

Recombination

H. Fujii, K. Itakura, K. Miyachi, and C. Nonaka
Phys. Rev. C 106, 034906 (2022)

Electromagnetic fields

J. A. Sun and L. Yan
Phys. Rev. C 109, 034917 (2024).

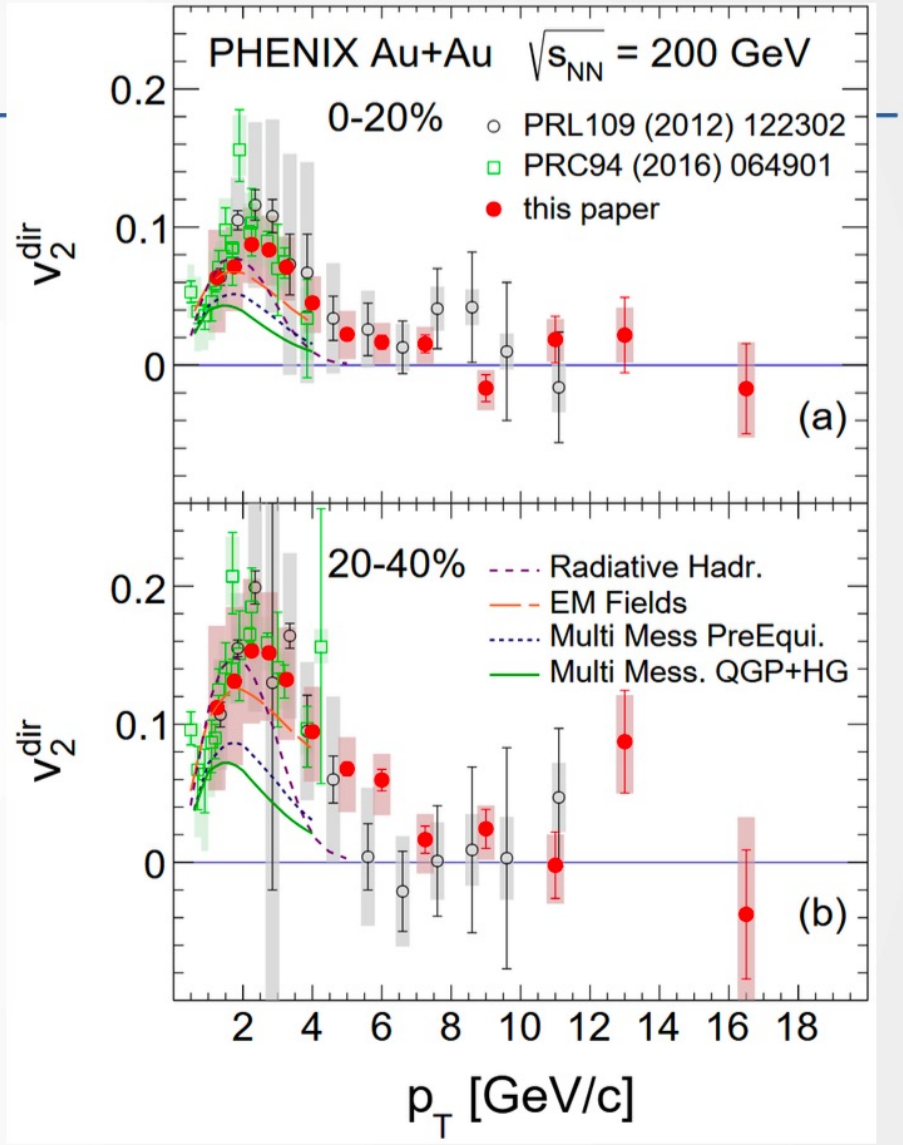

PHENIX collab., arXiv:2504.02955

EM fields acting on the medium

Do the EM fields act on the medium?

- Recent STAR results suggest yes STAR; PRX 14, 011028 (2024)
- We can simulate the EM field effects in our RRMHD model

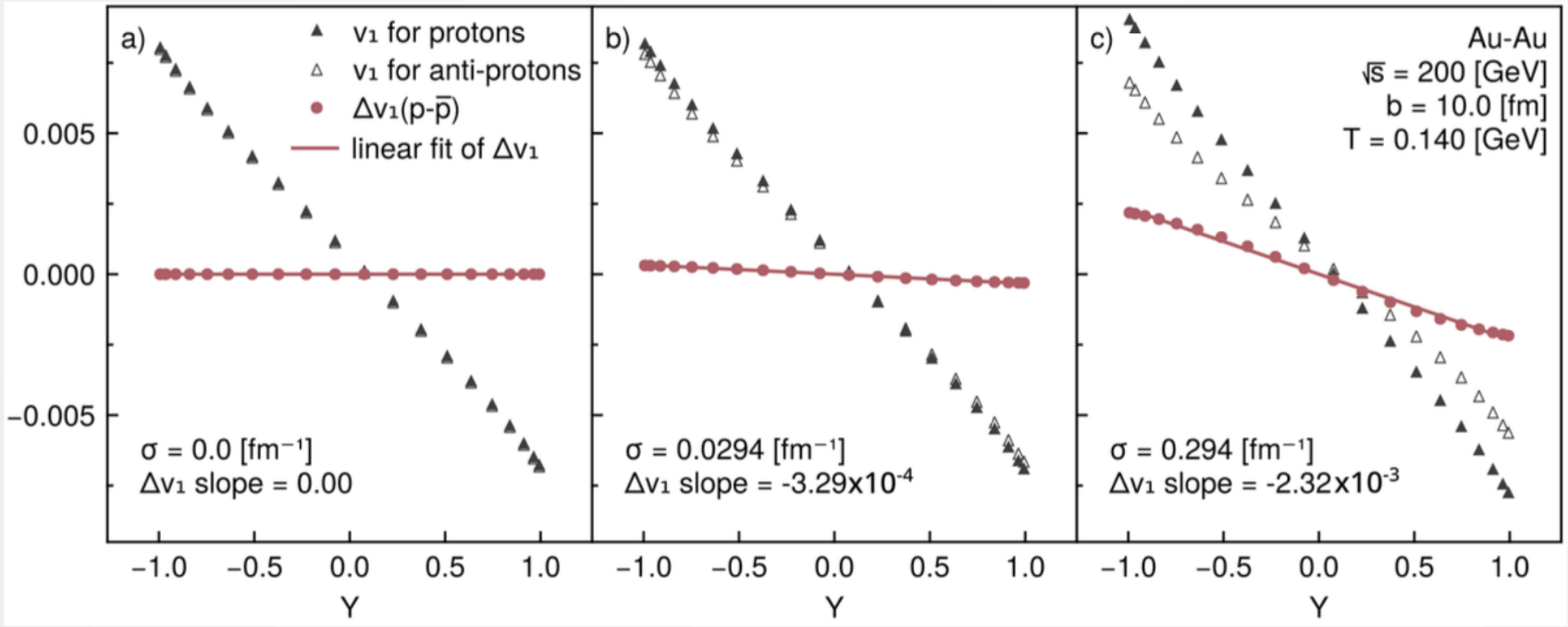

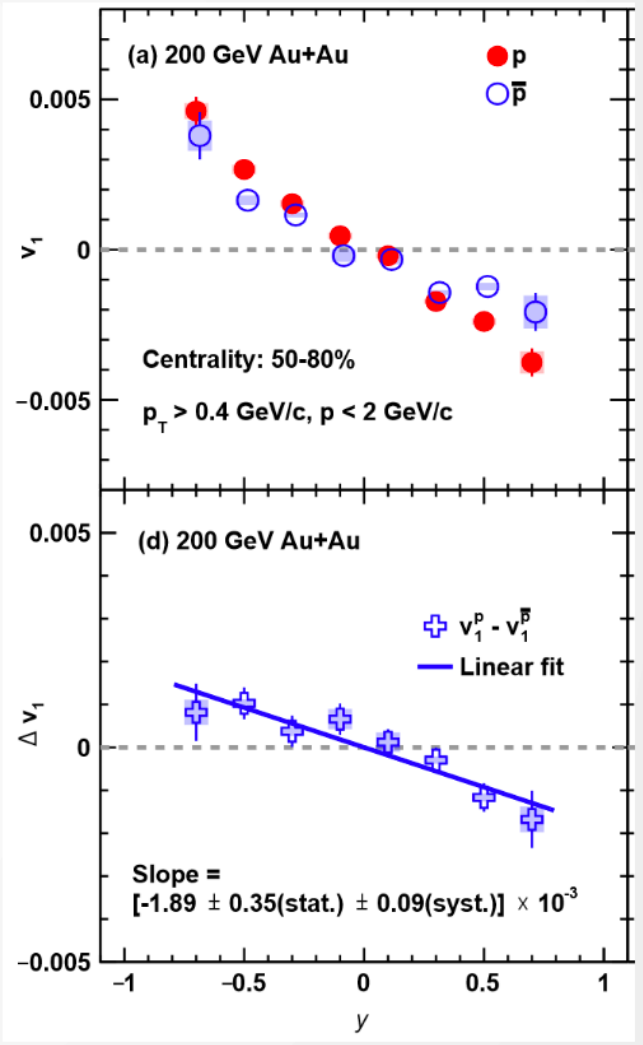

N J Benoit, T Miyoshi, C Nonaka, and H R Takahashi; PRC 112, 024911, arXiv:2502.04611 [nuc-th]

Photon Yield

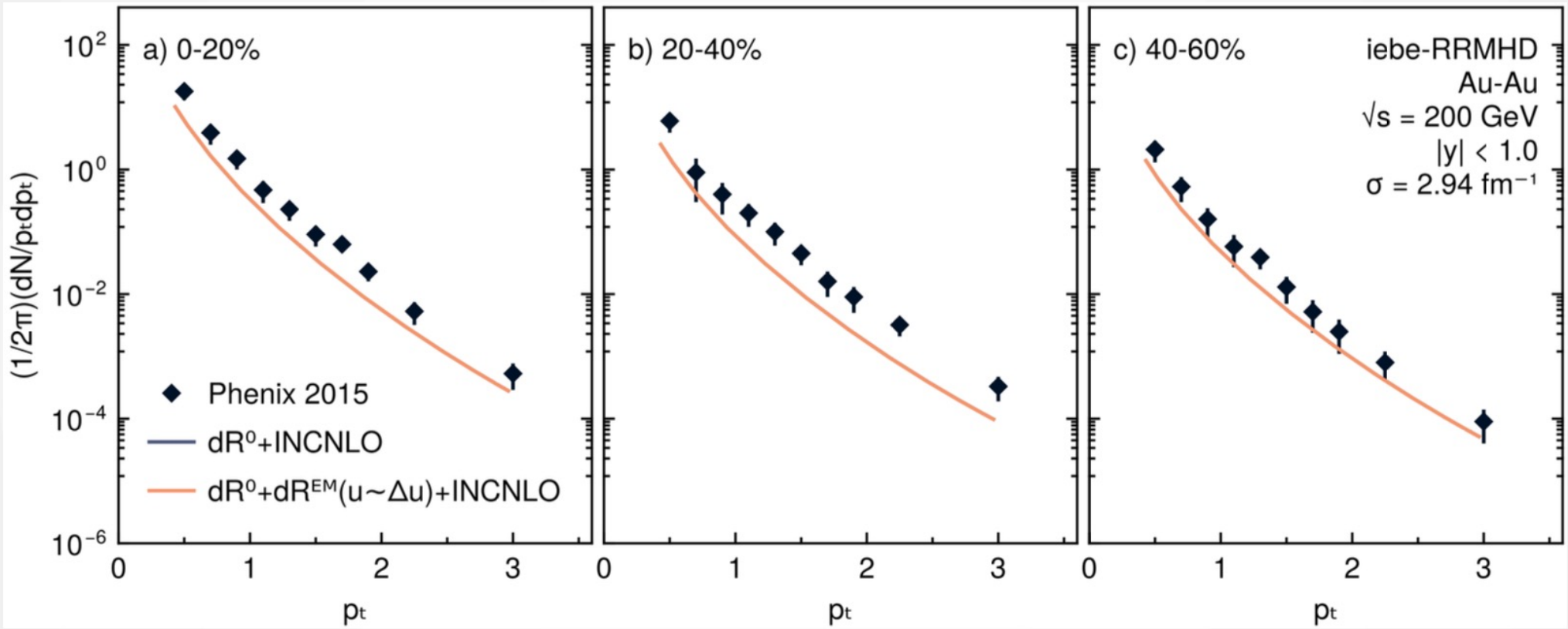

RHIC 200 GeV

τ_0 = 0.4 fm/c

EM fields create almost no change to photon yield

Systematic explorations of the space-time dynamics of QCD with N-point Energy Correlators

International Symposium on Multiparticle Dynamics
NCU Taiwan
August 17th, 2026

Rithya Kunnawalkam Elayavalli (She/They)
Vanderbilt University



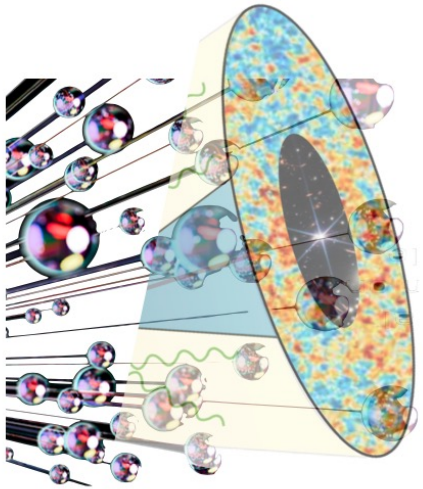

N-point Correlators

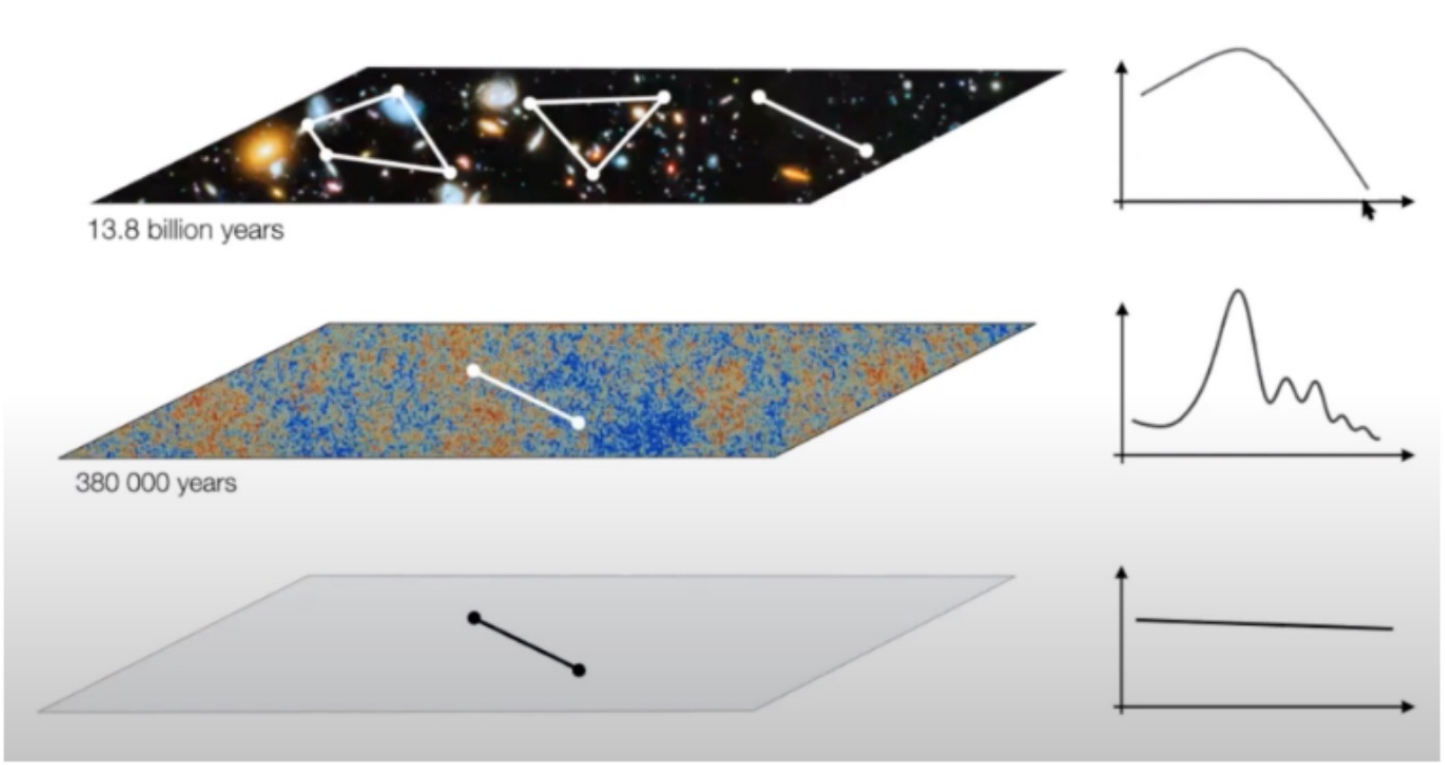

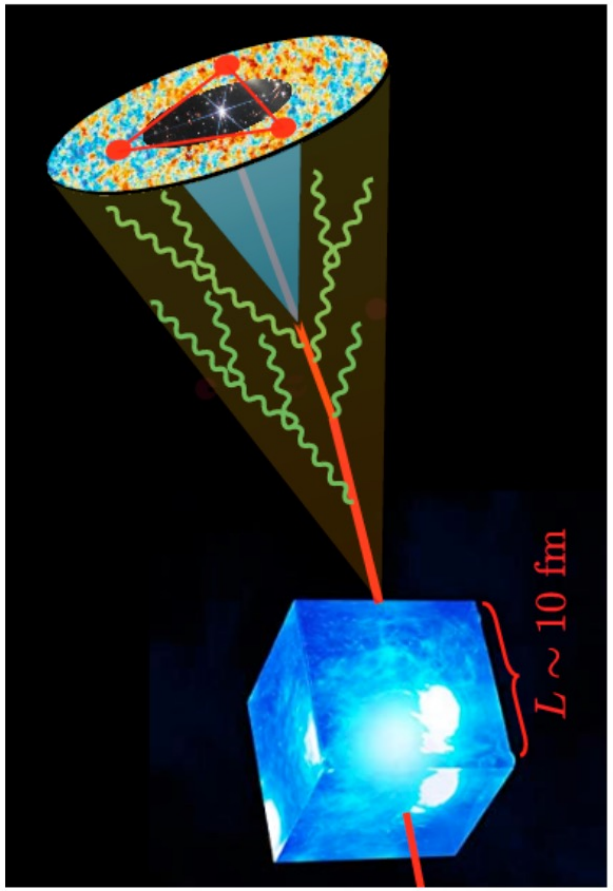

Quantifies the connection between correlation lengths and emergent structures

Projected ENC

Energy weighted pairwise distance of particles within your jet (or the event!)

$$\frac{\mathrm{d}\Sigma^{(n)}}{\mathrm{d}\theta} = \int \mathrm{d}\vec{n}_{1,2} \frac{\langle \mathcal{E}^n(\vec{n}_1)\mathcal{E}^n(\vec{n}_2)\rangle}{Q^{2n}} \delta(\vec{n}_2 \cdot \vec{n}_1 - \cos\theta)$$

$$\text{Normalized EEC} = \frac{1}{\sum_{Jets}\sum_{i\neq j}\frac{E_i E_j}{p_{T,Jet}{}^2}} \frac{d\left(\sum_{Jets}\sum_{i\neq j}\frac{E_i E_j}{p_{T,Jet}{}^2}\right)}{d\,(\Delta R)}$$

Hofman, Maldacena JHEP 0805 (2008) 012
Dixon, Moult, Zhu PRD 100, 014009 (2019)
Andres, Holguin et. al PRL. 130, 26, 262301 (2023)
Andres, Holguin et. al JHEP 09 (2023) 088

$$R_{\mathrm{L}} = \sqrt{(\Delta y)^2 + (\Delta\phi)^2}$$

LHCb:2610.14221[hep-ex]

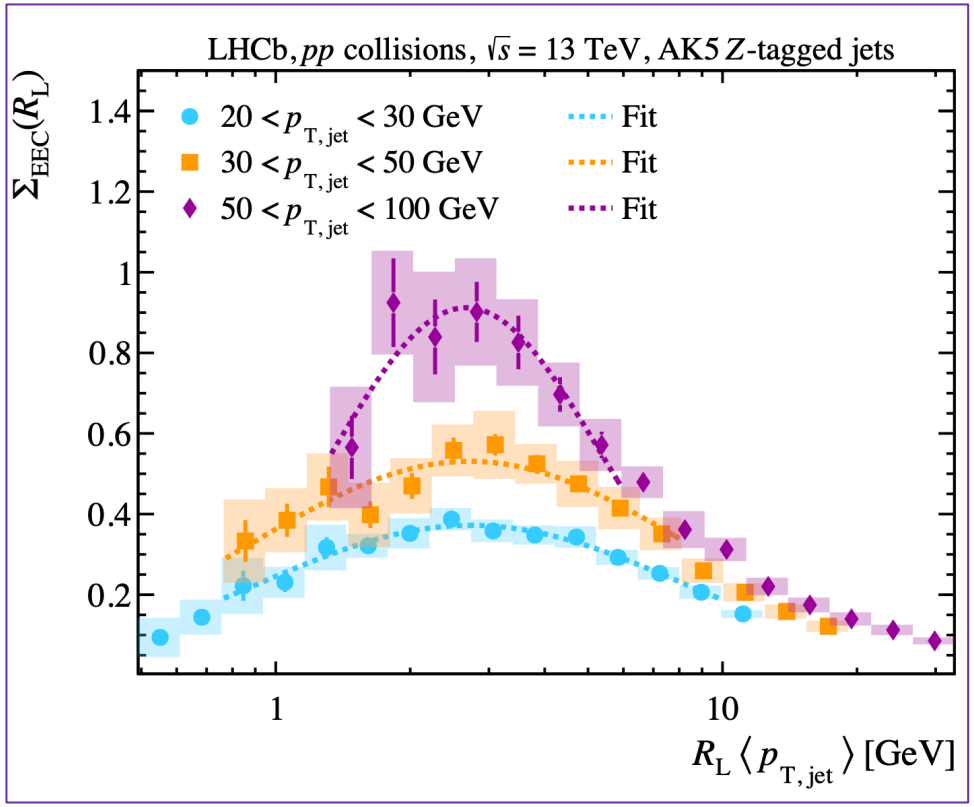

$$\Sigma_{\mathrm{EEC}}(R_{\mathrm{L}}, p_{\mathrm{T,jet}}) = \frac{1}{N_{Z+\mathrm{jets}} \cdot \Delta_{R_{\mathrm{L}}}} \times$$

$$\sum_{\{Z+\mathrm{jets}\}} \sum_{i<j} \int_{\Delta_{R_{\mathrm{L}}}} w_{p_{\mathrm{T}}}^{ij} \delta(R'_{\mathrm{L}} - R_{\mathrm{L}}^{ij}) \mathrm{d}R'_{\mathrm{L}},$$

How exactly do we plot this?

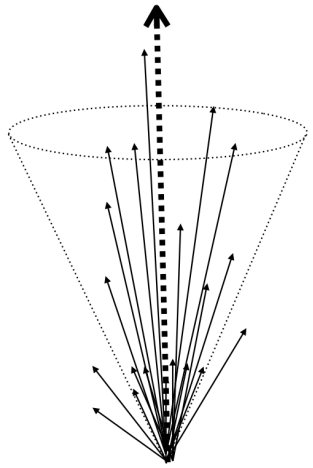

Step 1 - reconstruct your jets!

Step 2a - decide on an axis - jet $\vec{p}$ or WTA

Step 2b - draw a circle around the jet axis and choose your particles/fighters

How exactly do we plot this?

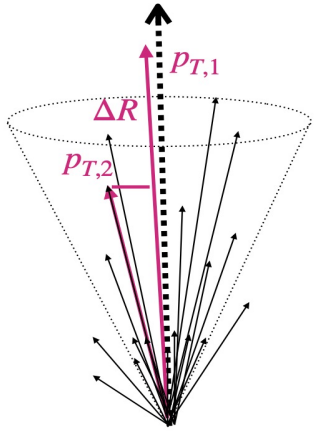

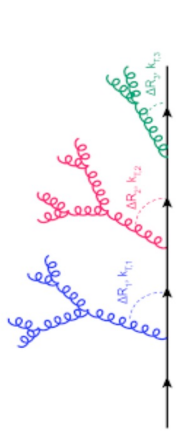

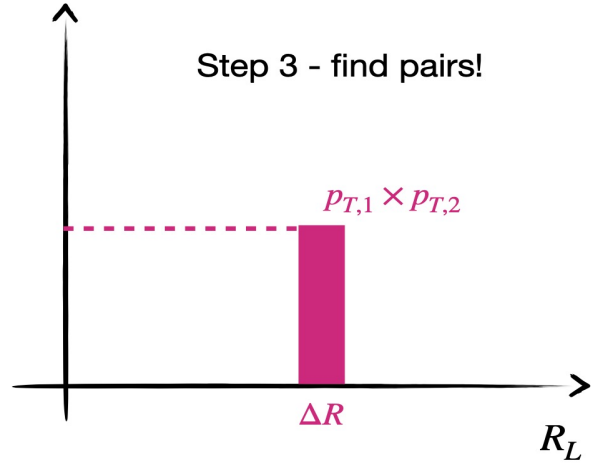

How exactly do we plot this?

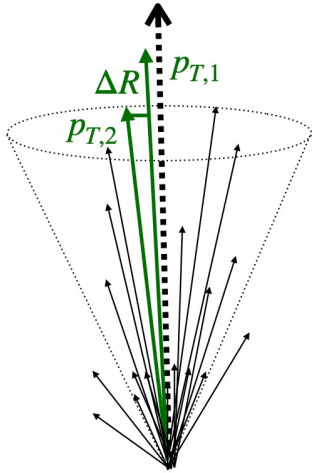

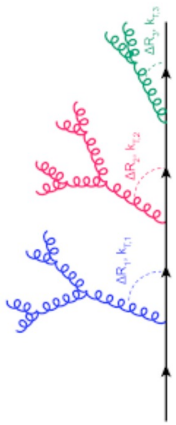

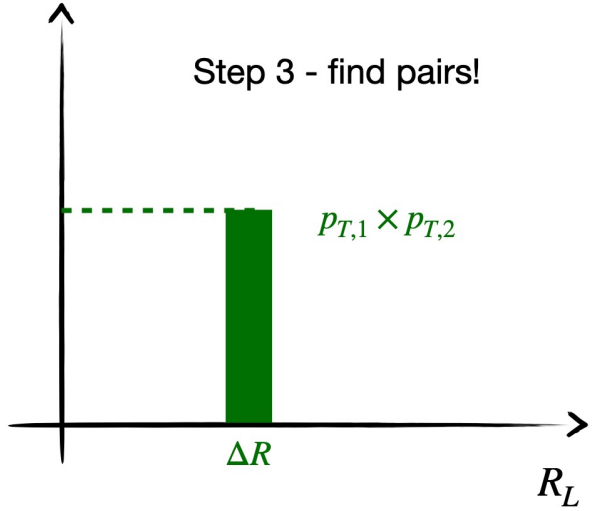

How exactly do we plot this?

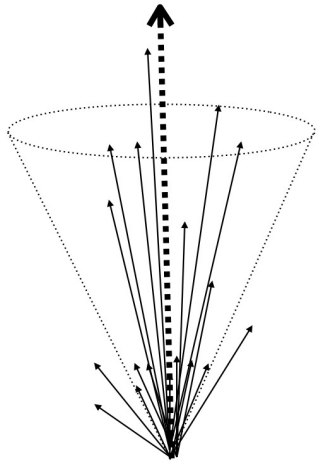

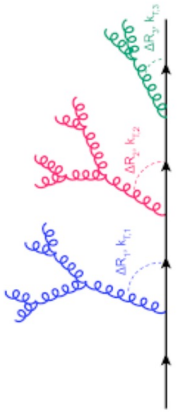

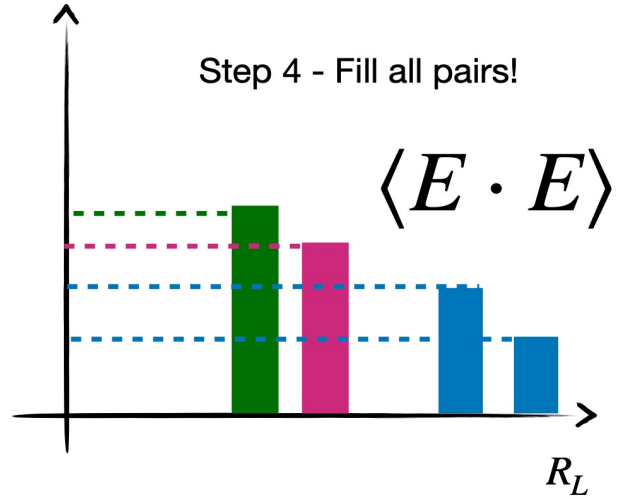

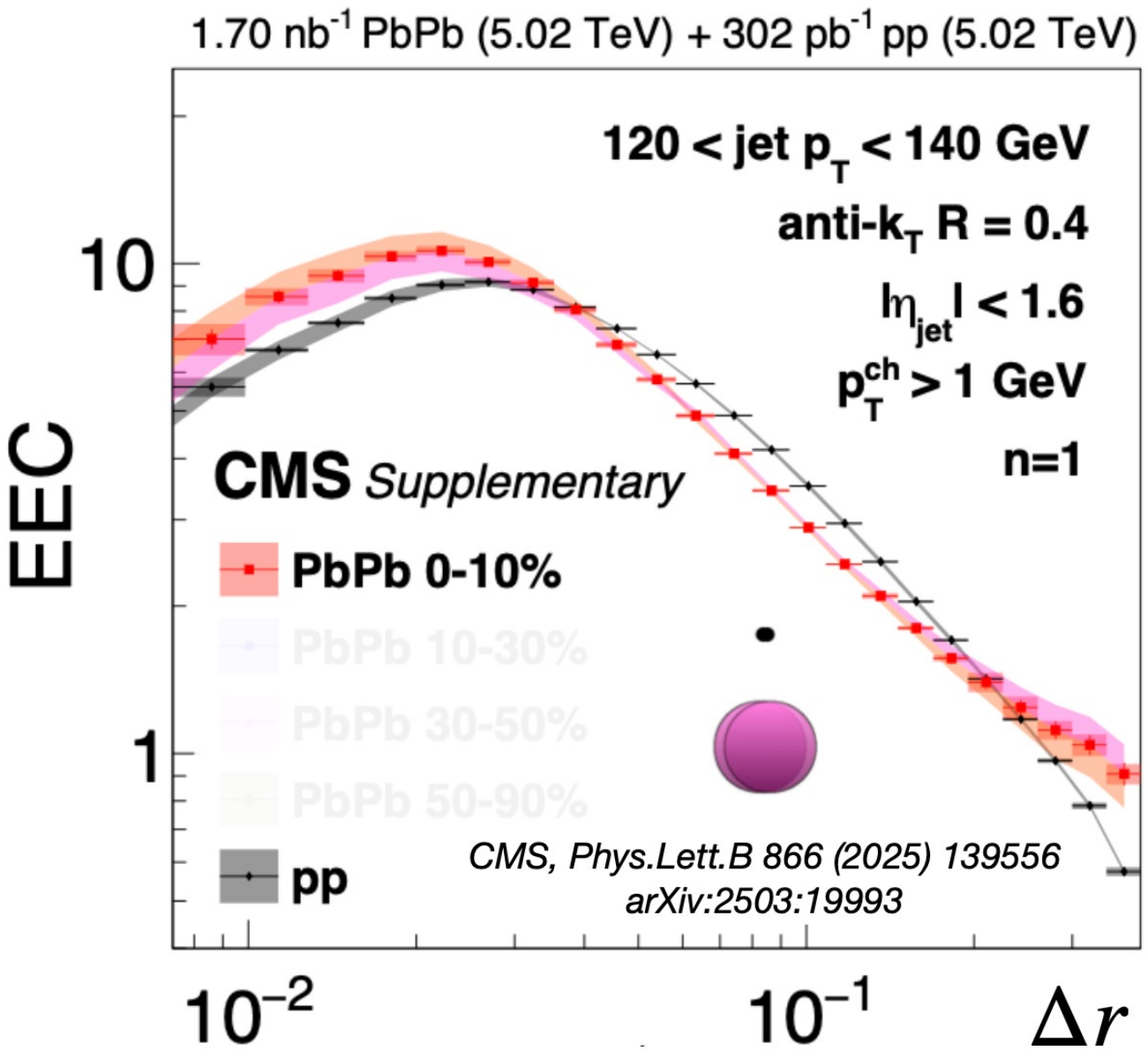

Start with this measurement

- Jet (sub)structure **is** modified in heavy ion collisions compared to pp collisions
- Peak of the EEC shifts to smaller angle (higher virtuality) - **direct evidence** of energy loss
- Improvements to models based on data!
- What are some next steps?

EEC Modification in Heavy Ions

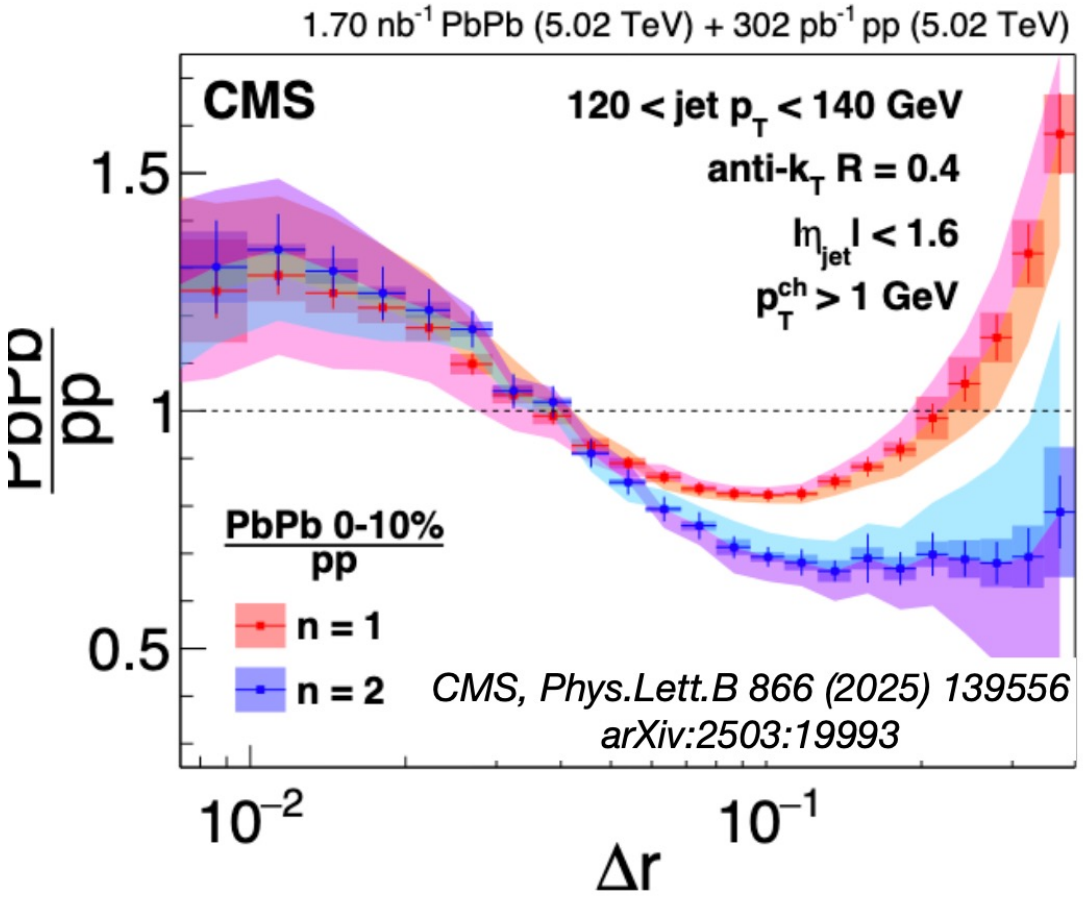

See refs here

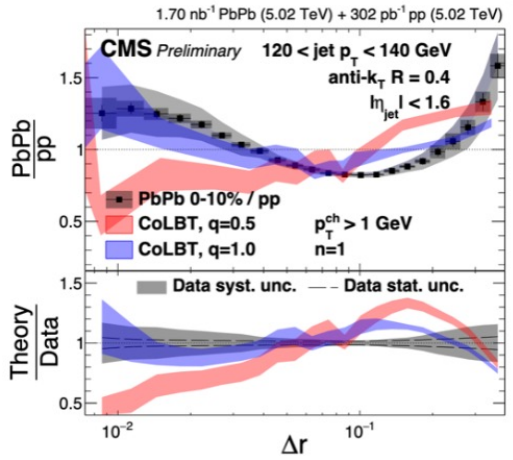

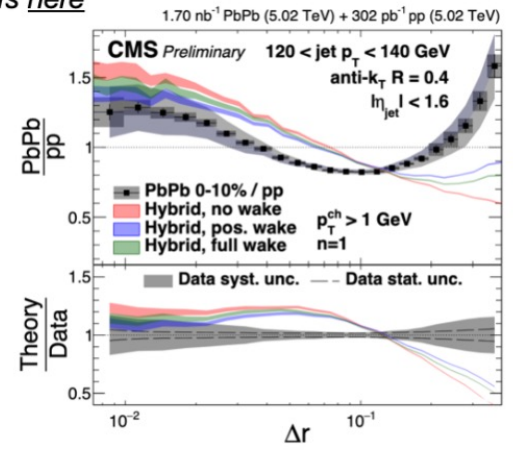

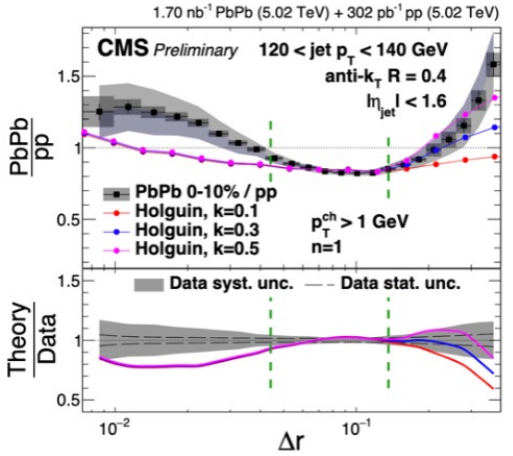

IN-23-004

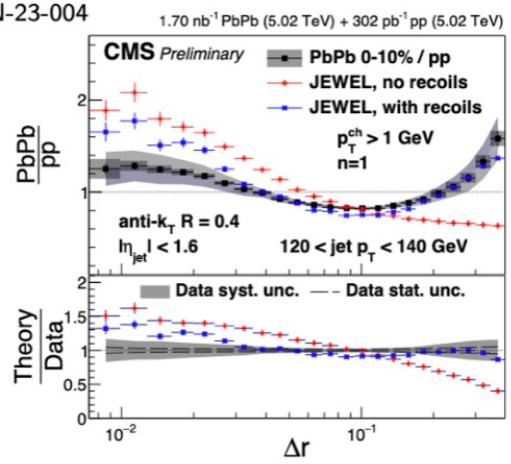

Enhancement at the large angle → indicative of medium response

Rithva KE @ ISMD. NCU. Taiwan Aug 2026

2-х точечные EEC различают следующие области образования струй.

Пертурбативная область при больших угловых расстояниях связана с более ранними моментами формирования струи (партонного ливня), подходит для Р-предсказаний КХД (pQCD).

Область свободных адронов при малых значениях углового расстояния связана с более поздними моментами формирования струи. При малых угловых расстояниях адроны полностью сформированы и распространяются без взаимодействия друг с другом. Эта область подходит для изучения npQCD, таких как модели адронизации (кинематические распределения адронов чувствительны к этим моделям).

Переходная область определяется изменением масштабирующего поведения между пертурбативной и областью свободных адронов и указывает на начало адронизации. В случае струй, инициированных легкими кварками или глюонами, переходная область соответствует угловым расстояниям порядка ΛQCD, деленным на поперечный импульс струи относительно оси pp-столкновения, p_T, струи, при этом предсказывается, что струи, инициированные легкими кварками, будут иметь переходную область при несколько меньшем угловом расстоянии, чем струи, инициированные глюонами.

Where are we now and next steps!

- **Energy N-point Correlators carry a wealth of information regarding the different regimes of QCD**
- **Large angle and small angle regions are fundamentally different in their physics interpretation - measurements drive progress**
- **ENCs offer varying insight regarding how jets are modified in heavy ion collisions (based on many measurements)**
- **Newer observables w/ ENCs enable us to study the phase-space in a multi-differential fashion!**

Measurements of Jets and Energy-Energy Correlators in Archival e^+e^- Data from LEP

Chris McGinn

ISMD, Taiwan

17 August 2026





MITHIG's work is supported by US DOE-NP



Collisions of e^+e^- for Studying QCD

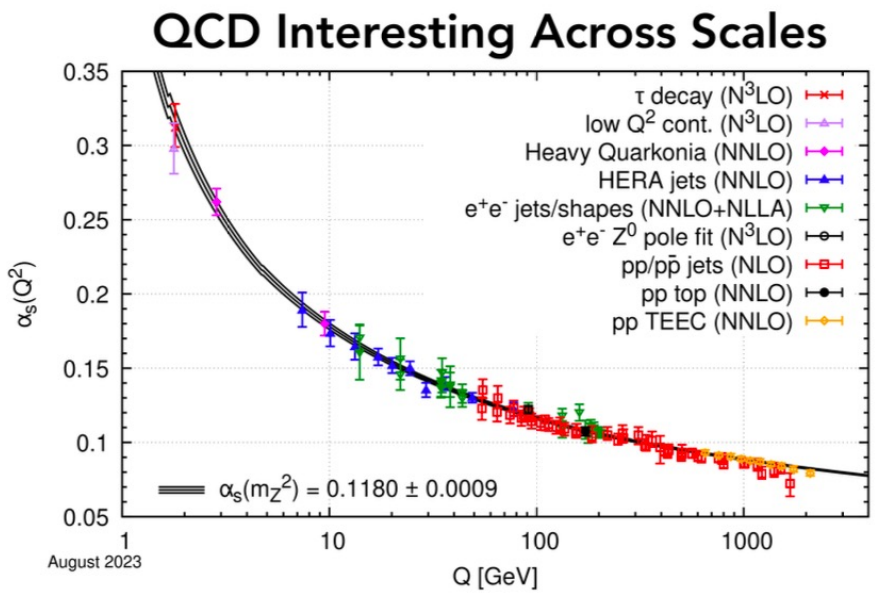

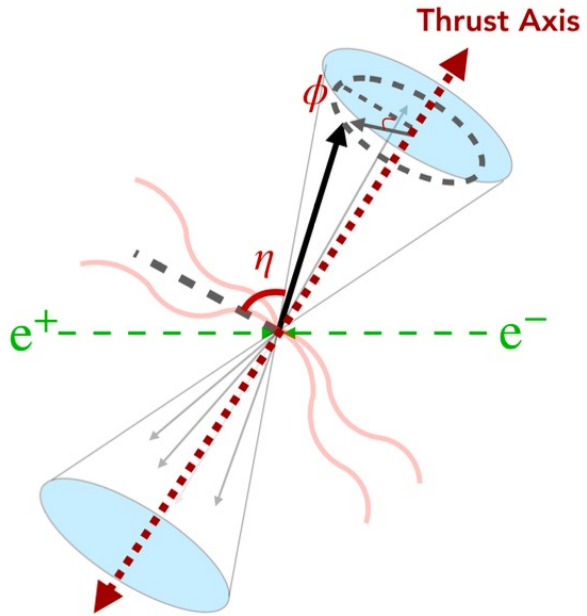

$$T = \max\left(\frac{\sum_i |\vec{p}_i \cdot \hat{n}|}{\sum_i |\vec{p}_i|}\right),$$

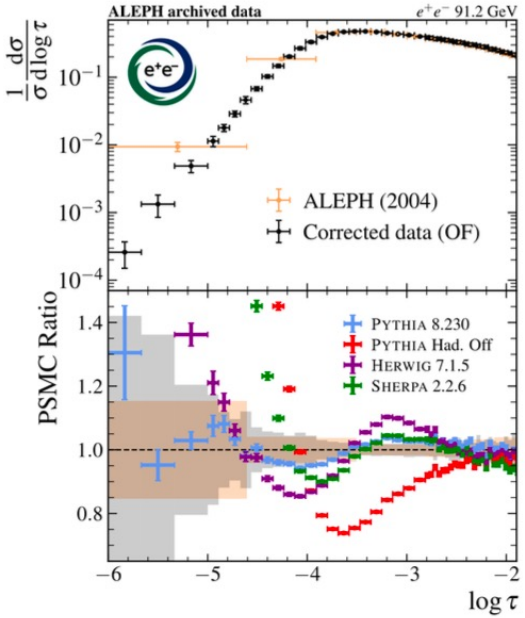

Farhi, PRL 39 (1977) 1587

- Quantum Chromodynamics (QCD) is central to the Standard Model arxiv:2510.22038
- Essential to study QCD from perturbative to nonperturbative regimes
  - Phenomena evolve with hard scale (running coupling!), manifests in observables
  - Example: Thrust-based extraction of α_s has significant nonperturbative corrections

Advantages of e^+e^- Collisions

Consider $e^+e^- \to q\bar{q}$:

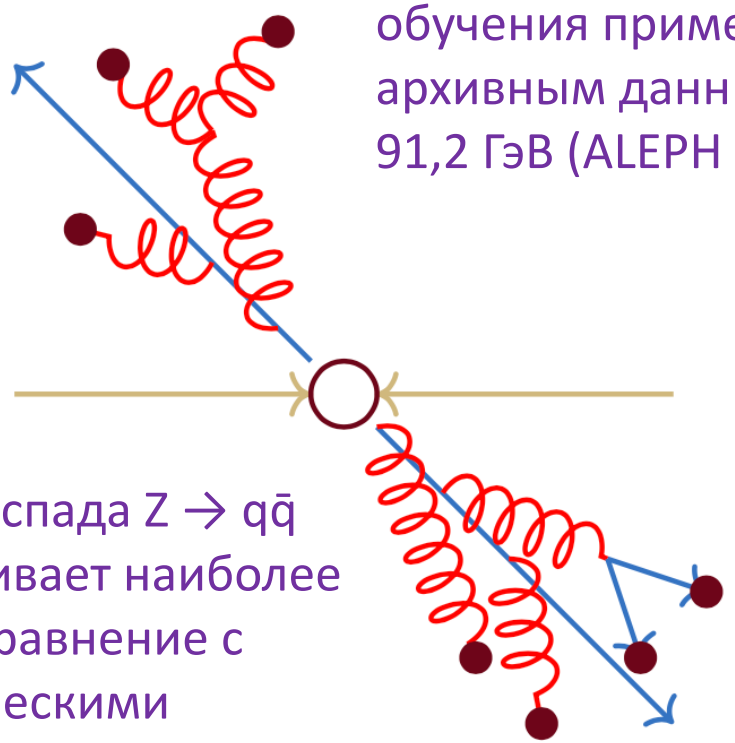

Метод машинного обучения применяется к архивным данным √s = 91,2 ГэВ (ALEPH на LEP).

Канал распада Z → qq̄ обеспечивает наиболее точное сравнение с теоретическими расчетами КХД на Z-полюсе.

Advantages over pp/AA collisions:

- **Pointlike initial state**
  - **No PDFs or nPDFs**
  - **No gluon ISR**
- **Hard scale is fixed!**
  - **Full collision energy → final state**
- **Kinematics fully constrained**
- **Quark jets dominate production**
- **MPI contributions reduced**
- **Clean, signal-dominated final state**

Example: Event Display for Low-Thrust Event

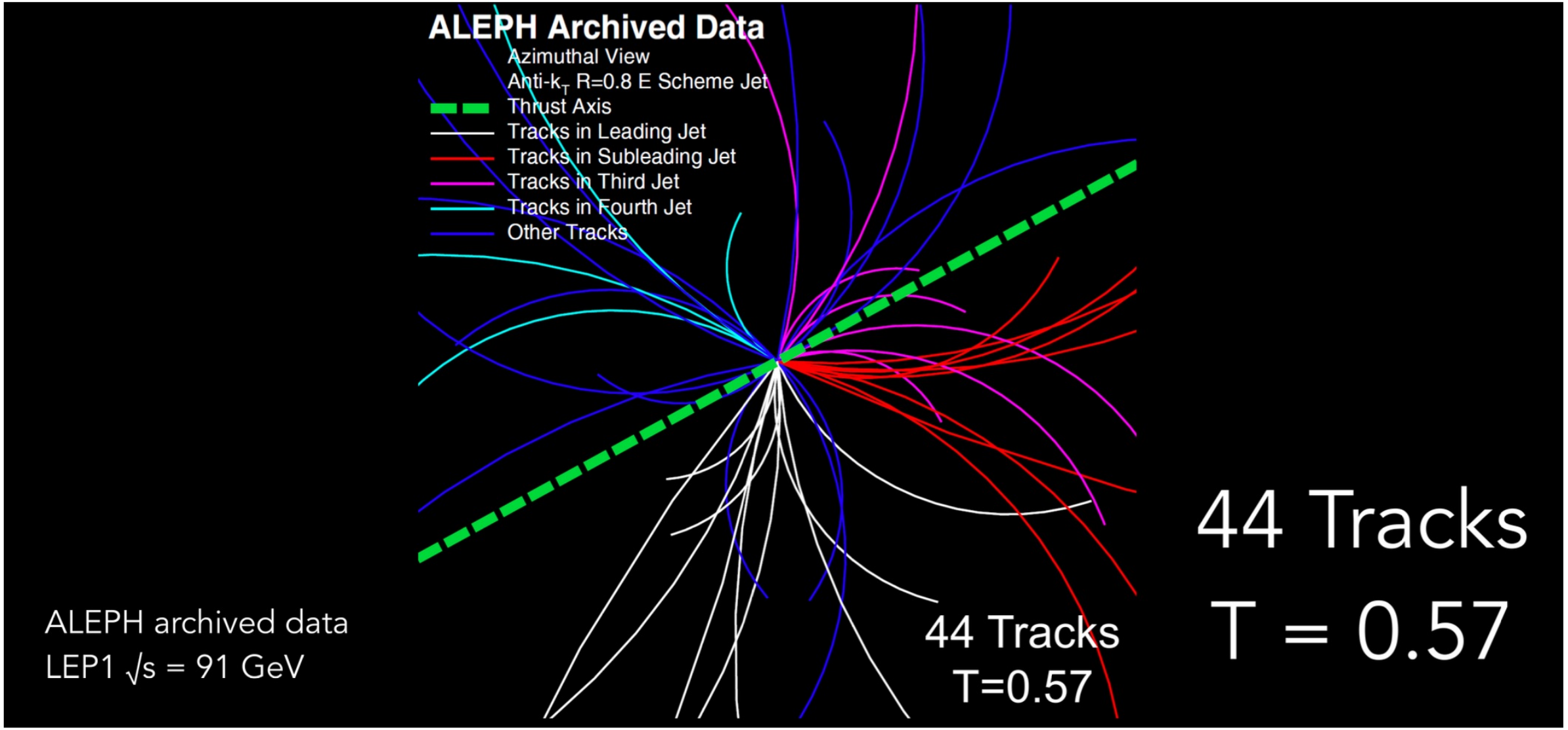

Example: Event Display for High-Thrust Event

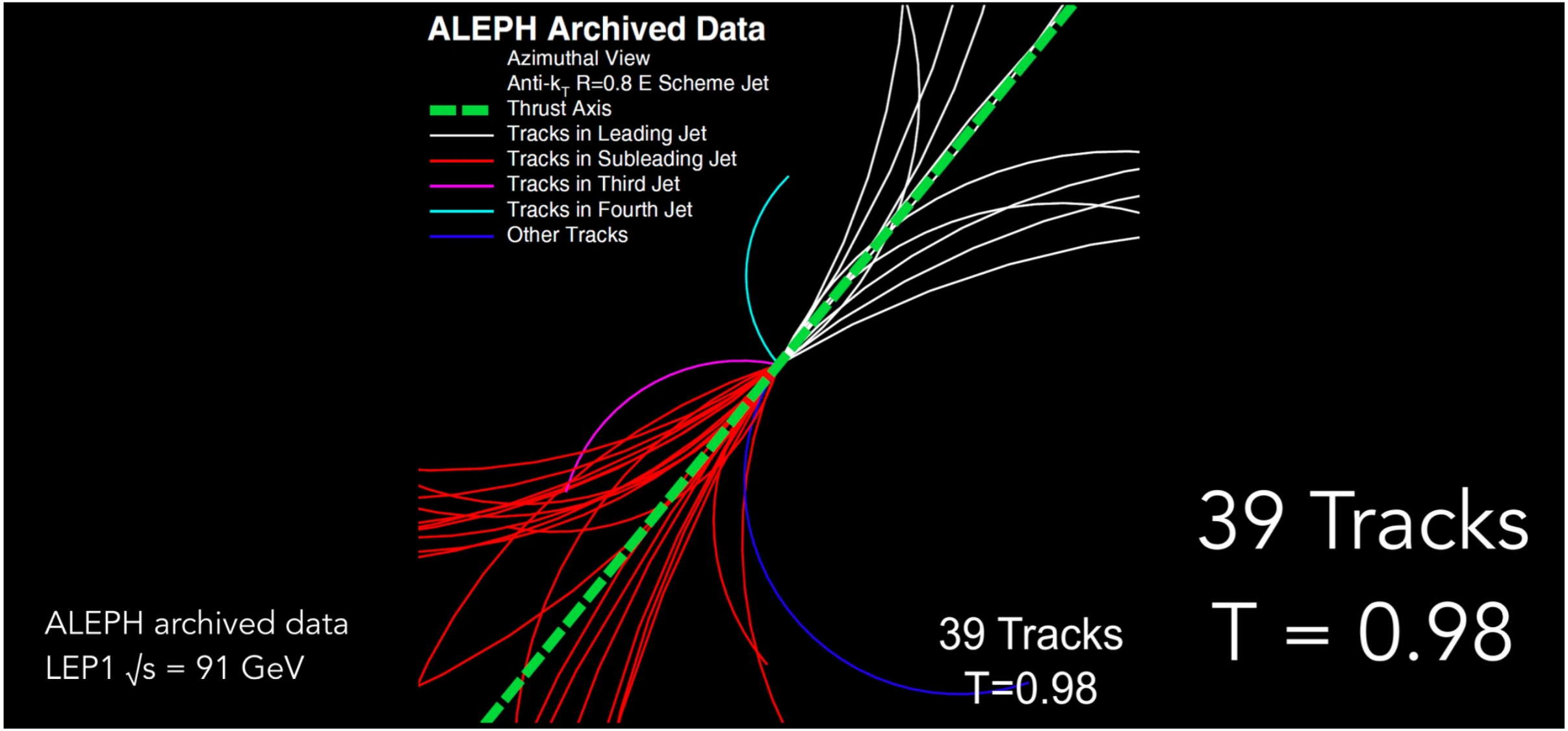

Timeline of e^+e^- Colliders

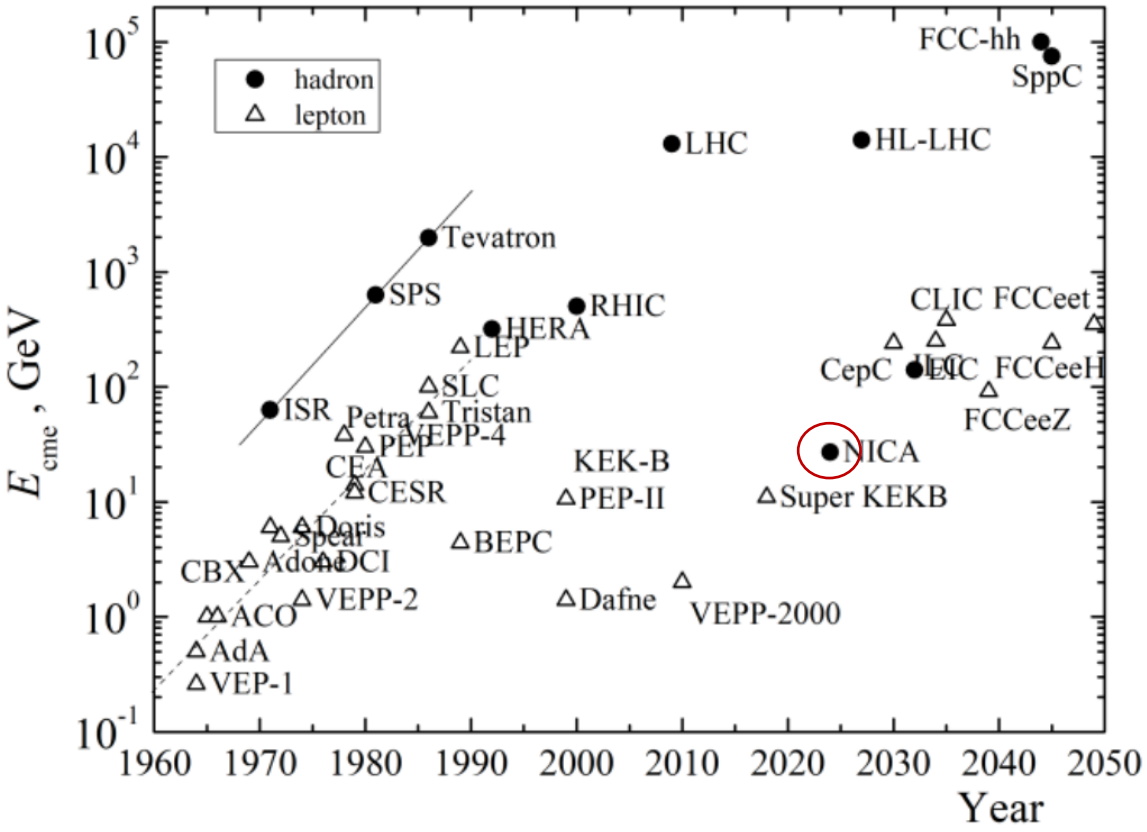

Via **Ultimate Limits of Future Colliders**

- **Current existing machines <= 11 GeV**
- **For best dynamic range, we should look at older data that collided at the Z pole**
  - **Also informs physics at the FCCee**
- **Archival data → a "recycling frontier"**

The e^+e^- Alliance



- **Please find us at https://ee-alliance.org**

Evolution of Jet Algorithms w/ Time

EPJC 35 (2004) 457

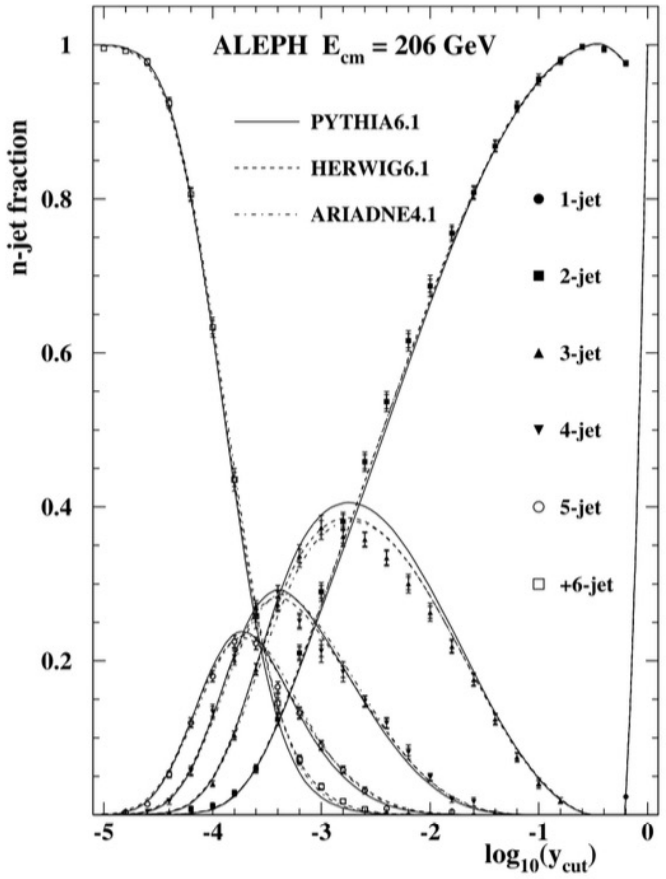

Fig. 7. Measured n-jet fractions for $n = 1, 2, 3, 4, 5$ and $n \geq 6$ and the predictions of Monte Carlo models, at a centre-of-mass energy of 206 GeV

JHEP 04 (2008) 063

February 2008
LPTHE-07-03

The anti-k_t jet clustering algorithm

Matteo Cacciari and Gavin P. Salam
LPTHE
UPMC Université Paris 6,
Université Paris Diderot – Paris 7,
CNRS UMR 7589, Paris, France

Gregory Soyez
Brookhaven National Laboratory, Upton, NY, USA

89v2 [hep-ph] 21 Apr 2008

Abstract: The k_t and Cambridge/Aachen inclusive jet finding algorithms for hadron-hadron collisions can be seen as belonging to a broader class of sequential recombination jet algorithms, parametrised by the power of the energy scale in the distance measure. We examine some properties of a new member of this class, for which the power is negative. This "anti-k_t" algorithm essentially behaves like an idealised cone algorithm, in that jets with only soft fragmentation are conical, active and passive areas are equal, the area anomalous dimensions are zero, the non-global logarithms are those of a rigid boundary and the Milan factor is universal. None of these properties hold for existing sequential recombination algorithms, nor for cone algorithms with split–merge steps, such as SISCone. They are however the identifying characteristics of the collinear unsafe plain "iterative cone" algorithm, for which the anti-k_t algorithm provides a natural, fast, infrared and collinear safe replacement.

- **Jets at LEP were very different from jets today**
  - **Largely studied w/ event shape observables (thrust)**
  - **Dominant algo. anti-k_T only available after 2008!**

Two-particle Correlations with LEP-I Data

The sharp near-side peaks arise from jet correlations and have been truncated to better illustrate the structure outside that region.

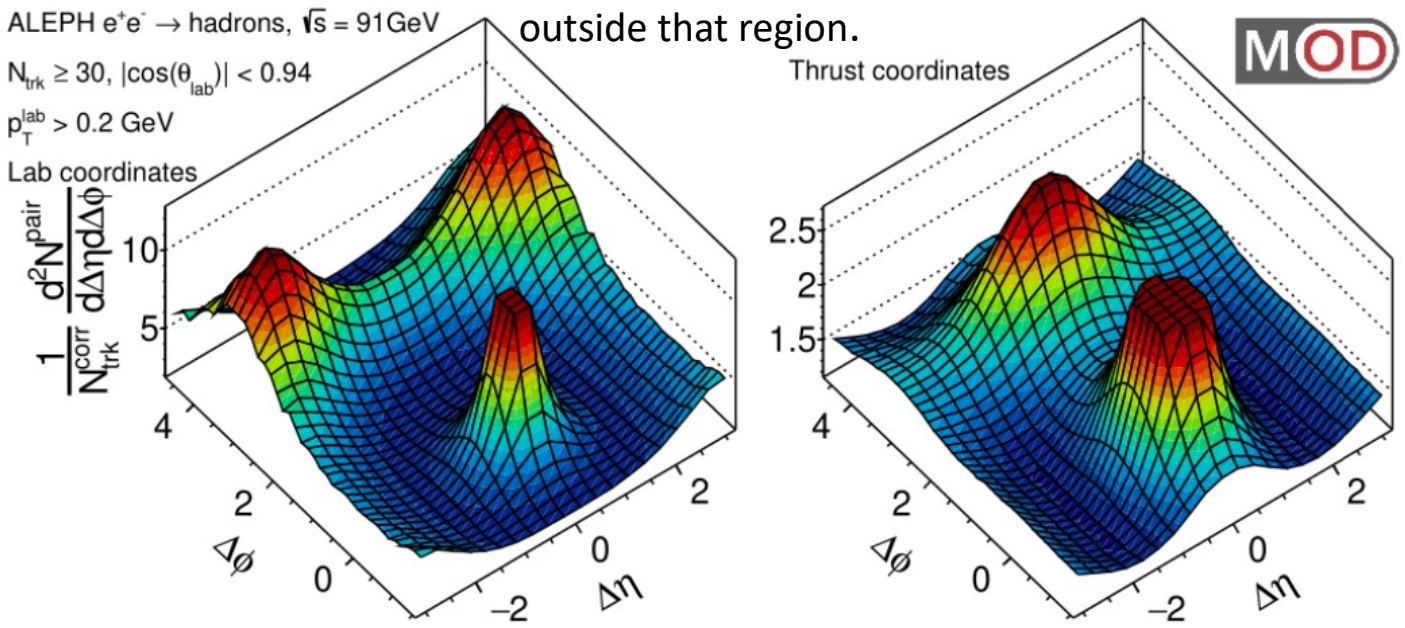

PRL 123 (2019) 21, 212002

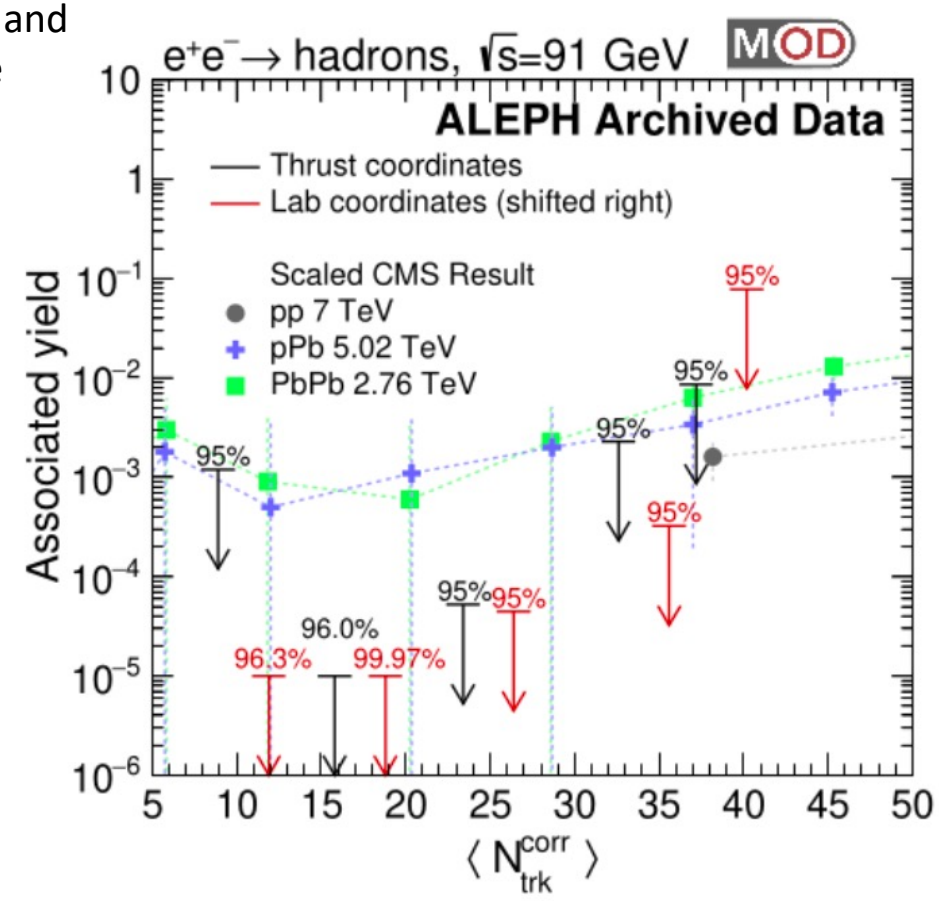

- **Search for associated particle yield that in AA indicates flow**
- **Correlate particles with each other in lab and thrust coordinates**
  - **Very similar procedurally to measuring EECs! Add energy weights, and use single angle**

"В отличие от pp-, pA- и AA-столкновений с большой n_{ch}, где наблюдают дальнодействующие корреляции с большим интервалом по η, в e^+e^--столкновениях их значительного усиления не обнаружено. Данные сравниваются с результатами работы генераторов, не учитывающих дополнительные взаимодействия партонов в конечном состоянии. Полученные результаты лучше описываются генераторами PYTHIA и SHERPA, чем HERWIG. Есть веские основания полагать, что мы правильно обрабатываем архивные данные."

ISMD 2026

Measurements of particle production in light ion collisions with the ATLAS detector

Krzysztof W. Woźniak
INP PAS, Kraków, Poland
for the ATLAS Collaboration

2026
8.17 → 8.21
Chungli **Taiwan**
我很高興能造訪台灣

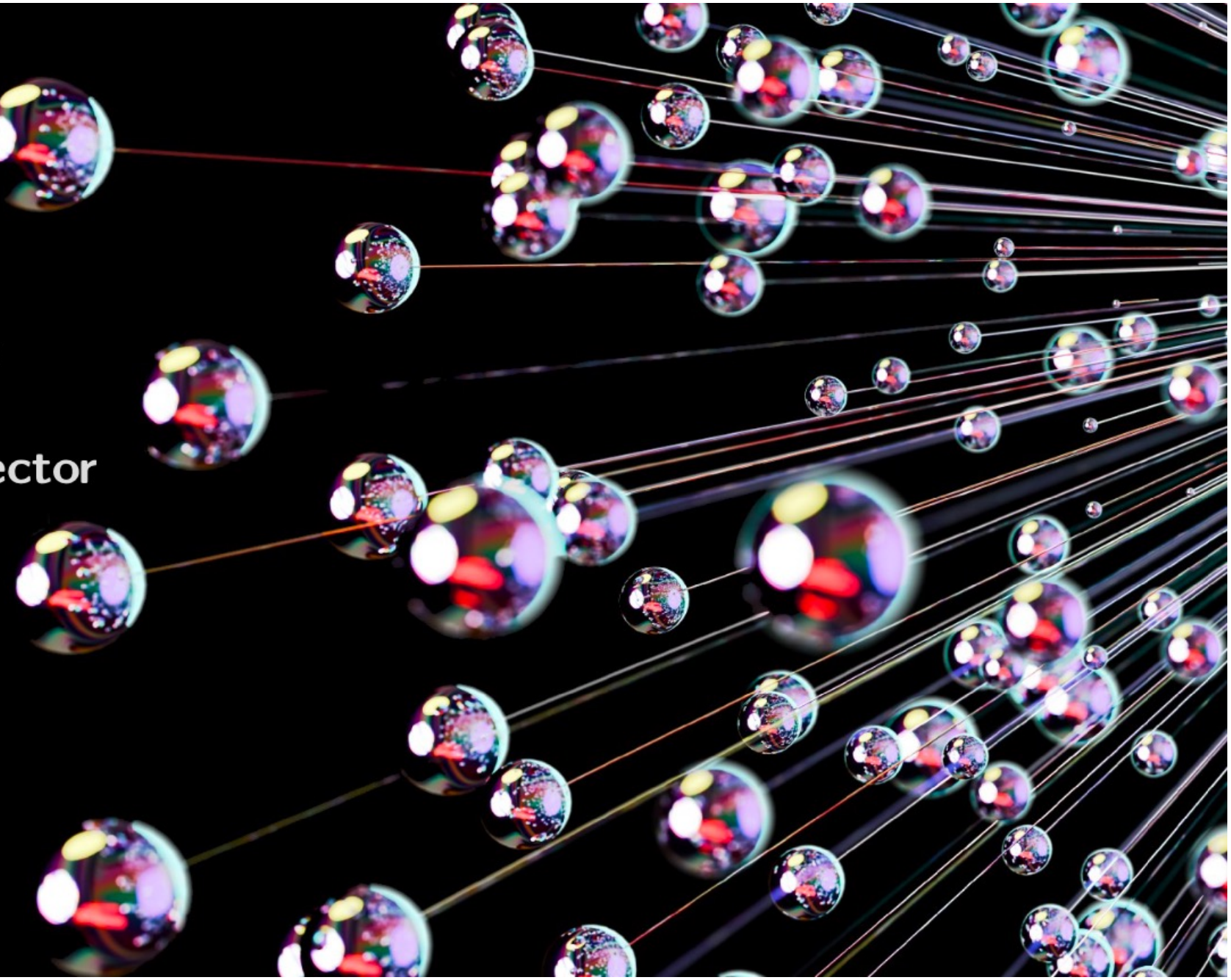

Outline

List of light ion collisions:
- *p*+O - for cosmic ray interactions (11 nb^{-1})
- O+O - light nucleus at the highest energy (8 nb^{-1})
- Ne+Ne - different light nucleus (1 nb^{-1})

Analyses
- multiplicity of charged particles
- pseudorapidity and p_T distributions
- particle flow
- jets flow and fragmentation

p+O collisions at 9.62 TeV

Crucial for correct simulation of particle cascades initiated by cosmic rays of high energy
- high energy cosmic ray are protons (90%), He (9%) and heavier nuclei (1%)
- air composition: N_2 (78.08%), O_2 (20.95%), Ar (0.93%), other (0.04%)
- earlier data available at LHC: *pp* (up to 13.6 TeV) and *p*+Pb (up to 8.16 TeV)
- imprecise extrapolations to obtain *p*+N and *p*+O interactions

pp collisions at 7 TeV and 13 TeV

at 7 TeV (20.3 μb^{-1}):
σ_{inel} = 69.1 ±2.4 (exp.) ±6.9 (extr.) mb

at 13 TeV (60.1 μb^{-1}):
σ_{inel} = 78.1 ±0.6 (exp.) ±1.3 (lum.) ±2.6 (extr.) mb

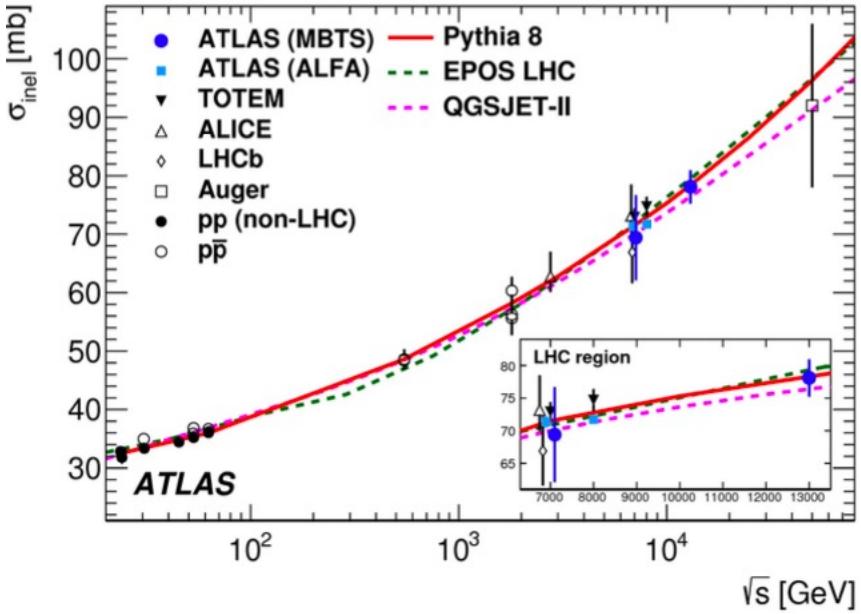

p+O collisions at 9.62 TeV

Inelastic cross section (measured):

$\sigma^{pO}_{inel,fid}$ = 396 ± 6 (exp.) ± 9 (lumi.) mb

compared to predictions from several models

Extrapolated to full phase space:

σ^{pO}_{inel} = 438 ± 6 (exp.) ± 10 (lumi.) ± 30 (th.) mb

Estimated proton-air inelastic cross section:

σ^{p+air}_{inel} = 406 ± 6 (exp.) ± 9 (lumi.) ± 28 (th.) mb

compared to model predictions and indirect estimates obtained from measurements of cosmic-ray cascades

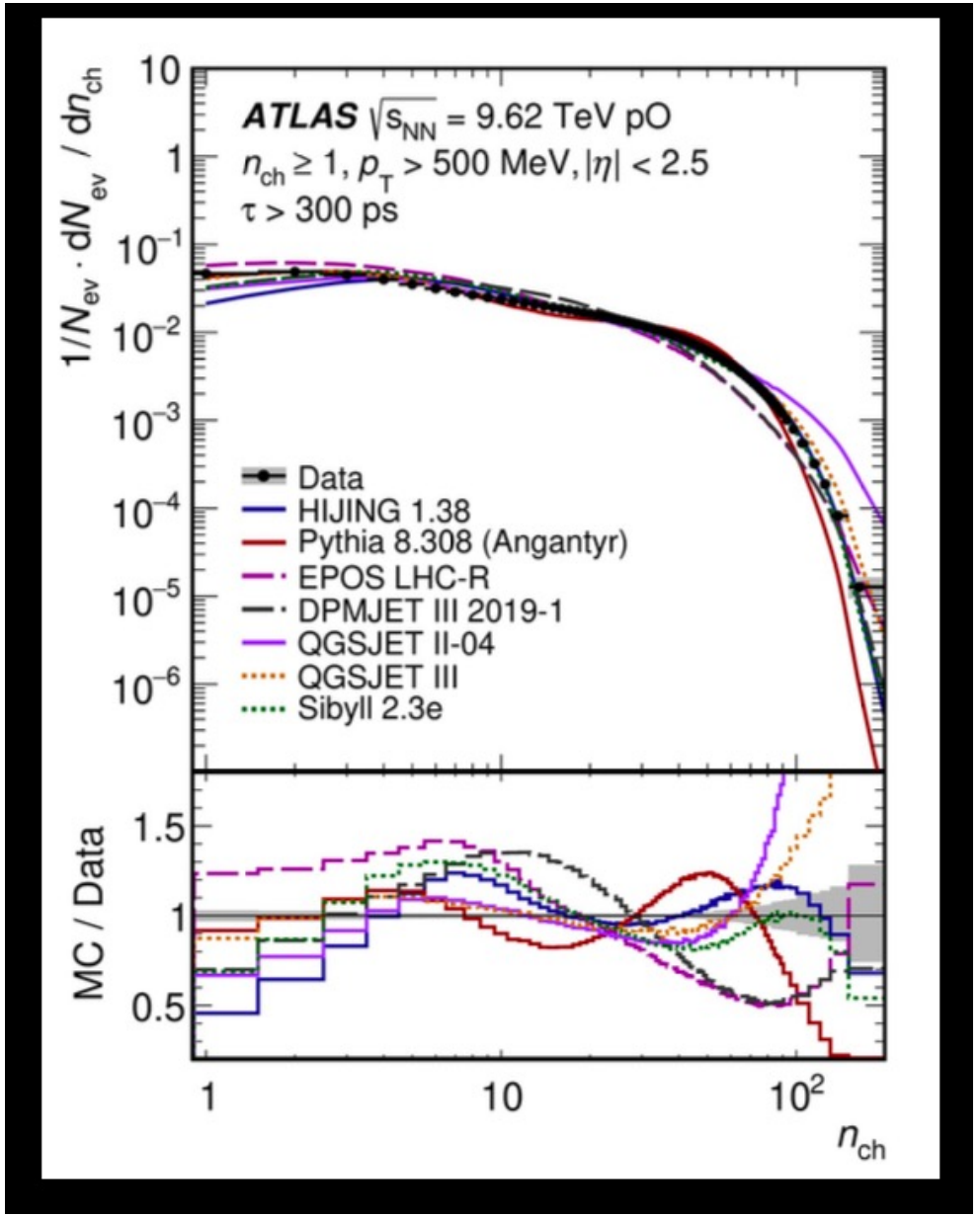

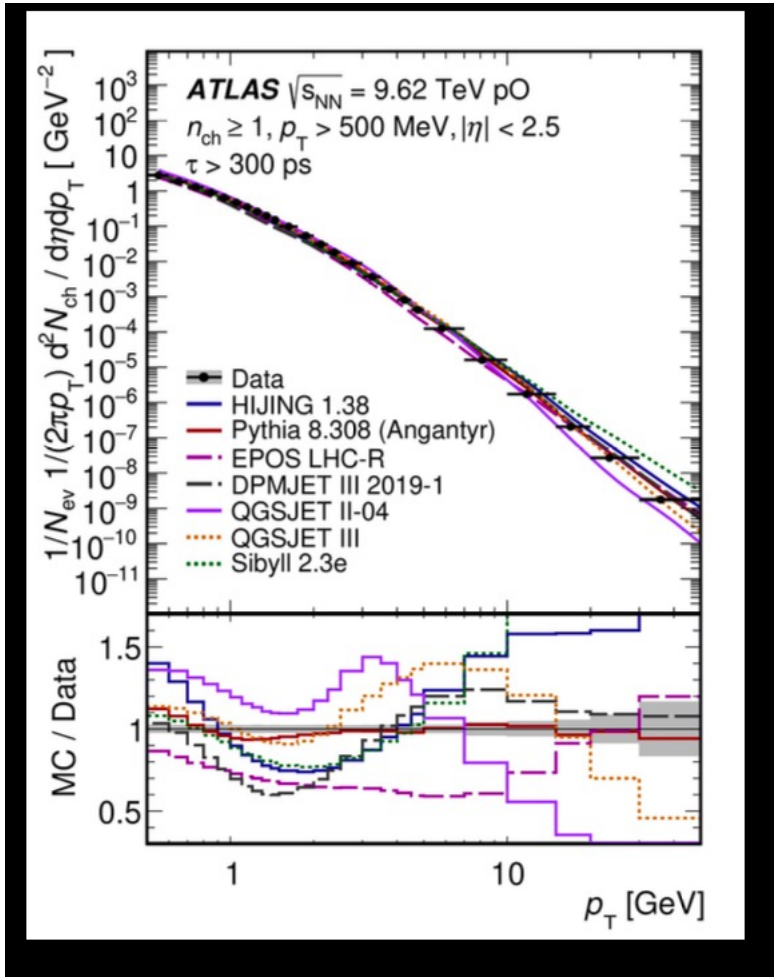
ATLAS $\sqrt{s_{NN}}$ = 9.62 TeV pO
$n_{ch} \geq 1$, $p_T > 500$ MeV, $|\eta| < 2.5$
$\tau > 300$ ps
Data
HIJING 1.38
Pythia 8.308 (Angantyr)
EPOS LHC-R
DPMJET III 2019-1
QGSJET II-04
QGSJET III
Sibyll 2.3e
$1/N_{ev}\ 1/(2\pi p_T)\ d^2N_{ch}/d\eta dp_T$ [GeV^{-2}]
MC / Data
p_T [GeV]

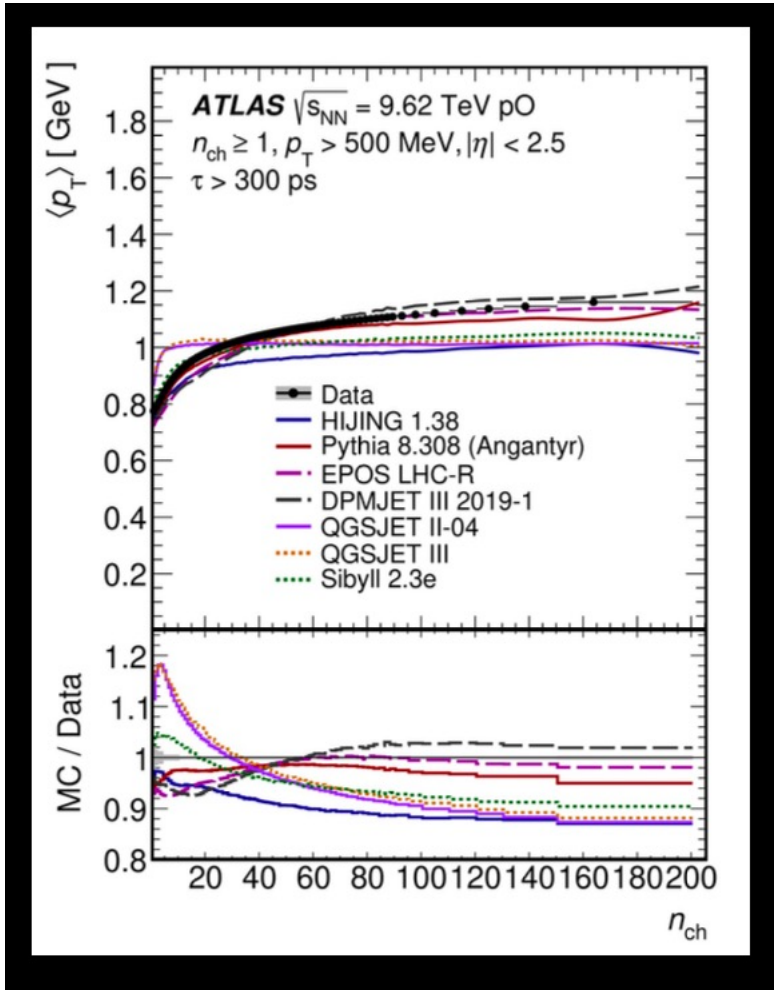
ATLAS $\sqrt{s_{NN}}$ = 9.62 TeV pO
$n_{ch} \geq 1$, $p_T > 500$ MeV, $|\eta| < 2.5$
$\tau > 300$ ps
Data
HIJING 1.38
Pythia 8.308 (Angantyr)
EPOS LHC-R
DPMJET III 2019-1
QGSJET II-04
QGSJET III
Sibyll 2.3e
$\langle p_T \rangle$ [GeV]
MC / Data
n_{ch}

O+O and Ne+Ne collisions

Nuclei of very similar size Z=8, A=16 (O) and Z=10, A=20 (Ne) but **different shape** opportunity to study dependencies on geometry of nuclei collisions

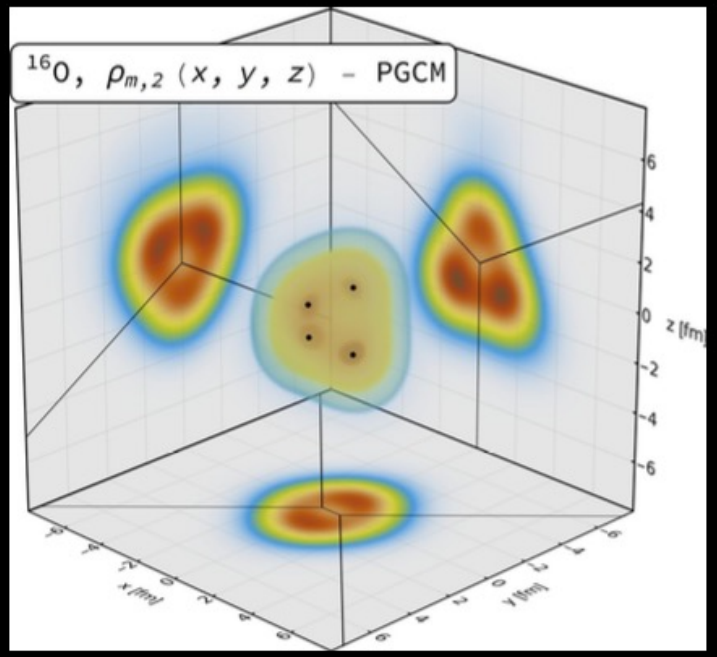

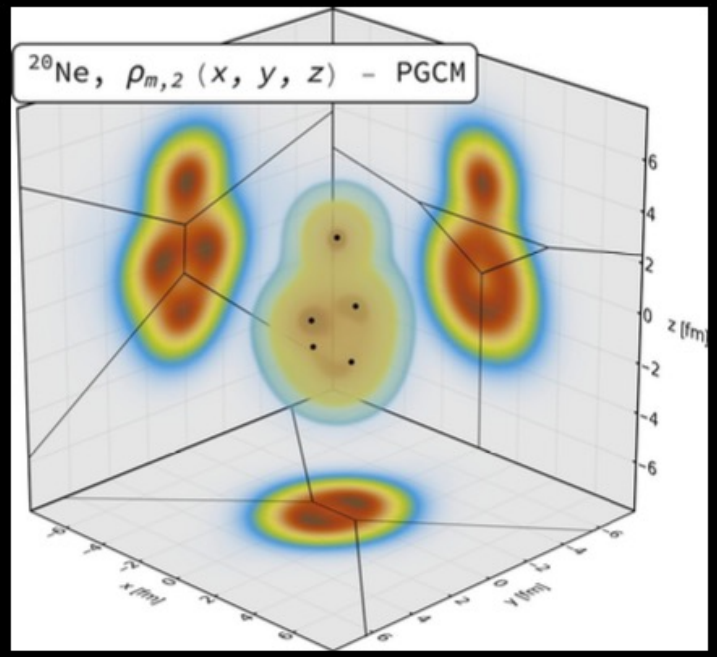

oxygen: spherical



橘子

neon: elongated



梨

Images by 冰韵 汤 from pixabay.com

G. Giacalone *et al.*, arXiv:2402.05995 [nucl-th]

O+O and Ne+Ne collisions - particle flow

O+O, Ne+Ne, Xe+Xe - flow harmonics $v_n(p_T)$

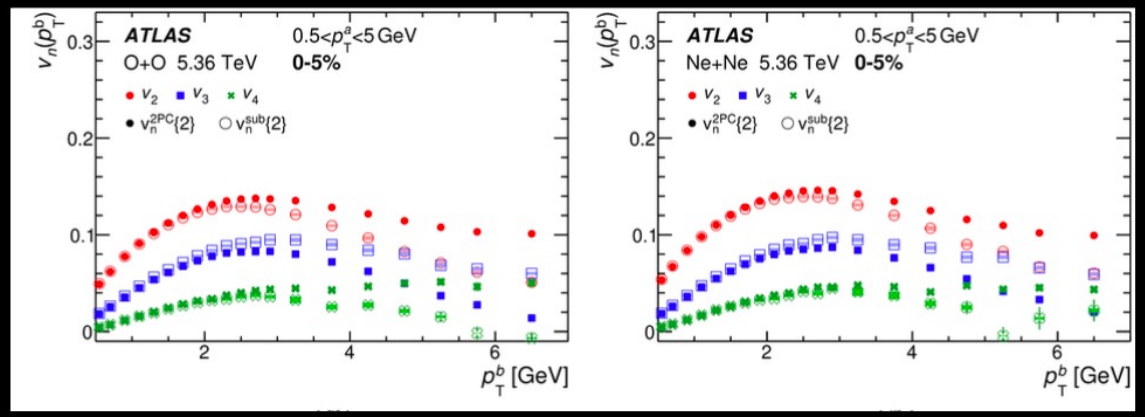

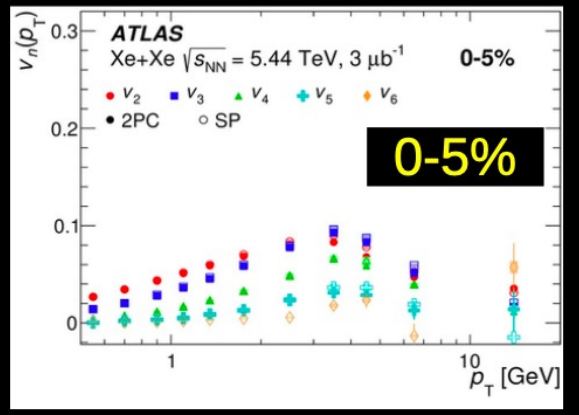

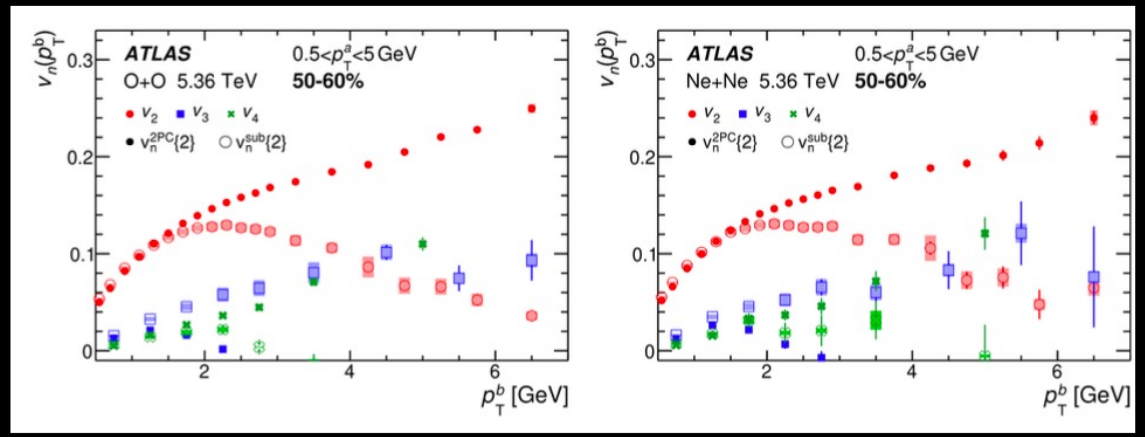

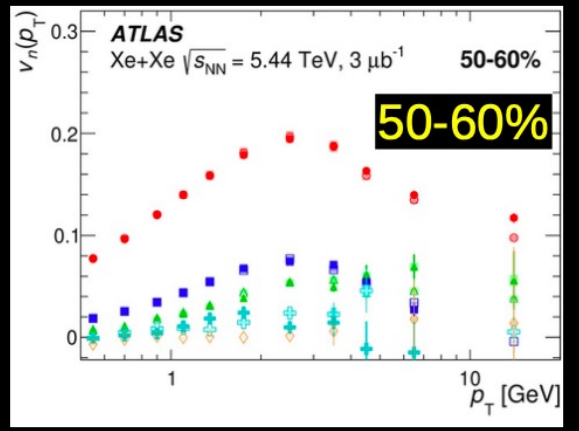

Phys. Rev. C 113 (2026) 045205

p_T dependence:

central events
- similar shape
- in Xe+Xe collisions smaller v_2

peripheral events
- similar shape
- in Xe+Xe collisions larger v_2
- non-flow contribution to v_2^{2PC} in O+O and Ne+Ne collisions

Conclusions

For the first time the light nuclei, oxygen and nitrogen, were accelerated and collided in the Large Hadron Collider last year. The data collected are used to obtain several new results:

- measurement of global characteristics of *p*+O collisions are especially important for proper simulations of development of cosmic-ray cascades in the atmosphere - crucial for studies of cosmic rays
- O+O and Ne+Ne collisions fill the gap between collisions of relatively heavy Xe nuclei and very light p+Pb and *pp* collisions and provide:
  - global characteristics useful for comparisons of models
  - measurement of particle flow in small systems
  - parton interactions in the medium - by measurement of dijet balance and correlations in events with photon-tagged jets

The 54th International Symposium on Multiparticle Dynamics (ISMD 2026)

System-size dependence of charged-particle production at mid and forward pseudorapidity with ALICE

Tulika Tripathy
(for the ALICE Collaboration)

National Central University in Chungli, Taiwan
18th August 2026.

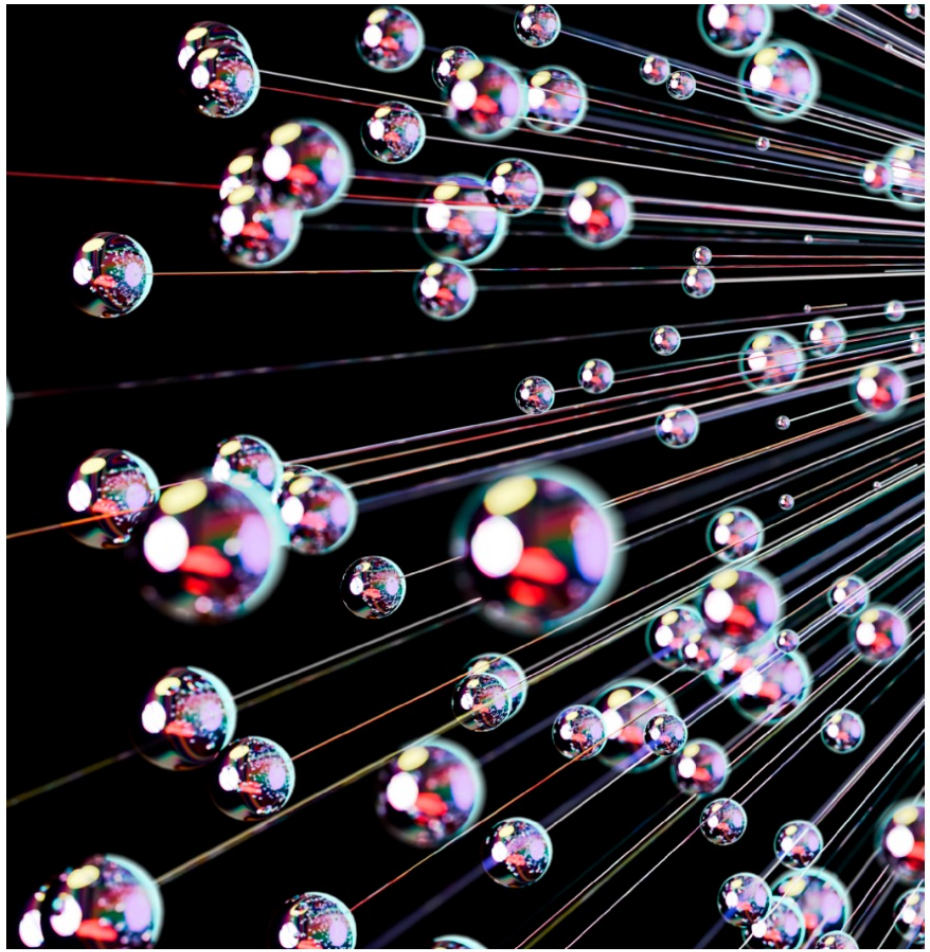

Charged-particle multiplicity density ($\mathrm{d}N_{\mathrm{ch}}/\mathrm{d}\eta$):

- Directly related to the **initial energy density** in heavy-ion collisions (QGP formation studies)

Key role:

Observable vs Multiplicity:

- Observables like particle yields, mean p_{T} can be measured as a function of $\langle \mathrm{d}N_{\mathrm{ch}}/\mathrm{d}\eta \rangle$ in centrality classes.
- Centrality classes can be estimated from N_{ch} for AA collisions

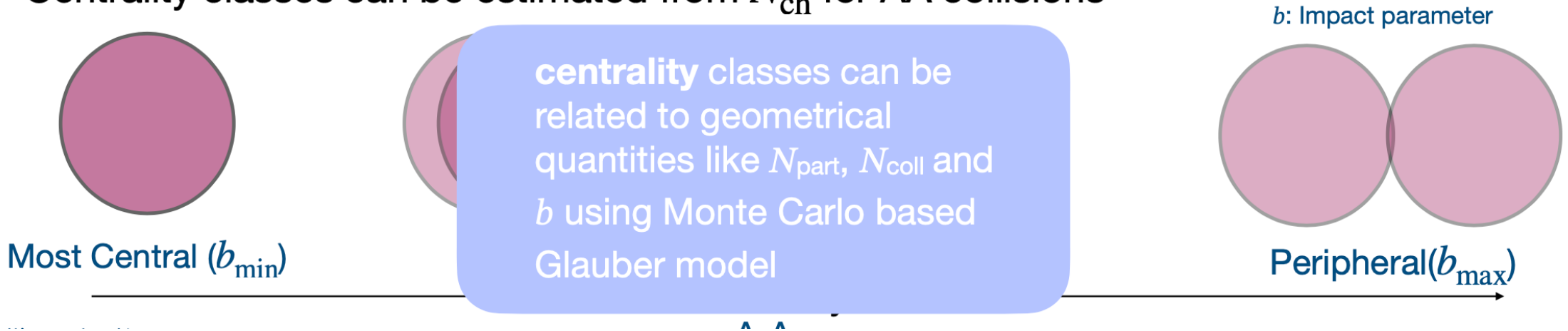

centrality classes can be related to geometrical quantities like N_{part}, N_{coll} and b using Monte Carlo based Glauber model

Small systems:
The reference and the puzzle

pp pO

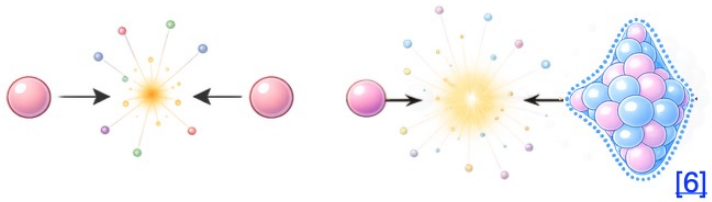

How do particle production and event activity evolve from elementary proton collisions to proton—nucleus system?

- Baseline for QCD particle production
- Collective-like signatures observed in high-multiplicity pp collisions [7, 8]
- pO bridges pp and ion collisions

Soft QCD processes Low pT
Non-perturbative in nature

Hard QCD processes High pT
Described by pQCD: precise calculation

Heavy ions:
The QGP benchmark

Pb—Pb

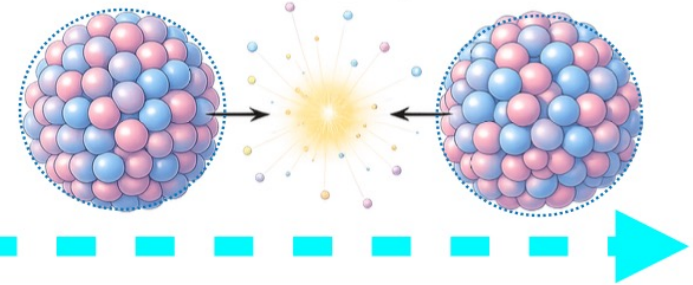

Pb–Pb collisions:
The established QGP reference at LHC

- QGP formation [1]
- Strong collective flow [2]
- Parton energy loss and jet quenching [3, 4]
- quarkonia suppression [5]

sPHENIX jet and photon measurements in p+p, O+O, and Au+Au collisions

Virginia Bailey
for the sPHENIX Collaboration

54th International Symposium on Multiparticle Dynamics

August 18, 2026

MPS Ascend Fellow

Why jet measurements at **RHIC *and* LHC**?

- Different QGP:
  - Temperature and temperature evolution different between LHC and RHIC
- Different probes:
  - Different quark vs. gluon jet mixture
  - Lower kinematic range- radiation close to the QGP medium scale early in collision

arXiv:1501.06197

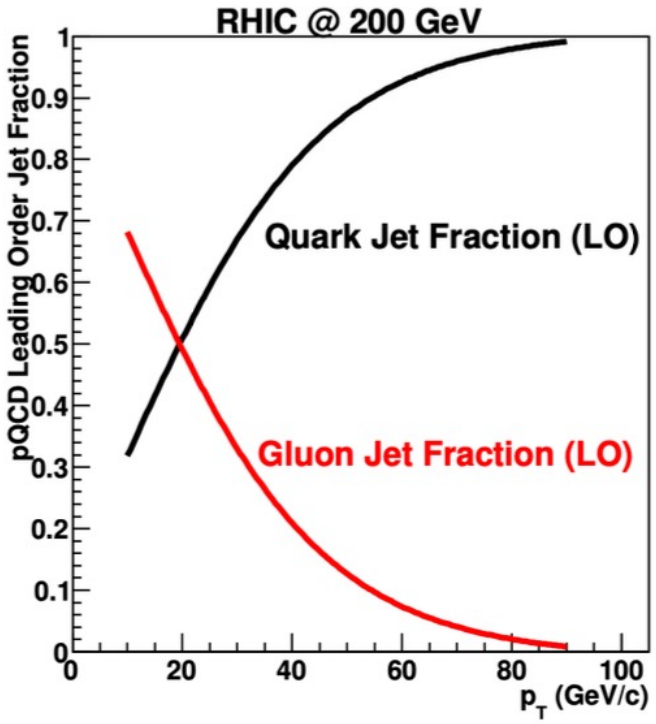

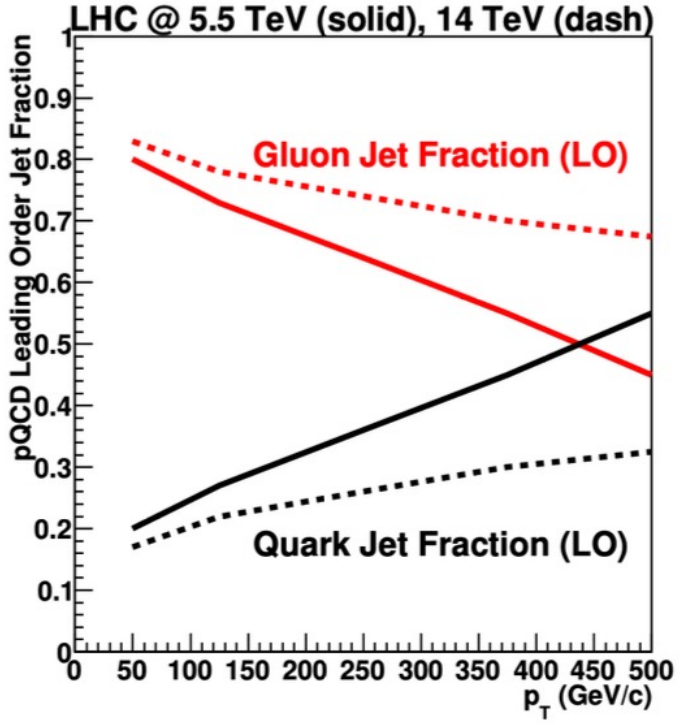

Courtesy of Misaki Ouchida (Hokkaido University)

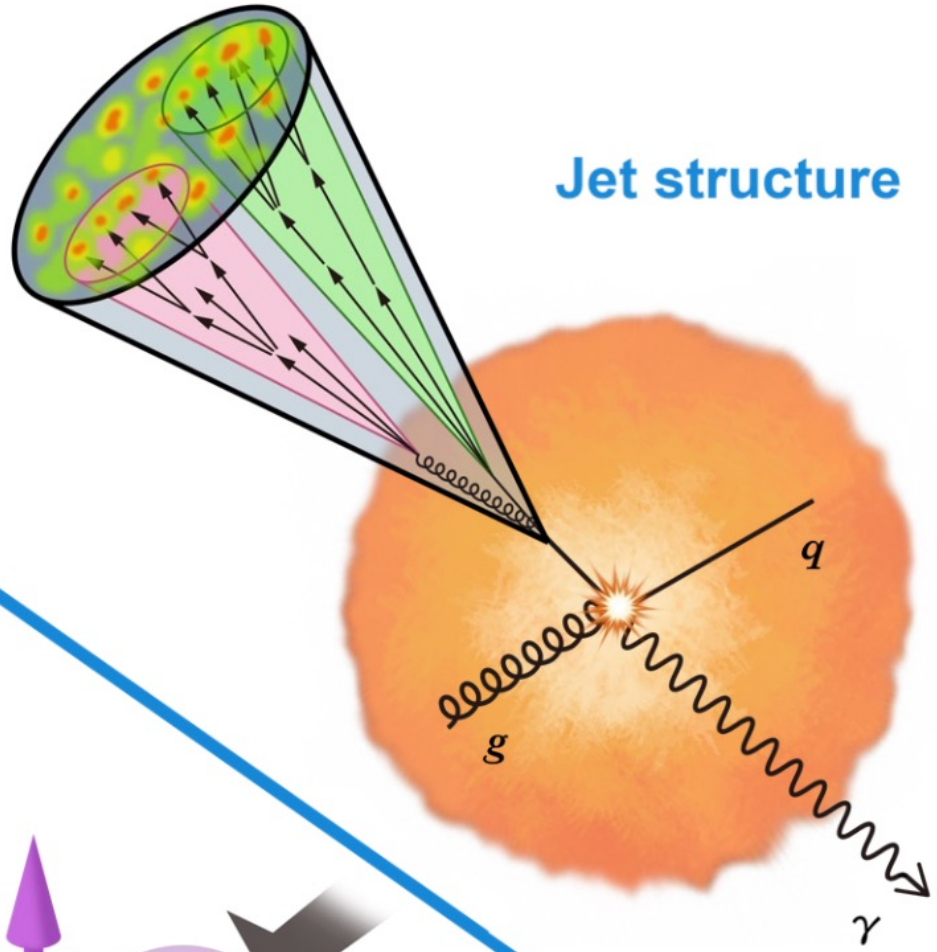

Jet structure

Quarkonium spectroscopy

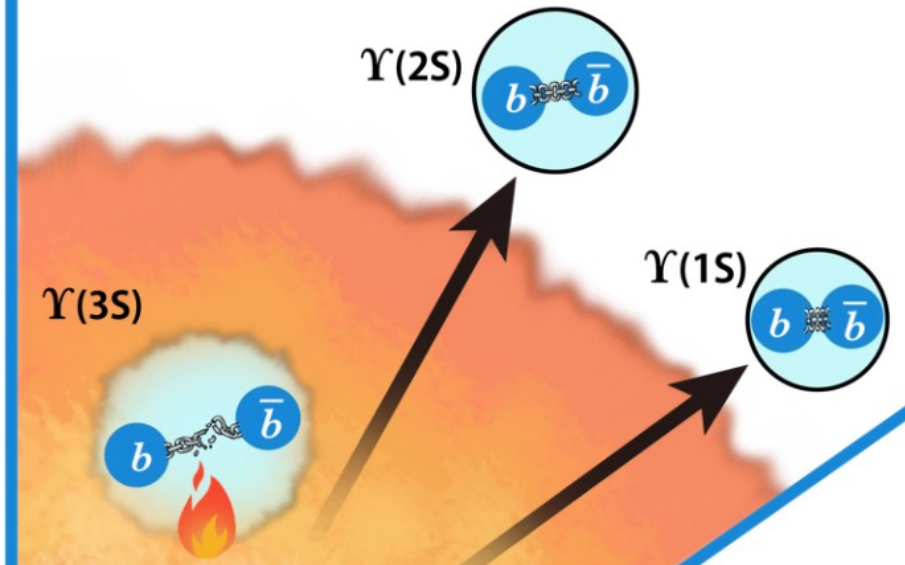

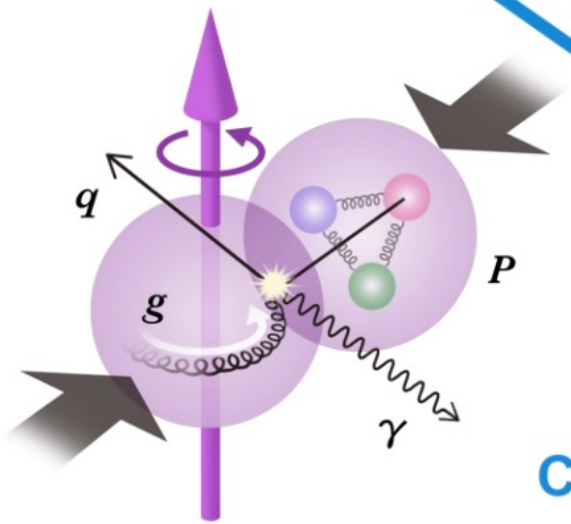

Cold QCD

sPHENIX

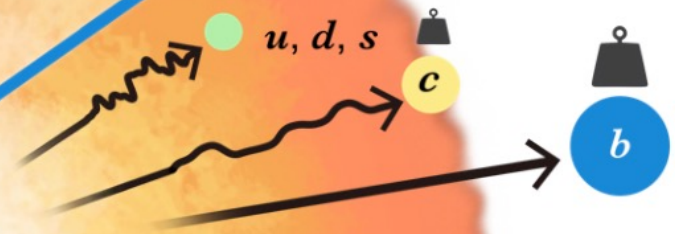

Parton energy loss

sPHENIX

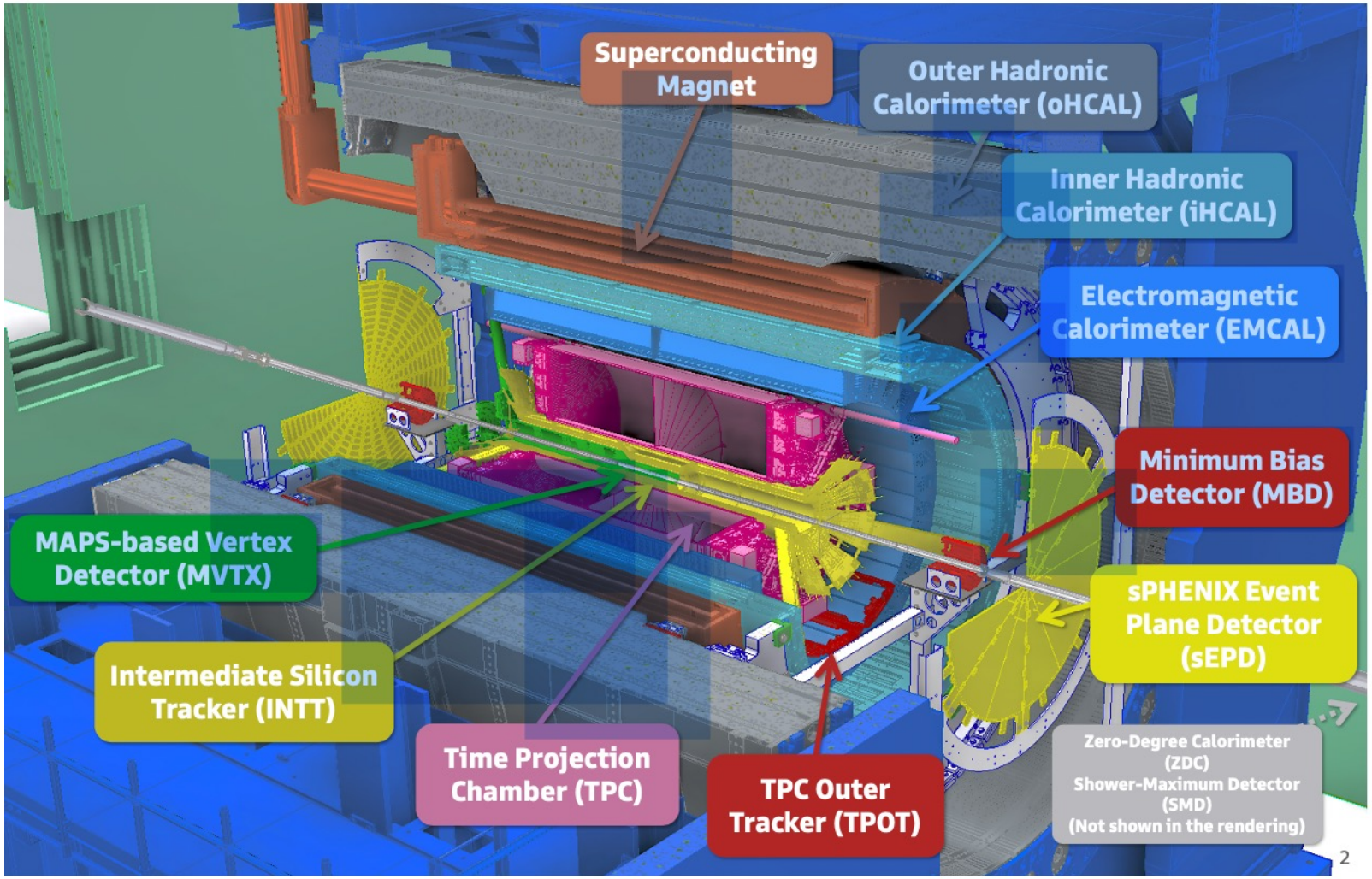

- **New detector** built at RHIC- first commissioning data in 2023
- Full calorimetry allows for **unbiased calorimeter jet reconstruction**
- **Precision tracking** allows for tagging heavy flavor decays, jet substructure, etc.
- Fast readout allows for **high statistics datasets**
  - 15kHz trigger system + capability for streaming tracking detectors

Isolated prompt photons

sPH-JET-2026-02, arXiv:2607.03892

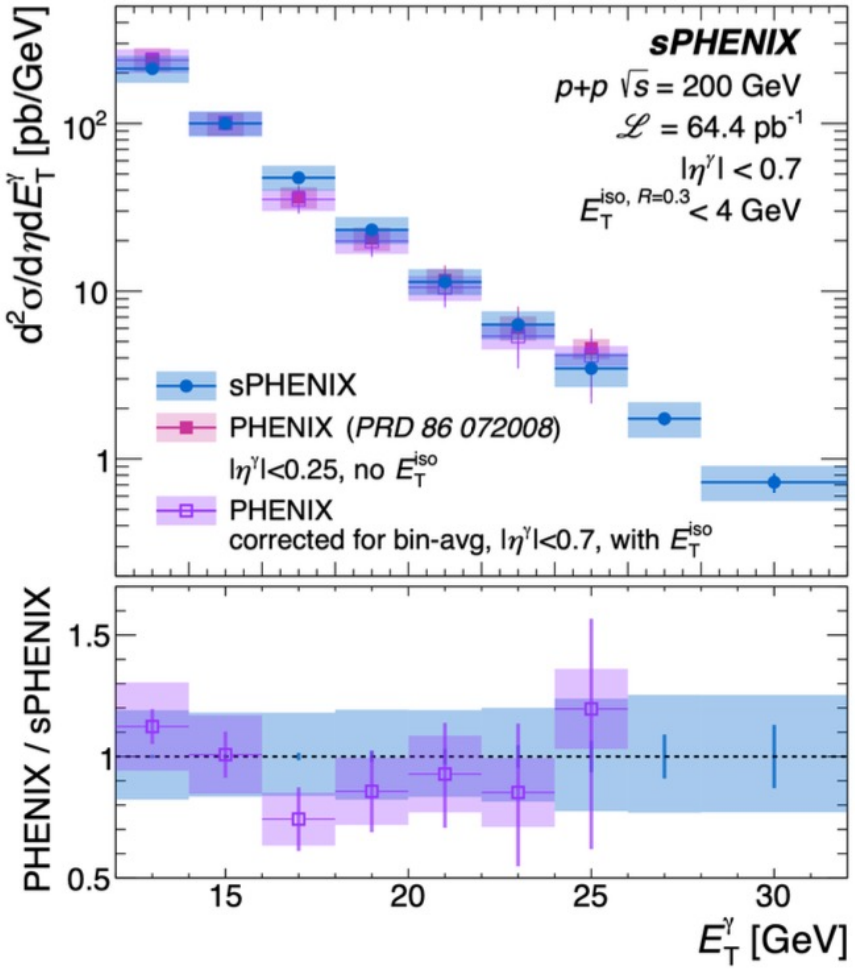

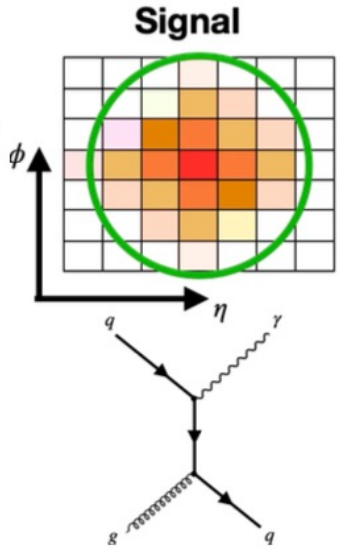

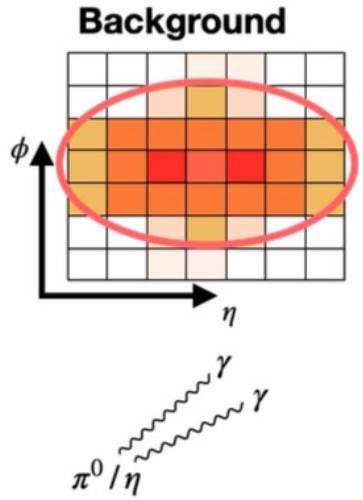

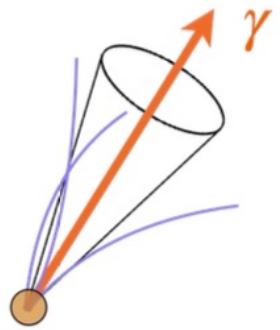

- Backgrounds suppressed using **ML identification** (BDT) based on shower shapes
- Isolation includes both **EMCal and HCal**
- Good agreement with pQCD calculations
- Improved **kinematic reach** and statistical precision from previous measurements at RHIC

Key for future photon+jet measurements

Jets are suppressed in large systems not in small systems

arXiv:2308.05743

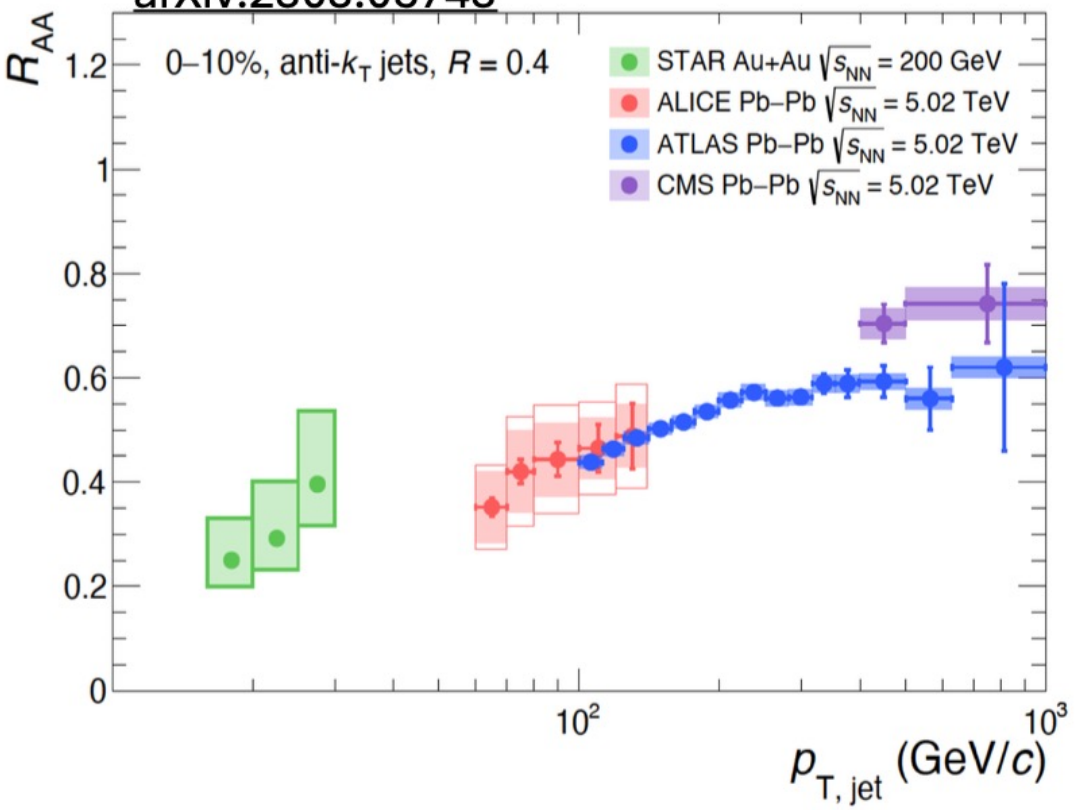

JHEP05(2024)041

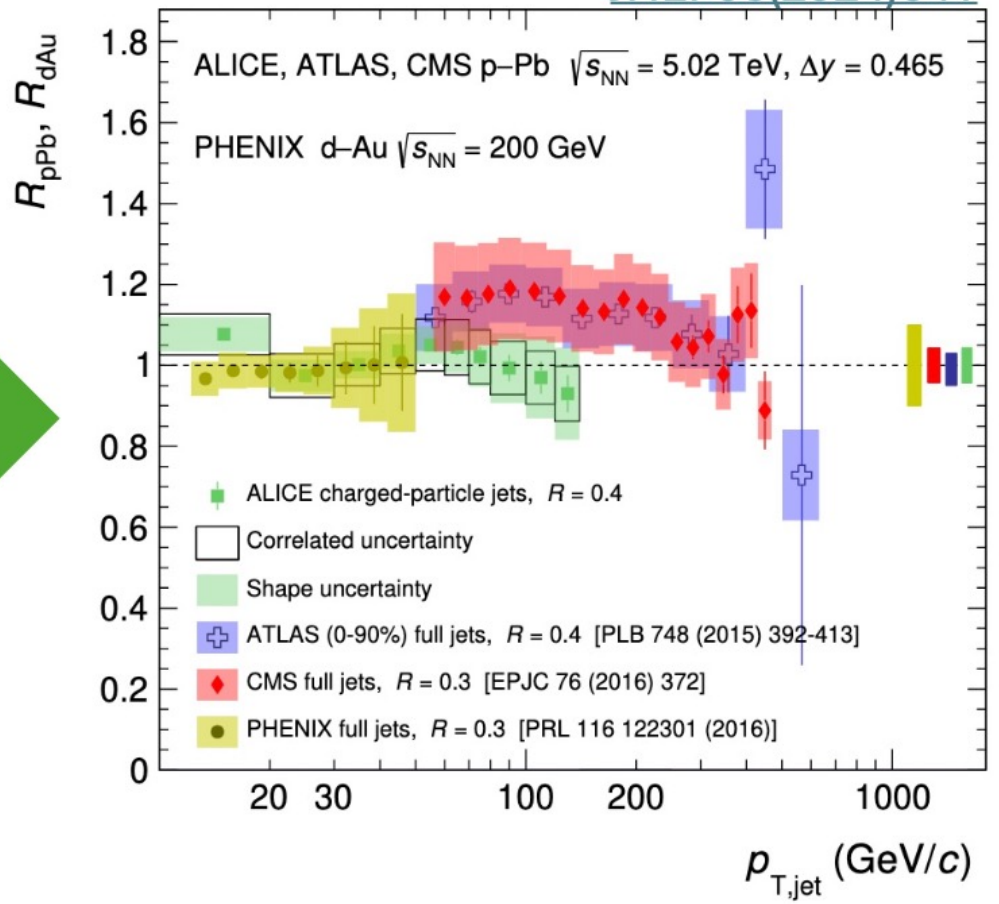

Evidence for jet quenching in O+O

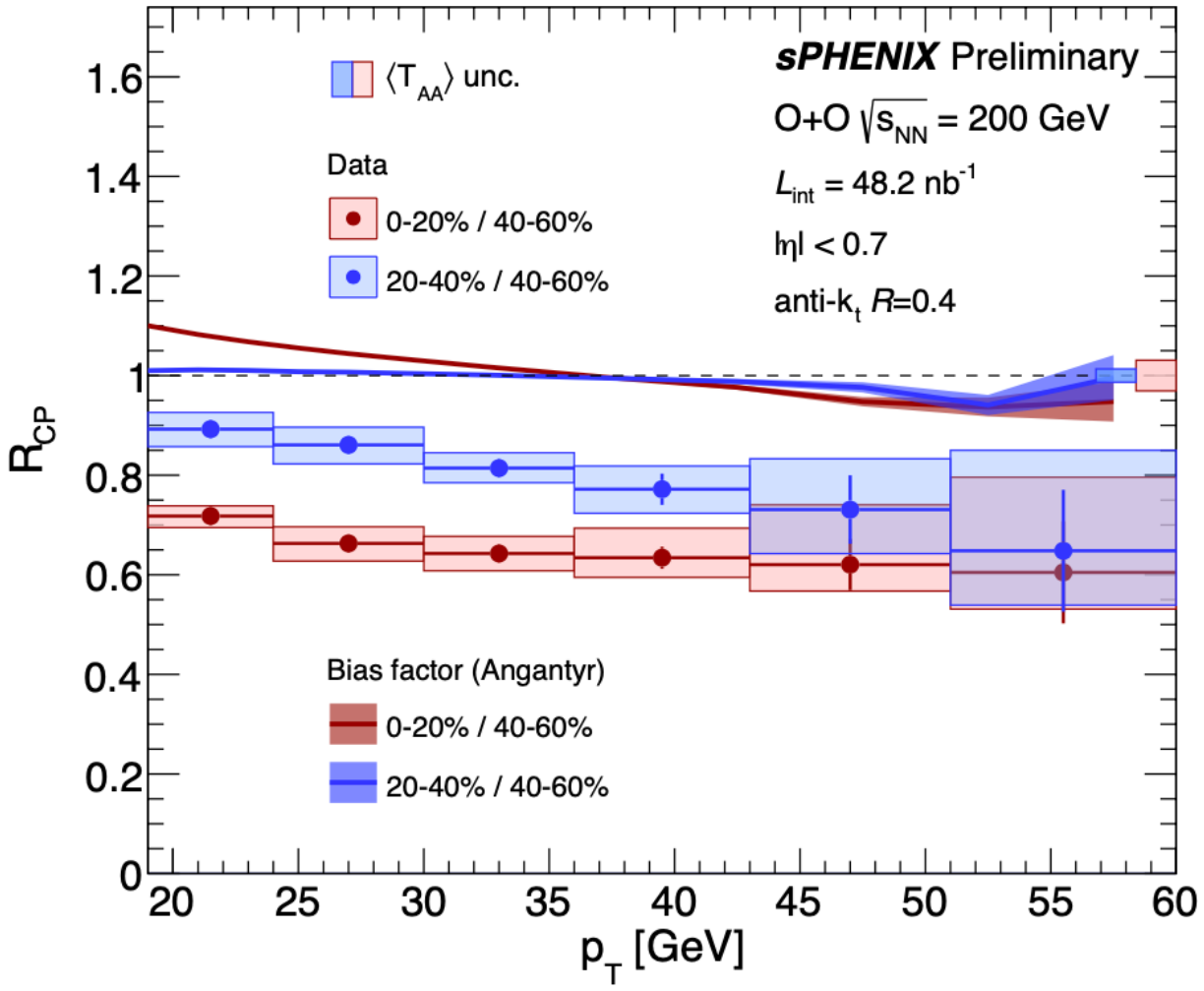

- Jets in O+O collisions are **suppressed** compared to p+p
- Important to consider **nuclear PDF effects**
- Central to peripheral ratio also shows evidence for quenching
  - Beyond level of **selection bias** effects modeled in Angantyr

Conclusions

- sPHENIX has performed **baseline jet and photon measurements** in p+p collisions
  - **Data-driven** JES and JER calibrations
- Also sPHENIX's first **jet quenching** results in large (Au+Au) and intermediate (O+O) systems
- Together set the stage for **precision jet and jet substructure** physics program

See all sPHENIX public results:
https://www.sphenix.bnl.gov/PublicResults

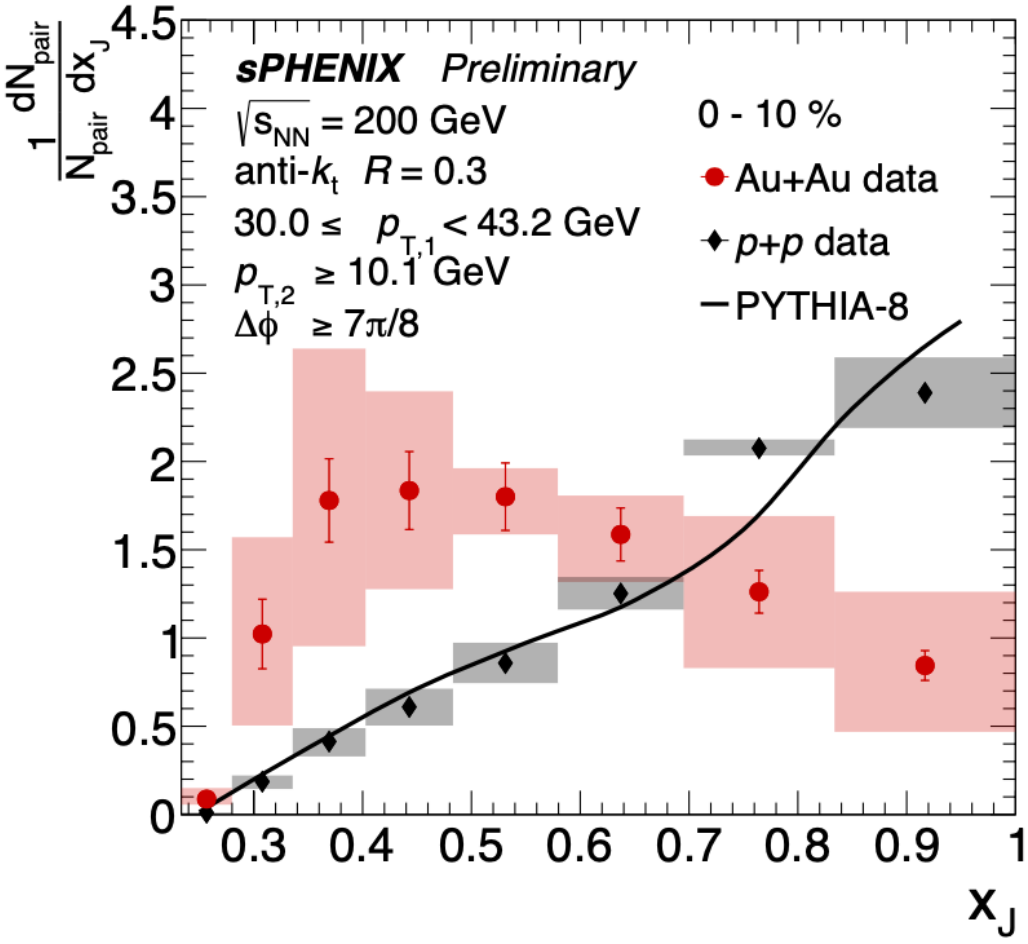

Accessing hadronic interactions via femtoscopy with ALICE

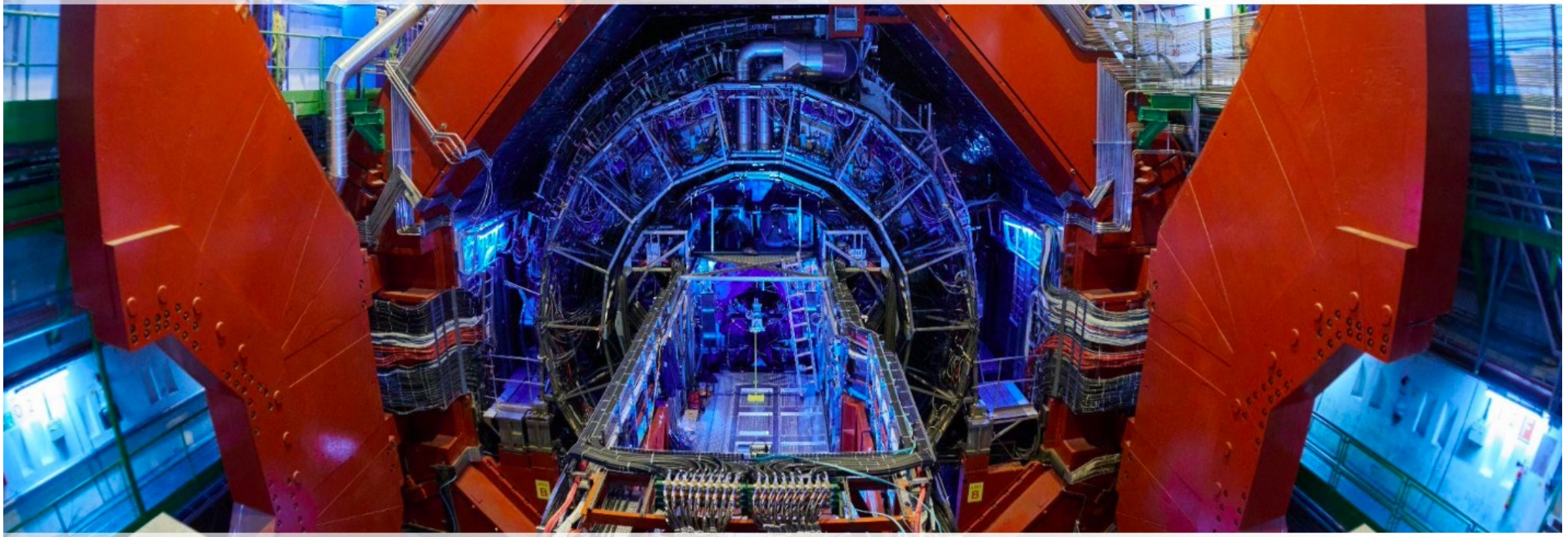

Daniel Battistini, on behalf of the ALICE Collaboration
Czech Technical University in Prague

International Symposium on Multiparticle Dynamics
Chungli, Taiwan | 17th - 21st Aug 2026

ISMD 2026

European Research Council

Femtoscopy for interactions A

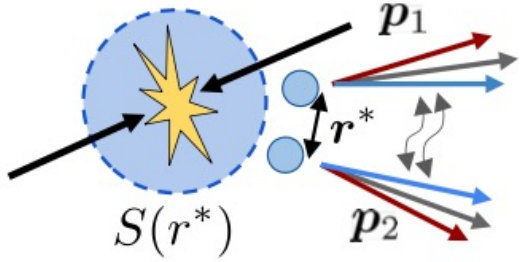

$$k^* = \frac{1}{2}|\boldsymbol{p}_1^* - \boldsymbol{p}_2^*|$$

Experimental correlation function (CF)

$$C(k^*) = \frac{N_{\text{same}}(k^*)}{N_{\text{mixed}}(k^*)}$$

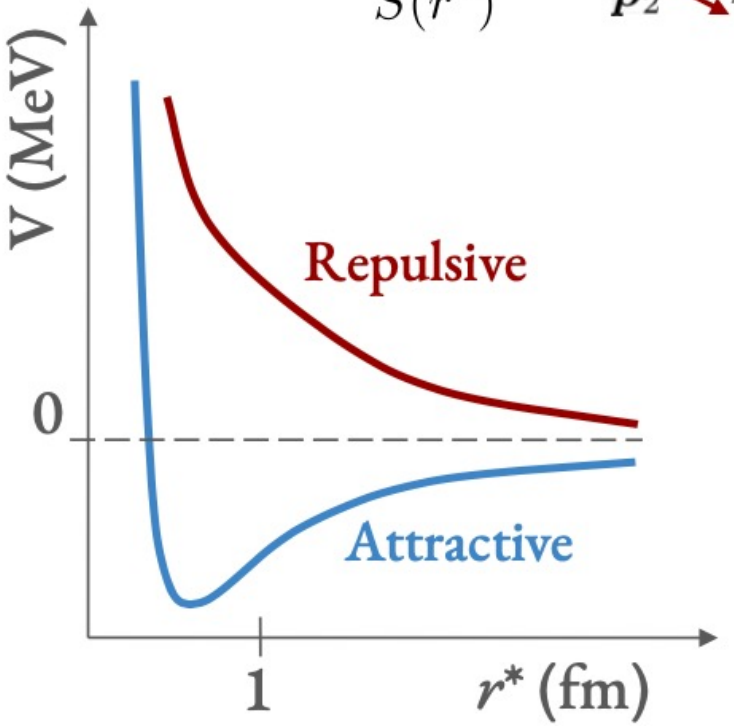

Koonin-Pratt formula

$$C(k^*) = \int \mathrm{d}\boldsymbol{r}^*\, S(\boldsymbol{r}^*)|\psi(k^*, \boldsymbol{r}^*)|^2$$

M. Lisa, S. Pratt et al., ARNPS 55 (2005), 357-402
L. Fabbietti et al., ARNPS 71 (2021), 377-402
D. Mihaylov et al., EPJC 78 (2018), 5, 394

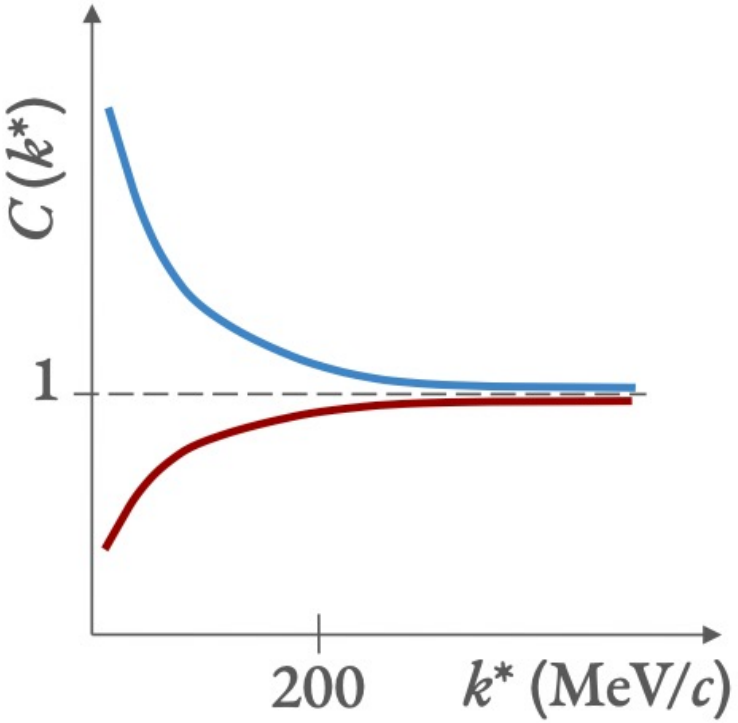

The source function

The pp interaction is very well known from scattering
→ used to determine the source

$$C(k^*) = \int \mathrm{d}\boldsymbol{r}^*\, S(\boldsymbol{r}^*)|\psi(k^*, \boldsymbol{r}^*)|^2$$

Measure — Constrain ← Known

Resonance Source Model:

$$S(r^*) = \frac{1}{(4\pi r_{\mathrm{core}}^2)^{3/2}} \exp\left(-\frac{r^{*2}}{4r_{\mathrm{core}}^2}\right) \oplus \text{ resonances}$$

Common emission source for all hadrons observed experimentally in Run 2

New double-differential study in Run 3 of the source size with m_{T} and multiplicity

$$m_{\mathrm{T}} = \sqrt{k_{\mathrm{T}}^2 + m^2}, \quad k_{\mathrm{T}} = |p_{\mathrm{T},1} + p_{\mathrm{T},2}|/2$$

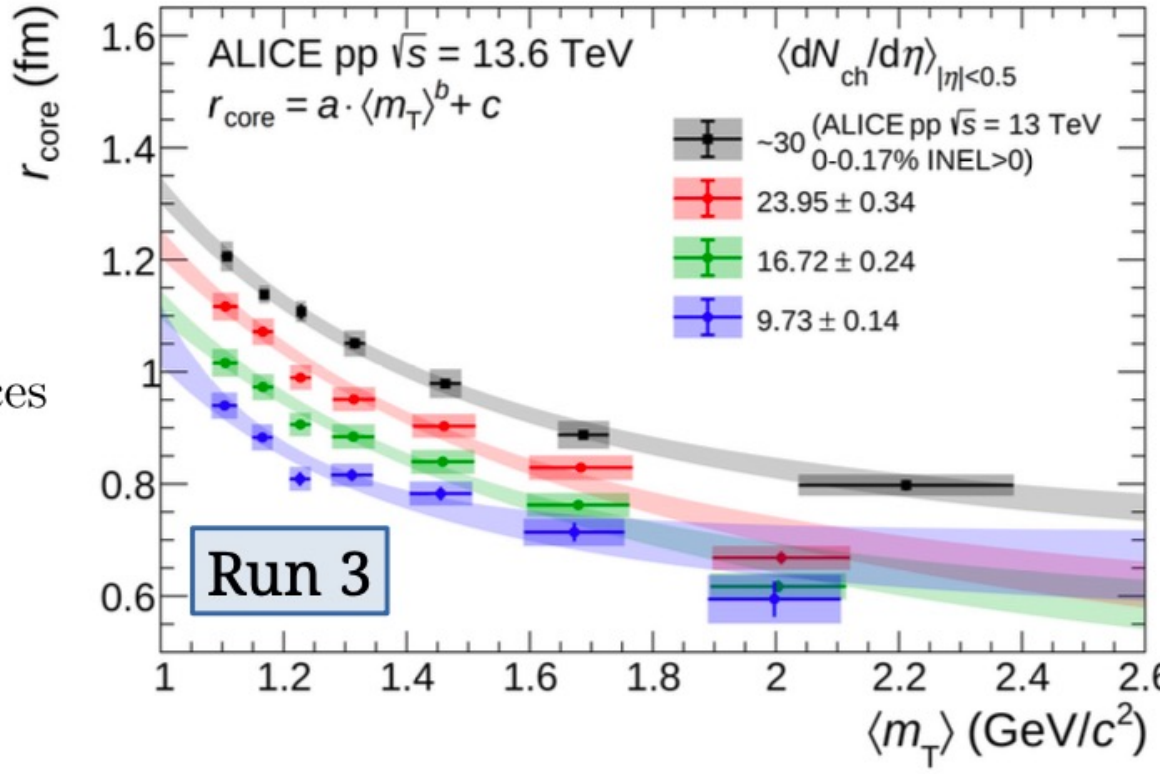

ALICE Coll., arXiv:2606.28098

The $p\Sigma^-$ interaction ($|S| = 1$)

$p\Sigma^-$: very challenging measurement ($\Sigma^- \rightarrow n\pi^-$)

Σ^- reconstructed with direct tracking in the ITS2

Strong interaction based on chiral effective field theory + Lednicky-Lyuboshits model

Deviations from Coulomb-only interaction
→ sensitive to the strong nuclear force

Tension with theoretical predictions

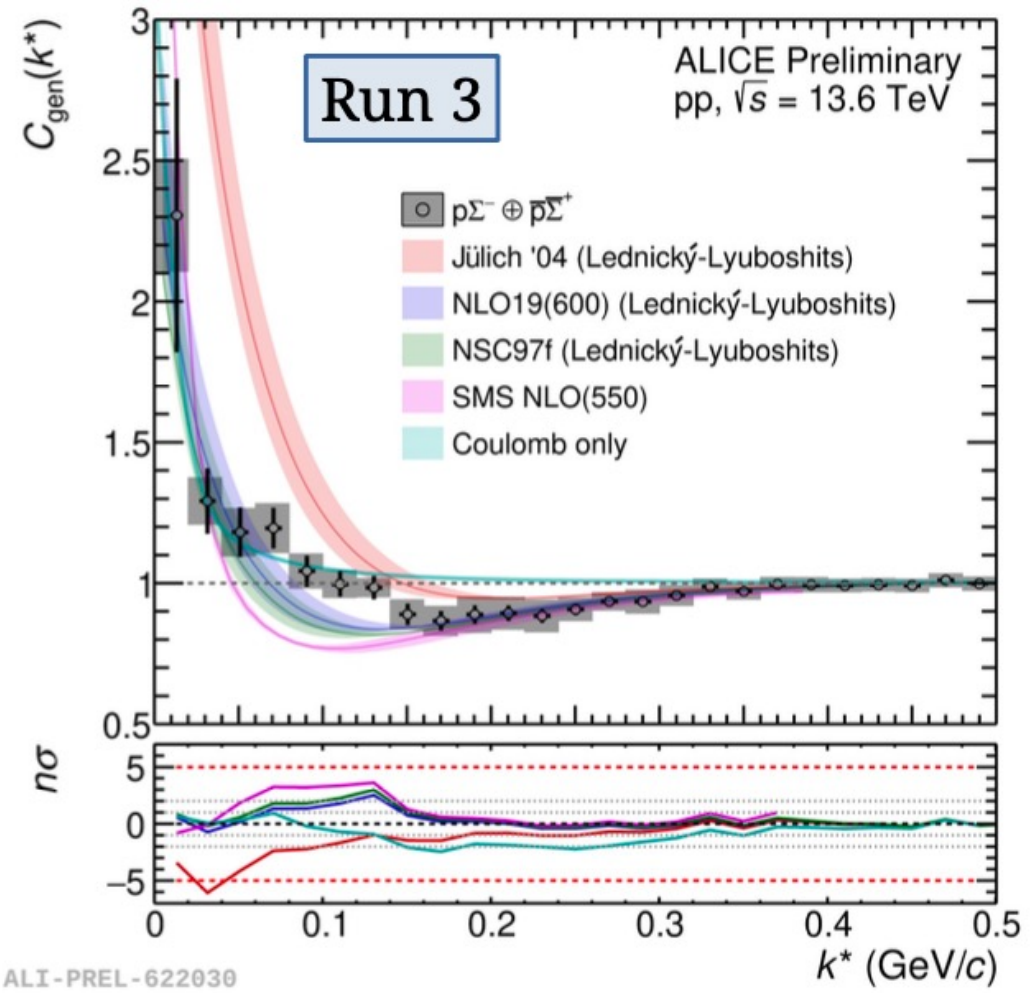

"… We resolve the problem by regularizing the generalized Lednicky-Lyuboshitz formula with a cut-off and validate it using the Koonin-Pratt formula as a reference. We also show the relationship between the cut-off in the regularized Lednicky-Lyuboshitz and the effective-range correction in the original Lednicky-Lyuboshitz formula. Using the obtained formula, we investigate the source-size dependence, the validity of the effective range expansion, and the cutoff dependence of the correlation function."

Conclusions

Femtoscopy: excellent tool for accessing the strong interaction between hadrons
→ several high-precision measurements in Run 2 and Run 3
→ valuable input for low-energy QCD

Hyperon interactions:
→ pΛ: improved precision w.r.t. scattering, singlet channel is less attractive
→ $p\Sigma^-$: tension with theoretical models
→ pΞ: first evidence of $p\Xi \rightarrow \Lambda\Sigma^0$ coupling
Heavy neutron stars remain unexplained… 3-body forces?

3-body forces:
→ ppp: demonstrates sensitivity to the 2- and 3-body partial-wave structure
→ ppΛ: sizeable effect of 3-body forces compared to available models
→ ppΞ: significant deviations at intermediate Q_3

Probing light nuclei formation at the LHC with balance functions and long-lived resonances tagging

Sushanta Tripathy, Peter Christiansen
Email: sushanta.tripathy@cern.ch

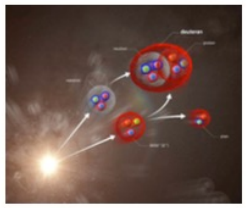

ALICE, Nature 648 306 (2025)

Explore content · About the journal · Publish with us

nature > articles > article

Article | Open access | Published: 10 December 2025

Observation of deuteron and antideuteron formation from resonance-decay nucleons

The ALICE Collaboration

Nature 648, 306–311 (2025) | Cite this article

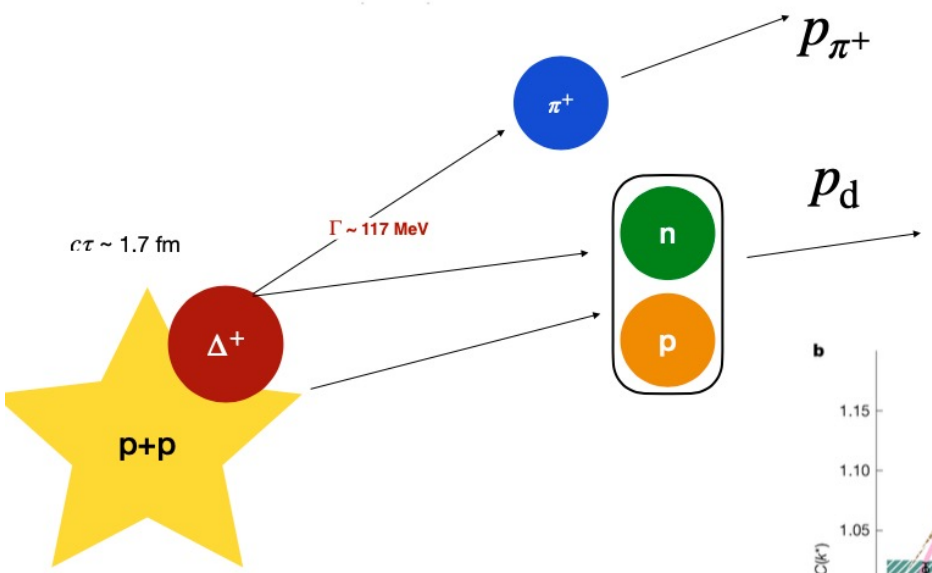

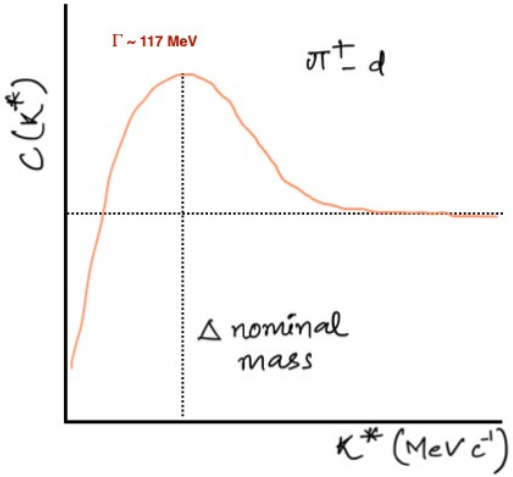

$$C(k^*) = N \frac{N_{\text{same}}(k^*)}{N_{\text{mixed}}(k^*)}$$

k* is the single-particle momentum in the pair rest frame. For non-interacting particles, C(k*) ≈ 1 everywhere

EPOS + coalescence afterburner

- the nucleon from the decay coalesces with another nucleon to form d
- a **peak** in C(k*) near the Δ nominal mass

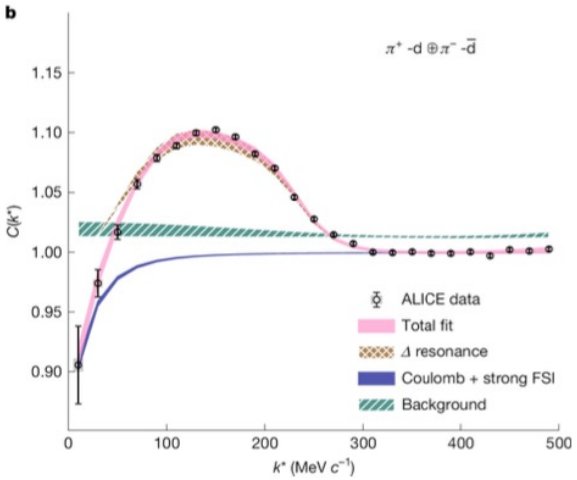

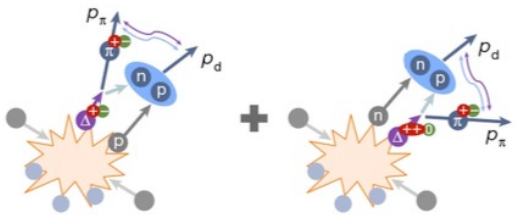

Most of the deuterons are produced in nuclear reactions following the decay of short-lived resonances



LUND UNIVERSITY

Summary and outlook



- Light nuclei production at the LHC remains a puzzle
- Proton/deuteron balance functions can provide strong separation between production mechanisms.
- Pion-deuteron correlations study by ALICE support coalescence and presents an important role of resonance-decay nucleons.
- Resonance-tagged observables such as $\Lambda(1520)$ can offer a direct handle on deuteron formation.
- Future precision measurements can establish the microscopic origin of light nuclei and improve inputs for dark matter searches

Recent RHIC results from prospects for the EIC

Yuji Goto (RIKEN)

Outline

RHIC & EIC introduction

- EIC physics
  - Tomography
  - Gluon saturation
- Ultraperipheral collision (UPC) in heavy-ion collision
  - Recent STAR results
- Summary

RHIC & EIC introduction

- RHIC
  - World's first heavy-ion & polarized-proton collider constructed in BNL
  - First gold-ion collision in 2000
  - Polarized-proton collision at √s = 200 GeV in 2001
  - Polarized-proton collision at √s = 500 GeV in 2009
- Concluded 26-year operation
  - 2026.2.6



Dario Gil, US-DOE Under Secretary officially ended the operational era of the RHIC

- EIC
  - World's first polarized electron + proton / light-ion / heavy-ion collider
  - BNL determined to host EIC in 2020
  - To be constructed in 2034

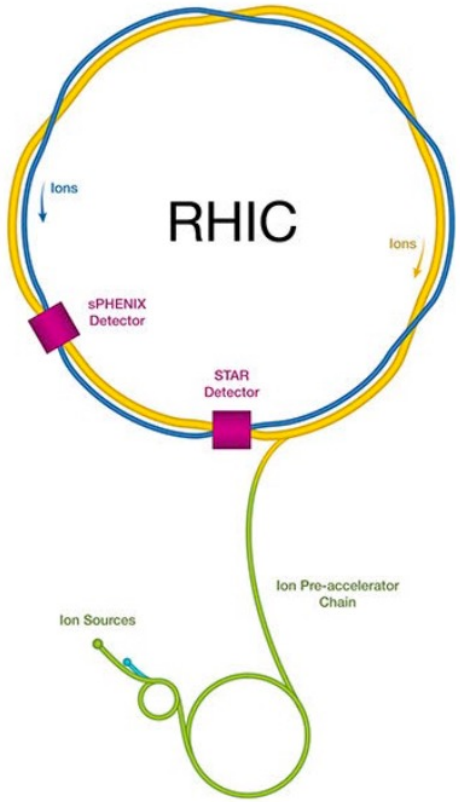

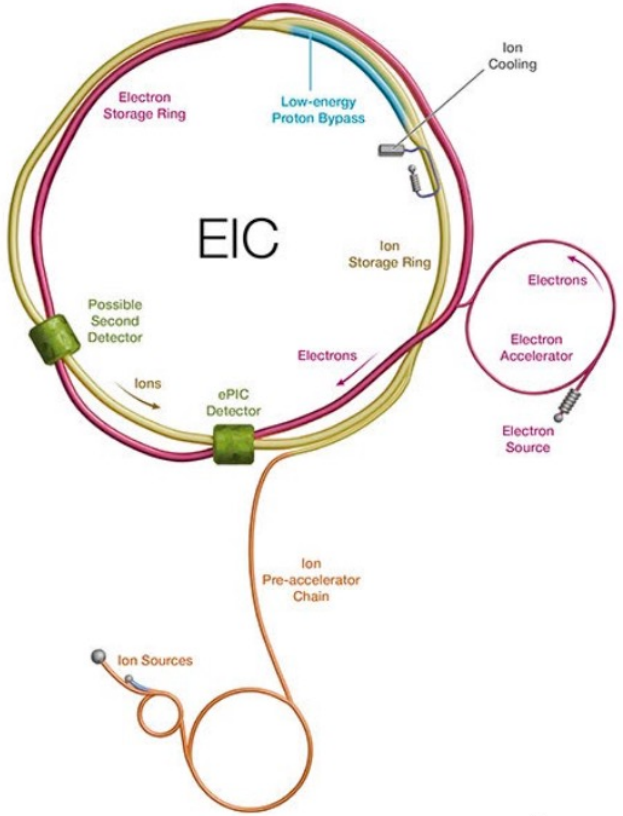

Physics at EIC

- How does the mass of the nucleon arise?
  - The Higgs mechanism accounts for only ~1% of the mass of the proton.
- How does the spin of the nucleon arise?
  - The spin of the quarks accounts for only one-third of the spin of the proton.
- What are the emergent properties of dense system of gluons?
  - The gluon saturation describes a new state of matter at extreme high density.

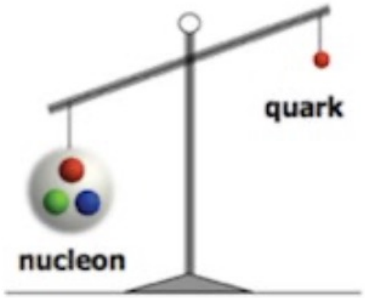

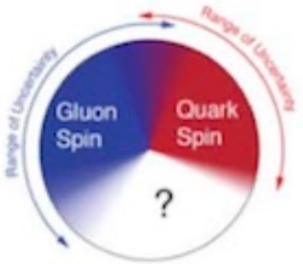

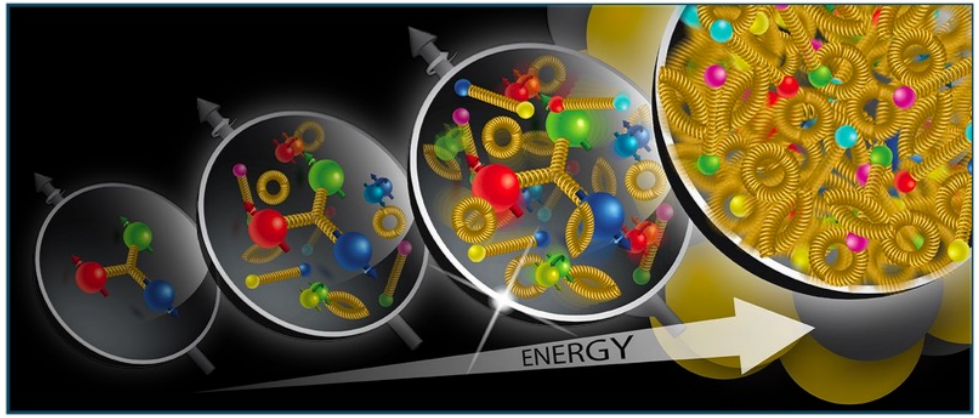

Tomography of the nucleon / nucleus

- EIC = color dipole microscope
  - Exclusive process and diffractive process
  - 3D distribution: transverse spatial distribution

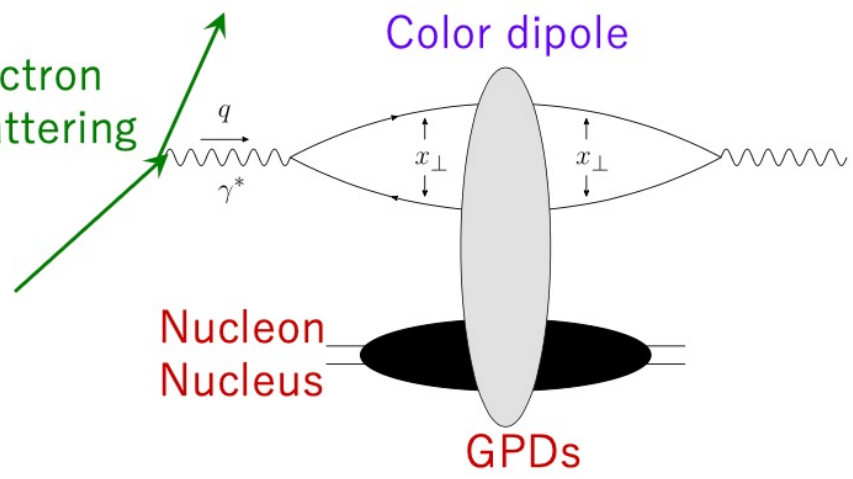

DVCS (Deeply Virtual Compton Scattering)

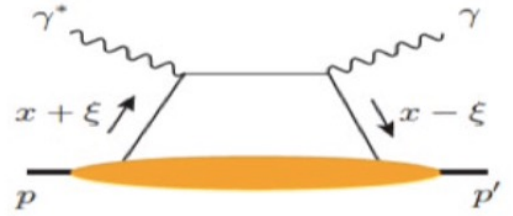

Meson Production

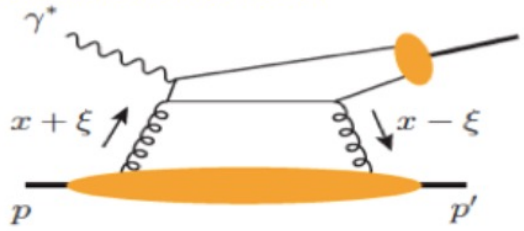

J/ψ, ϕ, ρ, etc.

- GPD (Generalized Parton Distribution)
  - Spatial imaging of gluons and quarks = tomography
  - Orbital angular momentum
    - Ji's sum rule
    - Origin of the nucleon spin

$$J_q^z = \frac{1}{2}\sum_q \Delta q + \sum_q L_q = \frac{1}{2}\left(\int_{-1}^{1} x dx (H^q + E^q)\right)_{t\to 0}$$

Gluon saturation

- Gluon emission
  - Divergence at small *x*
- Gluon recombination
  - Restriction of divergence
- Gluon saturation in balanced
  - Based on classical idea of the saturation
- Discovery of quantum collective gluon
  - Saturated gluon model, the color glass condensate (CGC) model, allows precision comparison with experiments
- Precision understanding of nucleus with the quark-gluon picture necessary as the initial state of the QGP for understanding its production mechanism

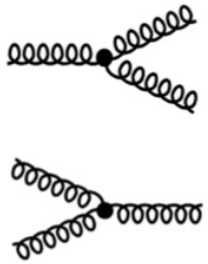

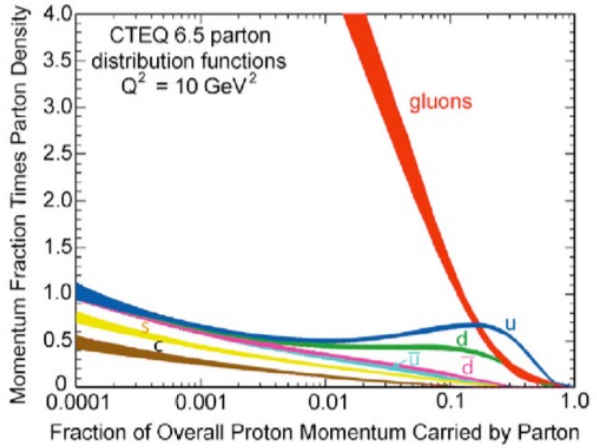

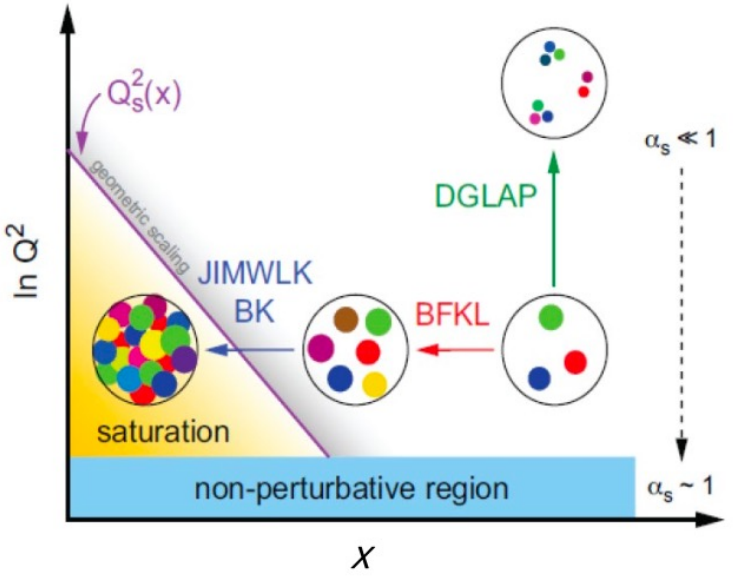

$$\tau = \frac{Q^2}{Q_s^2(s)},$$
$$Q_s^2(s) \propto x^{-\lambda}.$$

Gluon saturation at extreme density

- Exclusive vector meson production
  - Momentum transfer t dependence translated to the transverse spatial distribution of gluons in the nucleus
- Incoherent process (nucleus breaks up)
  - Spatial density fluctuation in nucleus
  - Much larger than the coherent process
- Coherent process (nucleus remains intact)
  - Sensitive to the gluon saturation
  - Identify & veto breakup of the excited nucleus

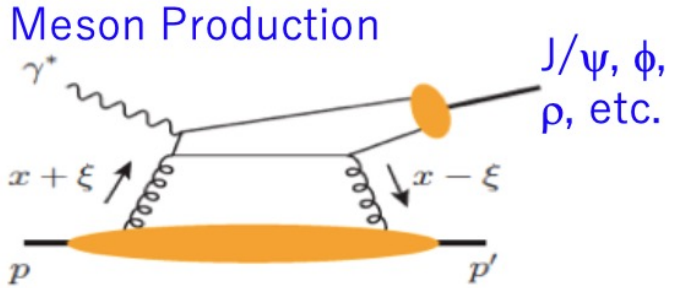

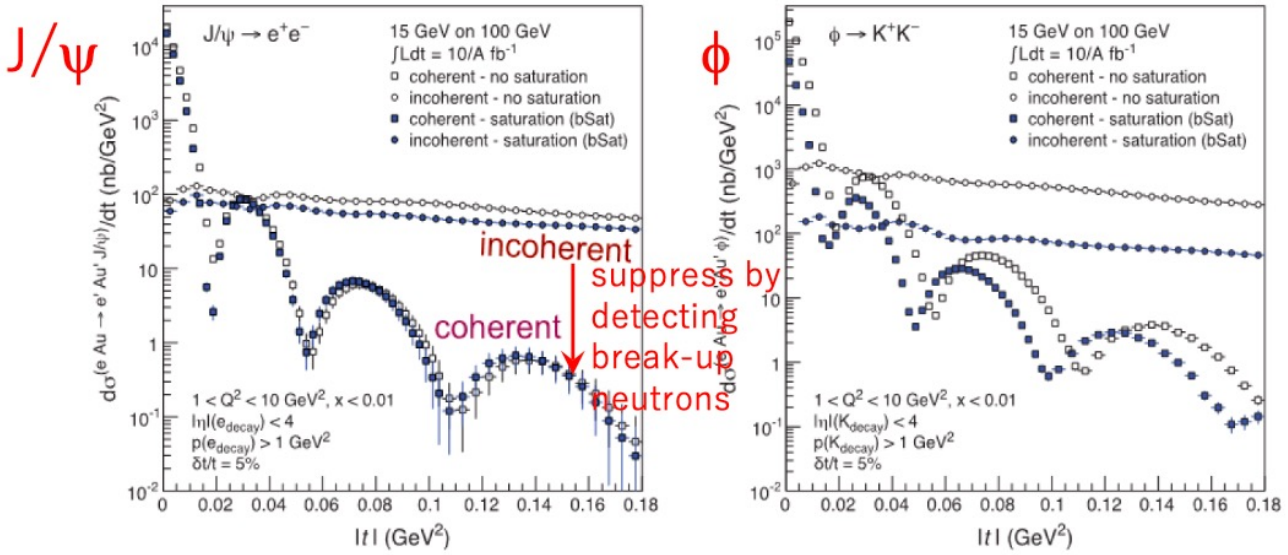

UPC introduction

- Ultraperipheral collision (UPC) in heavy-ion collision
  - No hadronic overlap
  - Long-range electromagnetic interactions dominant
- Quasi-real photon from UPC
  - Highly Lorents-boosted EM field
  - Virtuality $k_\perp \sim 1/R_p \sim 30$ MeV (R_p: nuclear charged radius)
- Pomeron exchange
  - Color-singlet two-gluon exchange
- Vector meson exclusive production in UPC
- Clean tool for probing gluon density down to the very low-x

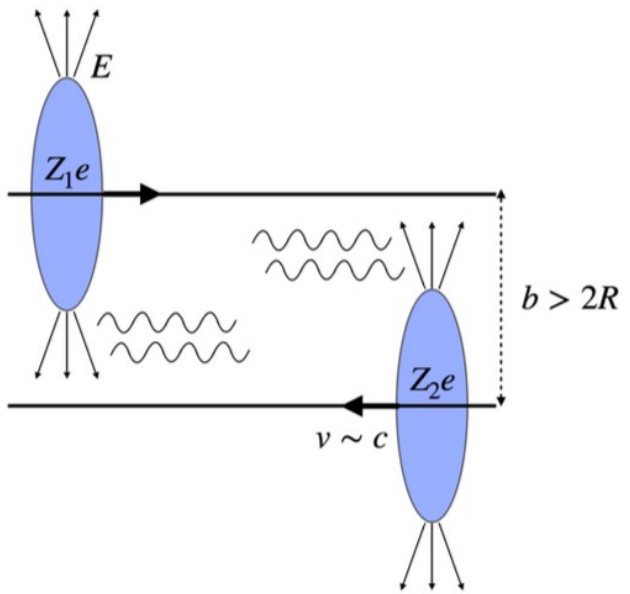

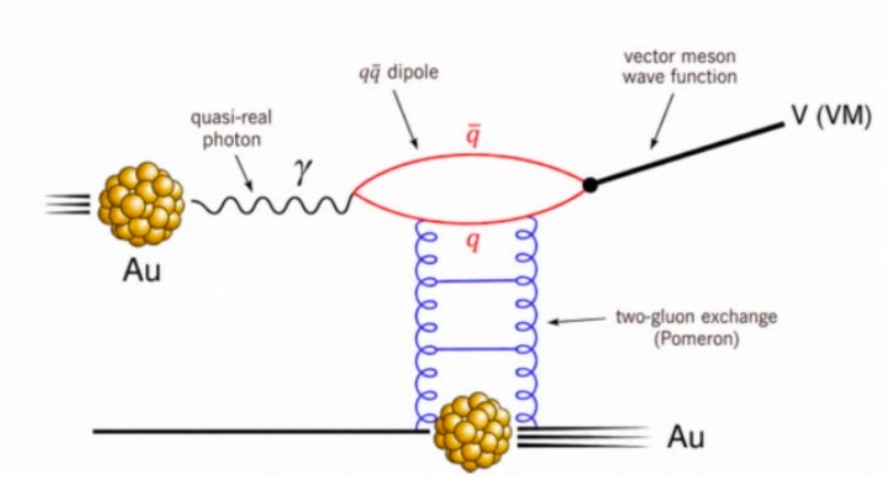

Recent STAR results

- Spin interference in J/ψ
  - Phys. Rev. Lett. 136 (2026) 242302
- Negative modulation for J/ψ, weaker than ρ
- Spin interference
  - New experimentally accessible handle on gluon structure
  - Constrain on models

